2020

APOE AS A METABOLIC REGULATOR IN HUMANS, MICE, AND ASTROCYTES

Brandon C. Farmer
University of Kentucky, brandon.c.farmer@uky.edu
Author ORCID Identifier:
https://orcid.org/0000-0003-1698-2283
Digital Object Identifier: https://doi.org/10.13023/etd.2020.298

STUDENT AGREEMENT:

I represent that my thesis or dissertation and abstract are my original work. Proper attribution has been given to all outside sources. I understand that I am solely responsible for obtaining any needed copyright permissions. I have obtained needed written permission statement(s) from the owner(s) of each third-party copyrighted matter to be included in my work, allowing electronic distribution (if such use is not permitted by the fair use doctrine) which will be submitted to UKnowledge as Additional File.

I hereby grant to The University of Kentucky and its agents the irrevocable, non-exclusive, and royalty-free license to archive and make accessible my work in whole or in part in all forms of media, now or hereafter known. I agree that the document mentioned above may be made available immediately for worldwide access unless an embargo applies.

I retain all other ownership rights to the copyright of my work. I also retain the right to use in future works (such as articles or books) all or part of my work. I understand that I am free to register the copyright to my work.

REVIEW, APPROVAL AND ACCEPTANCE

The document mentioned above has been reviewed and accepted by the student's advisor, on behalf of the advisory committee, and by the Director of Graduate Studies (DGS), on behalf of the program; we verify that this is the final, approved version of the student's thesis including all changes required by the advisory committee. The undersigned agree to abide by the statements above.

Brandon C. Farmer, Student

Dr. Lance A. Johnson, Major Professor

Dr. Kenneth Campbell, Director of Graduate Studies

APOE AS A METABOLIC REGULATOR IN HUMANS, MICE, AND ASTROCYTES

DISSERTATION

A dissertation submitted in partial fulfillment of the
requirements for the degree of Doctor of Philosophy in the
College of Medicine
at the University of Kentucky

By

Brandon Charles Farmer
Lexington, Kentucky

Co- Directors: Dr. Lance A. Johnson, Assistant Professor of Physiology

and Dr. Steven Estus, Professor of Physiology

Lexington, Kentucky

2020

https://orcid.org/0000-0003-1698-2283

ABSTRACT OF DISSERTATION

APOE AS A METABOLIC REGULATOR IN HUMANS, MICE, AND ASTROCYTES

Altered metabolic pathways appear to play central roles in the pathophysiology of late-onset Alzheimer's disease (AD). Carrier status of the E4 allele of the *APOE* gene is the strongest genetic risk factor for late-onset AD, and increasing evidence suggests that E4 carriers may be at an increased risk for neurodegeneration based on inherent metabolic impairments. A new appreciation is forming for the role of *APOE* in cerebral metabolism, and how nutritional factors may impact this role. In chapter 1, the literature on nutritional interventions in E4 carriers aimed at mitigating disease risk is reviewed. Studies investigating the mechanism by which E4 increases disease risk have focused primarily on the association of E4 with the neuropathological hallmarks. While these studies have aided in our understanding of the role of E4 in late-disease pathology, investigating metabolic signatures of E4 carriers who have not yet developed neuropathology gives insight into the potential earlier mechanisms of E4 as a risk factor for AD. For example, an early and consistent biological hallmark of AD is cerebral glucose hypometabolism as observed by fluorodeoxyglucose positron emission tomography (FDG-PET). Interestingly, E4 carriers also display an AD-like pattern of decreased glucose metabolism by FDG-PET far before clinical symptomology. Since glucose hypometabolism occurs early in AD and early in E4 carriers, it may represent a critical prodromal phase of AD. Beyond this brain imaging finding, it is unclear if APOE has any other discernable metabolic effects in cognitively unimpaired young people. In chapter 2 we bridge this knowledge gap in the field. We utilized indirect calorimetry (IC) as a method for assessing metabolism in young and middle aged volunteers with and without the E4 allele. While IC is commonly used in clinical settings to assess nutritional status, it has never been used to assess risk for cognitive decline. Thus, repurposing IC to study the metabolic effects of an AD risk factor such as E4 represents a simple, cost-effective, and innovative new approach. We found that young female E4 carriers show a lower resting energy expenditure compared to non-carriers. We also tested how E4 carriage affects response to a glucose challenge by administering a glucose rich beverage in conjunction with IC measurements and plasma metabolomics. We found that female E4 carriers were unable to increase oxygen consumption relative to non-carriers, reflecting an impairment in glucose oxidation. Additionally, the plasma metabolome of E4 carriers showed increased lactate and an overall metabolic profile consistent with aerobic glycolysis. We translated these findings to mice expressing the human alleles of *APOE*. We found that E4 mice on a normal chow diet have lower energy expenditure than E3 mice, a difference further exacerbated by high carbohydrate diet feeding. Stable isotope tracing in mice whole brains and astrocytes

implicate increased utilization of aerobic glycolysis as a mechanism for altered glucose handling in E4 carriers. Another pathological feature of the Alzheimer's brain is glial lipid accumulation. The mechanism for this is largely unknown. In chapter 3, the literature pertaining to lipid droplets (LD) in the brain is reviewed. We show that LDs are much more than simple fat depots, playing critical roles in metabolism, inflammation, and various neurodegenerative diseases. In chapter 4, the effect of the E4 allele on astrocyte LD accumulation and turnover is assessed. Using an *in vitro* model of *APOE* we probed the storage and oxidation capacity of fatty acids in E3 and E4 astrocytes. We observed that E4 astrocytes exhibit greater storage of fatty acids as LDs under control and lipid loaded conditions compared to E3 astrocytes. Furthermore, we found that E4 astrocytes rely on these LDs as a source of fuel for oxidation. Therefore, *APOE* appears to regulate whole body energy expenditure, cerebral glucose oxidation, astrocyte LD metabolism, and risk for a host of metabolic diseases. In chapter 5, the evolutionary history of *APOE* is presented to posit a hypothesis for why E4 may be disadvantageous in modern times compared to its prior advantages in the pre-historic era. These results point toward a larger role for *APOE* in the regulation of metabolism than previously understood and advocates for alternative nutritional approaches including calorie reduction and intermittent fasting as plausible interventions to mitigate disease risk in E4 carriers.

KEYWORDS: Alzheimer's, APOE, astrocytes, metabolism, lactate, energetics

Brandon Charles Farmer

(Name of Student)

April 17th, 2020

Date

APOE AS A METABOLIC REGULATOR IN HUMANS, MICE, AND ASTROCYTES

By
Brandon Charles Farmer

Lance Johnson
Co-Director of Dissertation

Steven Estus
Co-Director of Dissertation

Kenneth Campbell
Director of Graduate Studies

April 17th, 2020
Date

DEDICATION

To my late grandmother Joyce Smoot Farmer and all other great minds that are taken far too early by Alzheimer's disease.

ACKNOWLEDGMENTS

MD/PhD training brings with it unique challenges that I do not possess the constitution to weather independently. These individuals formed my support structure and are due as much credit as I for this dissertation.

Lance, I approached you as an orphaned graduate student looking for a lab. I attempted to bribe you with pseudo-knowledge of your past publications, a promise of strong work ethic, and donuts. The bribery worked and you took a chance on me resulting in three years, three fellowships, five (six?) papers, countless lab/data/mentor meetings, poster and paper revisions, conferences, and oral presentations. But these "research products" do not compare with the training and mentorship that I have been privileged to receive as your first graduate student. The knowledge you have imparted with regards to leadership, grantsmanship, ethics, work-life balance, conflict resolution, and so many more invaluable lessons has truly shaped my scientific outlook. Your example as a PI will serve as my construct for how I manage my own laboratory one day, and if I approach any semblance of your management style I will be golden. I could not have asked for a better mentor who is so receptive to my ideas, who constructively redirects me when I need it, who supports me missing lab to go see a patient, who believes in my potential and is willing to work at 3am to ensure that I am successful. I was incredibly fortunate to stumble into your office in October 2017 and will forever be grateful for your mentorship and friendship.

To members of the Johnson Lab past and present, you created an environment that is rare in academia, one which is collaborative and socially pleasant. To DJ and Logan, the OGs, thank you for enduring my ramblings as a first year grad student who thought he had it all figured out. To Holden, thanks for being a co-graduate student that I can trust, bounce ideas off of, and academically develop with. Your humor and stories helped me to get through some tough times in grad school. To Grant, your assistance and organization of the clinical trial was pivotal to its success. To Jude, you were a workhorse for the projects in this dissertation. Your long days at the microscope, on the cryostat, reformatting of tables for the fiftieth time have paid off with dividends. I was a lucky grad student to have such a motivated and intelligent "minion" as you. Your can-do attitude will continue to serve you well, as well as your future patients. To Addie, Maggie, and Rebika you each contributed key comments, edits, or suggestions to shape this work and I am thankful for you all and excited to see what you do in the future.

I would also like to thank my committee members who helped guide me as I tackled this project. Dr. Estus, I recall finding you in your office one day as I anguished over a grant submission decision. Your calm and wise scientific input at that point, and throughout my PhD, was more valuable than you know. To Dr. Wilcock, thank you for teaching to refine ideas and ask good scientific questions. To Dr. Nelson, thank you for emphasizing the need for an appreciation of the human relevance of my work. Your example as a physician-scientist that takes time to mentor me at the microscope or in your office has impacted me and I'm grateful for that.

To my graduate student crew including Ben Shaw, Brooke Ahern, Beth Oates, Ryan Cloyd, and Laura Brown. Each of you played critical roles in the maintenance of my sanity during grad school. Through wallyball, “late-lunches” at KSR Bar, costume parties, bonfires, memes, Zoom happy hours, and Euchre games your companionship was the social outlet I needed. I am particularly thankful for Ben who taught me many fundamental research techniques in my brief stent in the Taylor Lab which I continue to rely on today.

There are not sufficient words to describe my gratitude for my parents Lisa and Charles Farmer. You enabled me to believe that I have the potential to accomplish anything, and through all of this I have only tried to do my best to make you proud of what I have done. I have felt nothing but love and support from you both as I have reached higher and gone further. I am the person, scientist, and doctor I am today because of my parents.

Mara, you likely did not know the full scope of my career when you agreed to marry me. But through your sincere commitment and love you have stuck with me despite my late nights in the office studying, my inability to think about anything but that upcoming paper, my rantings about astrocyte fatty acid metabolism, and my disgusting pictures of mice brains. You were the calming voice of reason in the darker moments of this journey where I questioned myself and my career path. You were the first person to celebrate the news of a publication or grant with me whether at two in the morning or in a Camaro on Mulholland Drive. Your constancy and your faith in me and my work has been so uplifting when I was most needed it. And though the training seems endless, and

pandemics come, and experiments fail, I will always have you. And that's what keeps me going.

TABLE OF CONTENTS

LIST OF TABLES

LIST OF FIGURES

CHAPTER 1. EFFECTS OF APOE IN NUTRITIONAL METABOLISM IN DEMENTIA

[This chapter consists of material adapted from a published manuscript: Farmer BC, Johnson LA, Hanson AJ. Effects of apolipoprotein E on nutritional metabolism in dementia. *Current Opinion in Lipidology*. 2019 Feb. PMID: 30550413]

1.1 Introduction

Apolipoprotein E (ApoE) is the major apolipoprotein in the central nervous system, responsible for lipid transport and cholesterol homeostasis. The gene that encodes ApoE (*APOE*) has three human isoforms– E2, E3, and E4 – with population frequencies of 8.4%, 77.9%, 13.7% respectively. The *APOE* gene has attracted much attention as the strongest genetic risk factor for the development of late onset Alzheimer's Disease (AD). Carriage of the E4 allele substantially raises one's risk of developing late onset AD, whereas the E2 allele is protective.(*1*) A new appreciation is forming for the role of *APOE* in cerebral metabolism of both glucose and lipid substrates. In this chapter, I will summarize recent findings in both humans and experimental *APOE* mouse models.

AD is characterized by several neuropathological hallmarks, including accumulation of extracellular amyloid plaques, intracellular tau tangles, and metabolic abnormalities including disruption of glucose metabolism and mitochondrial dysfunction.(*2*) The mechanisms by which E4 carrier status influences or causes these pathologies are still unclear, but there are likely both amyloid dependent and independent effects. Although it only differs from E3 and E2 by one or two amino acids, the structure of apoE4 protein is more compact and unstable which alters its ability to bind lipid, and in turn bind and clear amyloid breakdown products from the brain. The E4 isoform also appears to alter mitochondrial function, interfere with insulin signaling, and increase lipid

oxidation.(*2*) E4 carriers also demonstrate more pronounced and earlier defects in cerebral glucose metabolism.(*3, 4*) The effects of E4 are numerous, and many of the pathologies appear to involve cerebral energy metabolism, suggesting nutritional interventions could delay or prevent cognitive decline in these individuals.(*4*)

1.2 *APOE* influences the connection between diet and brain health

Abundant epidemiologic evidence shows high fat diets (HFD) and resultant metabolic abnormalities such as obesity and insulin resistance are risk factors for AD.(*5, 6*) Importantly, these findings are often modulated by *APOE* genotype. The association between HFD and AD in human epidemiological work is limited to E4 non-carriers in some(*7, 8*) but not all studies.(*9*) For example, we showed that acute high fat feeding improved cognition and plasma AD biomarkers in E4 carriers, but worsened these biomarkers in E4 non-carriers.(*10*) Reasons for this paradoxical response to HFD in E4 carriers is unknown, and could involve differences in transport of macronutrients, differences in lipidation status of the apoE protein, or differences in insulin and glucose metabolism.(*2, 11, 12*)

One major consequence of HFD is peripheral insulin resistance, which decreases brain insulin transport and subsequent function.(*13*) Both E4 carriers and non-carriers with AD have reduced CSF insulin and demonstrate signs of brain insulin resistance. However, the relationship between peripheral and brain insulin, and the connection between insulin resistance and brain aging, is less established in E4 carriers.(*14-16*) Similarly, E4 status influences the correlation between Aβ and insulin resistance. Only E4 non-carriers showed a correlation between CSF Aβ and CSF:plasma glucose ratio,(*15*) and showed reduced

plasma amyloid and memory improvement after an insulin infusion; E4 carriers had no changes in memory and their plasma amyloid increased in response to insulin.(*17*) Additionally, in an acute meal study, E4 non-carriers showed an increase in plasma Aβ42 after a high-fat meal compared to a high carbohydrate meal. Conversely, E4 carriers demonstrated higher plasma Aβ after the high carbohydrate meal accompanied by larger changes in insulin.(*10*) Given the brain insulin dysfunction in AD patients, insulin sensitizers and intranasal insulin are being investigated as treatments, and although the data are mixed, and the majority of these treatments improve cognition only in E4 non-carriers.(*12*)

Promisingly, healthy diets and certain nutritional factors improve cognition and reduce AD risk, but these findings are also influenced by *APOE* genotype. Perhaps the best studied diet for AD prevention is the Mediterranean (MeDi).(*18*) Most studies which have demonstrated cognitive or AD biomarker benefits of MeDi included *APOE* genotype as a covariate.(*19-21*) However, few if any have done pre-specified subgroup analyses by *APOE* status. A multicomponent interventional study involving a diet similar to MeDi showed that 2 years of a healthy Nordic diet (abundant fish, fruits and vegetables), exercise and brain training can prevent cognitive decline, although adherence to diet was not tracked and the control group also received information about the diet.(*22*) A subgroup analysis revealed that E4 carriers benefited more on tests of cognition from this intervention.(*23*) In another study, a hybrid Mediterranean diet was found to be protective against incident AD, but less protective in E4 carriers.(*24*)

Seafood intake is another dietary pattern associated with slower cognitive decline, but in one study this finding was only noted in E4 carriers.(*25*) Seafood contains high levels

of polyunsaturated fatty acids, or PUFAs, including DHA and EPA, and high intake of these nutrients is protective against AD. Despite the stronger protective effect of seafood in E4 carriers, studies specifically examining PUFAs show more benefit in non-carriers. In an intervention study in older adults, E4 non-carriers who received DHA for 18 months declined significantly less on a cognitive test compared to placebo, whereas DHA had no effect on E4 carriers.(*26*) In another study, there was a stronger association between fish consumption and increased plasma DHA levels in E4 non-carriers, whereas in E4 carriers there was a positive association between meat and DHA.(*27*) Follow-up studies have suggested several potential mechanisms, including decreased lipoprotein lipase activity and differential fatty acid processing, increased VLDL turnover, or higher levels of lipid peroxidation and beta-oxidation in E4 carriers.(*27, 28*) How these peripheral differences affect brain transport and utilization of PUFAs and other FFA remains unknown. (*27, 28*)

Since patients with AD have decreased cerebral glucose metabolism, diets and pharmacologic agents which induce ketosis and supply the brain with ketone bodies are being investigated as treatments.(*29*) Although E4 carriers have more pronounced and earlier cerebral glucose dysregulation, only E4 non-carriers with AD responded to a ketosis-inducing medium-chain triglyceride supplement. The authors speculated that the mitochondrial dysfunction in E4 carriers, renders this group less able to use ketone bodies in lieu of glucose for brain fuel; alternatively there could be differences in ketone body brain transport.(*30*)

The evidence continues to accumulate around the idea that *APOE* genotype influences cognitive and neurological responses to diet and dietary supplements. To understand the pathophysiology of diet and dementia risk, *in vitro* and *in vivo* mouse

models serve as ways to examine these mechanisms more carefully. As noted above, HFD and resultant metabolic abnormalities have been identified as risk factors for AD.(*5, 6*) The saturated FFA palmitate induces inflammation in cell lines and AD animal models.(*31, 32*) However most human cell lines are studied without respect to *APOE* status, and the most utilized rodent models of AD which have provided much of the data for the experimental link between dietary factors and AD pathology are analogous to E4 non-carriers.(*33*) However, new models of human induced pluripotent stem cells (iPSC) edited to include *APOE3* and *APOE4* hold promise, and recent studies have demonstrated important differences in function with respect to lipid and cholesterol metabolism in neuronal- and glial-derived iPSCs.(*34*) In the next sections we will discuss how humanized *APOE* mice can help us better understand the differences we are seeing *in vivo*, in particular the response to high fat diets and lipid-based therapies in E4 carriers.

1.3 Knowledge and tools available to study *APOE* effects on nutritional metabolism in dementia

Research into the effect of *APOE* on nutritional metabolism has often relied on mouse models as a correlate for human disease. While several mouse models of human *APOE* exist (Table 1.3.1), the most widely used are the targeted replacement (TR) mice developed by Sullivan et al in the laboratory of Dr. Nobuyo Maeda. These mice were created by mating C57BL/6J mice with chimeras whose embryos had been injected with embryonic stem cells electroporated with human *APOE2, APOE3, or APOE4* constructs.(*35*) The vector was inserted at the normal murine *APOE* locus to maintain physiologic expression of the human variant. The metabolic profiles of these mice have

been explored by many groups, specifically with respect to how they differ from wild type mice and humans.

While 5-10% of human E2 homozygotes develop type II hyperlipoproteinemia, all E2 TR mice display features of it, including spontaneous atherosclerosis, xanthomas, and decreased VLDL clearance.(*36*) It has been hypothesized that this is due to the low affinity of E2 for the main VLDL receptor, LDLR. While humans are able to clear VLDL through apoE independent mechanisms (apoB100-LDLR interactions) mice are wholly dependent on apoE for clearance, and thus magnify functional differences in the apoE isoforms. While the abnormal lipid profile confounds studies of E2's lipid associated role in mitigating AD risk, the model is still useful for probing alternative roles of E2. For example, some have posited that E2 provides a metabolic advantage and thereby decreases AD risk. Venzi and colleagues found E2 mice to exhibit a significant increase in cerebral glucose metabolism beyond 3 months of age. Compared to E3 mice at 6 months, E2 mice showed increased glucose uptake by [$_{18}$F]FDG imaging in whole brain, cingulate cortex, cortex, and hippocampus and then a global increase at 9 months of age.(*37*) However, the first comprehensive human study to examine E2 carriers with [$_{18}$F]FDG imaging showed that age-related decreases in glucose uptake did not significantly differ from E3 individuals.(*38*) Thus, the cerebral metabolic effects of E2 remain an important, but unsettled issue.

The E3 and E4 TR mice also express their human isoforms at physiologic levels.(*35, 36, 39*) They are normolipidemic but become hyperlipidemic in response to a westernized diet.(*36, 40*) While E4 confers a higher risk of dementia in humans, it is controversial what cognitive effects are present in in TR E4 mice (in the absence of amyloid or tau over

expressing mutations). Rodriguez and colleagues observed impairments in spatial learning and memory in young E4 TR mice in the Barnes maze test, but no difference in a hidden platform water maze experiment.(*41*) In contrast to mixed effects of E4 on behavioral outcomes and age-related cognitive decline, the association of E4 with cerebral metabolic changes is more clear. Several groups have demonstrated reductions in cerebral glucose uptake in E4 mice compared to mice expressing E3 (*42-44*) – similar to the well-established findings via FDG PET in human E4 carriers.

In humans, E4 carrier status is associated with a higher brain amyloid burden, but it has been more difficult to demonstrate this in E4 mice unless other AD-related genes are present.(*11*) When AD mice are crossed with *APOE* knockout mice, the resultant phenotype is less amyloid depositions, suggesting that the apoE protein is necessary for amyloid breakdown products to cause plaques. AD mice that express human *APOE* alleles do recapitulate what is seen in humans with more amyloid in E4 compared to E3, and less still in E2.(*45*) One important difference that may affect amyloid burden studies is that humanized E4 is less stable in mouse brain and is degraded, whereas this does not appear to be the case in humans.(*11, 46*)

As glucose uptake and utilization is impaired in E4 carriers and AD individuals, many groups have studied the insulin-signaling pathway as a potential target of *APOE* modulation. Hippocampal RNA from middle-aged female E2, E3, and E4 TR mice was arrayed for genes involved in insulin signaling. This revealed that E2 mice have higher levels of Igf1, insulin receptor substrates, and the glucose transporter GLUT4 than E3 and E4.(*47*) Furthermore, E4 mice showed a significant decrease in PPAR-gamma and insulin-degrading enzyme, pointing to a further compromise of insulin signaling and glucose

utility. These findings were confirmed by another group who used an array for glucose and ketone body metabolism and identified glucose transporters and hexokinases were robustly altered by *APOE* genotype.(*48*) The Bu group discovered that E4 restricts insulin receptors to endosomes and thereby impairs trafficking and signaling, an effect exacerbated by HFD.(*49*) To test the effect of *APOE* on peripheral insulin receptor sensitization, To et al. fed E3 and E4 mice a diabetogenic diet then treated the mice with a thiazolidinedione. They found a reduction in tau phosphorylation, but only in E3 mice.(*50*) These studies support the idea that E4 renders the brain insulin resistant, likely through regulation of insulin receptors and glucose transporters.

Despite growing evidence for a role of diet in AD and the potential of personalized medicine and gene-diet interactions, very few studies have attempted to tackle the interaction between *APOE* and diet in the context of AD or cognitive function. Our group explored the potential interactive effects of diet and E4 on cognition by using a mouse model of chronic high fat feeding. We found that disruption of glucose homeostasis following 6 months of HFD led to more pronounced cognitive impairments in E4 compared to E3 mice. These cognitive deficits were specific to hippocampal-dependent spatial learning and memory outcomes, and were accompanied by wide-ranging isoform-specific alterations in the epigenetic landscape and changes in cerebral metabolism.(*51*) It is hypothesized that its effects on cerebrovascular function could be the driving force of the cognitive impairing effects of HFD. We found that E4 mice fed a HFD exhibit reduced glucose uptake compared to both E4 mice on a control diet and E3 mice on both control and HFD.(*51*) Further, E4 carriage and HFD acted synergistically to lower cerebral blood flow.(*43*) Interestingly, when challenged with an acute glucose bolus, E4 but not E3 mice

responded beneficially in terms of both increased blood flow and enhanced performance in a memory task; hinting at a potential role for *APOE* in modulating neurovascular coupling and cognitive function. (*43*)

In the APP mouse model of distorted amyloid processing, expression of E4 along with a HFD significantly increases amyloid deposition compared to E3.(*52*) E4 was also found to increase amyloid and glial activation in the EFAD model of AD when fed a westernized diet. (*53*) E3 mice gain more weight on a HFD, while E4 mice seem to upregulate genes involved in fatty acid mobilization and utilization in the periphery.(*54*) This could parallel a central E4 promoted HFD induced bioenergetic shift toward fatty acids and away from glucose as the primary cerebral energy source. Together, these studies show that E4 seems to exacerbate the negative effects of a HFD on cognition.

1.4 Conclusions

As we continue to uncover the role of the *APOE* gene as a contributor to cognitive decline, we must take into account the additive effects that the westernized high fat diet and insulin resistance seem to have on disease progression. Human epidemiologic and experimental evidence suggests that *APOE* genotype changes the relationship between several lipid-related macronutrients and markers of brain health and cognition. Whether it is diet-induced insulin resistance, PUFAs from fatty fish, or ketone bodies from medium chain triglycerides, *APOE* status appears to modulate important responses to lipid-related therapies. Mouse models have been vital in confirming that E4 exacerbates the negative cognitive effects of diabetogenic and HFD, and also suggest reasons by which E2 carriers are less susceptible to developing AD. Future studies should utilize these and other

experimental models of *APOE* to implicate specific cells and tissues in the E4 response to nutritional interventions, and include *APOE* genotype as an important subgroup for analysis of human interventions.

Table 1.1 Summary of *APOE* Models by Expression and Original Report or Source

Model	**APOE Expression**	**Original Study**
Targeted Replacement Mice	Global E2, E3, E4	Sullivan et al. 1997(*35*)
NSE Promoter	Neuron	Raber et al. 1998(*55*)
GFAP Promoter	Astrocyte	Sun et al. 1998
Dox Inducible	Cell specific	Liu et al. 2017(*56*)
APOE* KI mice	Global E2, E3, E4	Jackson Laboratory
hApoE4 Knock-in Rat	Global E4	Horizon Discovery
hApoE Knock-in Fly	Global E3, E4	Haddadi et al. 2016(*57*)

CHAPTER 2. APOE4 LOWERS ENERGY EXPENDITURE BY INCREASING FLUX THROUGH AEROBIC GLYCOLYSIS

[This chapter consists of material adapted from a submitted manuscript that is under review. For supplementary materials pertaining to this chapter, see appendix 1.]

ABSTRACT

Cerebral glucose hypometabolism is consistently observed in individuals with Alzheimer's disease (AD) and also in young cognitively normal carriers of the E4 allele of Apolipoprotein E (*APOE)*. As E4 is the strongest genetic predictor of late-onset AD, identifying other metabolic signatures of young E4 carriers may provide insight into disease mechanisms and early screening criteria for AD. Here, we perform the first assessment of whole body energy expenditure (EE) in young and middle-aged human participants with and without the E4 allele. Strikingly, young female E4 carriers show a lower resting EE than non-carriers - a phenomenon exaggerated following a dietary glucose challenge due to stunted oxygen consumption. This E4 effect was not observed in middle-aged individuals, suggesting an "early-aged" E4 phenotype of oxidative impairment. When given a cognitive challenge, EE increased in all study volunteers, representing a strong cerebral contribution to EE. Plasma metabolites associated with glycolysis were elevated in E4 carriers and pathway analyses revealed a glucose-induced increase in aerobic glycolysis (i.e. the Warburg effect). Isotopic tracing of ^{13}C-glucose in mice and astrocytes expressing human *APOE* showed E4-associated increases in lactate synthesis and decreased pyruvate entry into the TCA cycle. Finally, E4 astrocytes had elevated glycolytic activity, decreased oxygen consumption, blunted oxidative flexibility, and a lower rate of glucose oxidation in the presence of lactate. Together, these results suggest system-level

metabolic reprogramming in young E4 carriers, an endophenotype observable by indirect calorimetry and plasma metabolomics decades prior to clinically manifest AD.

2.1 Introduction

The E4 allele of Apolipoprotein E (*APOE*) confers more risk for the development of late-onset Alzheimer's disease (AD) than any other gene (*58, 59*). While E4 is a strong contributor to late-onset AD risk, the effect is even greater in females (*60*). Female E4 carriers have an increased odds ratio for AD (*61*), increased incidence of AD (*62*), elevated hazard ratio for conversion to mild cognitive impairment (*63*), increased CSF tau (*64*), and reduced hippocampal volume (*65*), compared to male E4 carriers. To date, studies investigating the mechanism by which E4 and sex increase disease risk have primarily focused on the important associations of E4 with the neuropathological hallmarks of AD – i.e. the increased amyloid load seen in E4 carriers (*66, 67*) and the *APOE*-dependence of tau propagation (*68, 69*).

Alternatively, investigating E4 carriers who have not yet developed neuropathology may provide insight into early E4 mechanisms and unveil additional risk factors for AD. For example, an early and consistent biological hallmark of AD is cerebral glucose hypometabolism as observed by ^{18}F-fluorodeoxyglucose positron emission tomography (FDG-PET) imaging (*70-72*). Interestingly, E4 carriers also display an AD-like pattern of decreased glucose metabolism by FDG-PET long before clinical symptomology (*3, 73*). Since glucose hypometabolism occurs early in AD and early in E4 carriers, it may represent a critical initial phase of AD pathogenesis that predisposes individuals to subsequent symptomology. Beyond this FDG-PET finding, it is not clear if *APOE* has other

discernable metabolic effects in pre-cognitively impaired young people. Studying *APOE*'s association with glucose metabolism in E4 carriers decades prior to disease onset may be beneficial in designing early interventions for the metabolic derangements of AD.

In contrast to the robust FDG-PET literature, clinical research focused on how *APOE* may regulate metabolism outside of the brain is limited (*74*). Most studies have utilized a targeted replacement mouse model of *APOE* in which the murine *Apoe* alleles are replaced by the human orthologs (*35, 75*). For example, several studies have found E4 mice to exhibit increased susceptibility to insulin resistance, and one report characterized E4 mice as deficient in extracting energy from dietary sources (*49, 51, 54*). While these preclinical studies have been critical to our understanding of E4-associated impairments in glucose metabolism, the extent to which systemic glucose metabolism is regulated by *APOE* in young healthy humans is largely unknown.

Energy expenditure (EE) is defined as the energetic cost of processes essential for life. Indirect calorimetry (IC) assesses EE by measuring metabolic gases to calculate the energy released when substrates are oxidized, and is the gold standard in the clinical setting to assess nutritional status and dietary needs (*76*). The Weir equation ($EE = 3.9 * VO_2 + 1.11\ VCO_2$) estimates EE with the assumption that anaerobic respiration is negligible and substrates are fully oxidized to CO_2 (*77*). This assumption is confounded when energy is derived through non-oxidative processes such as aerobic glycolysis - when glucose is metabolized to the non-oxidative metabolite lactate rather than pyruvate despite normoxia (*78*). Increased flux through glycolysis also decreases EE since only 2 ATP are produced via glycolytic substrate level phosphorylation in contrast to the 34 ATP from oxidative

phosphorylation. Therefore, individuals who undergo extensive aerobic glycolysis show a low EE due to less oxygen consumption and less ATP turnover.

Here, we use IC to study *APOE* genotype-dependent metabolic phenotypes in healthy, cognitively normal young and middle-aged individuals. We observe that young E4 carriers expend significantly less energy at rest and exhibit greater utilization of the aerobic glycolysis pathway, as evidenced by elevated lactate abundance in the plasma metabolome. Additionally, E4 carriers and E4 mice displayed an inability to increase oxygen consumption after a high carbohydrate challenge – a sign of oxidative impairment consistent with aerobic glycolysis (*79*). *In vitro* studies in astrocytes indicate that these energy detriments are a result of increased glycolytic flux, thereby increasing lactate production at the expense of oxidative metabolism. Together, these findings point to a role for *APOE* as a critical regulator of systemic glucose metabolism.

2.2 Methods

2.2.1 Study Design

The study objectives were to i) determine if *APOE* genotype influences peripheral and cerebral metabolism in young cognitively normal human subjects, and if so, ii) elucidate potential mechanisms using mouse and cell models of human *APOE*. For the clinical research study, healthy volunteers between 18-65 were prescreened for diagnoses that may affect cognitive function (ex. stroke, Parkinson's), metabolic diseases (diabetes), alcoholism, drug abuse, chronic major psychiatric disorders, medications that interfere with cognition (narcotic analgesics, anti-depressants), medications that interfere with EE (stimulants, beta-blockers) and vision or hearing deficits that may interfere with testing.

The prescreening checklist with a full list of medications and conditions excluded for can be found in the supplemental materials. Eligible candidates were brought in for informed consent after a 12-hour fast in which subjects were asked not to exercise and to abstain from everything except for water. We employed a power analysis based on a feasibility study, and the required sample size per group for a power level of 0.9 was calculated to be n = 30 per "group" (i.e. E2+, E3/E3 and E4+), for a total of 90 subjects. To account for potential biological outliers, non-consenting subjects, and post-recruitment exclusion criteria being met, we recruited a total of 100 individuals for this observational study. Six individuals who had IC values more than 2 standard deviations from the mean were excluded from analysis leaving 94 individuals for analysis. As we were primarily interested in *APOE* effects in young individuals, we stratified our sample population into a young cohort (under 40 years old) and a middle-aged cohort (40-65 years old). We chose 40 as the age-cutoff based on a meta-analysis of *APOE* genotype and AD-risk which found the E4 effect on disease to be observable in individuals 40 and over (*61*). Data acquisition was blinded as *APOE* genotypes were determined after the study.

2.2.2 Human study

Body mass index (BMI), waist to hip ratio, and blood pressure were first recorded. Thereafter, participants were fitted with an airtight mask that was connected to an MGC Diagnostics Ultima CPX metabolic cart which measures VO_2, VCO_2, and respiratory rate. EE is defined as the amount of energy an individual uses to maintain homeostasis in kcal per day, and can be calculated using the Weir equation ($EE = 1.44\ (3.94\ VO_2 + 1.11\ VCO_2)$) (*77*). EE is composed of the resting energy expenditure (REE), the thermic effect of feeding

(TEF), and activity related energy expenditure (AEE). In motionless and fasted humans, EE is equivalent to the REE since the TEF and AEE have been controlled for. Participants were instructed to remain motionless and to refrain from sleep for 30 minutes as data was gathered. All testing occurred between 8:30-11:30 am in a temperature controlled (20–22 °C) out-patient research unit (Center for Clinical and Translational Science, University of Kentucky). Body temperature was taken periodically via temporal thermometer to ensure thermostasis and provide intermittent stimulation to ensure wakefulness. After the resting period came a 30 minute cognitive test period. We then introduced a novel-image-novel-location (NINL) object recognition test consisting of a series of images which participants were later asked to recall. This test has been shown previously to study *APOE* allele effects on cognition (*80*). After the cognitive test period, a blood draw was taken via venipuncture and placed on ice. Participants then consumed a sugary milk drink consisting of 50g of sugar dissolved in whole milk. The drink was consumed within a two minute time span. The mask was then refitted and participants were instructed to again remain motionless for 30 minutes for data collection. Data from the first 5 minutes of the study time periods were excluded to allow a five minute steady state adjustment (*81, 82*). After the glucose challenge, participants provided a second blood sample (~45 minutes after the initial blood draw). Participants then exited the study and were compensated for their participation. This study was approved by the University of Kentucky Institutional Review Board (#48365) and was listed as Clinical Trial #NCT03109661.

2.2.3 Genotyping

APOE genotype was determined by extracting genomic DNA from participants' blood samples using a GenElute Blood Genomic DNA Kit (Sigma). After confirming concentration and quality by Nanodrop, *APOE* genotype was determined using PCR with TaqMan assay primers for the two allele-determining SNPs of *APOE*: rs7412 and rs429358 (Thermo). Positive controls for the six possible *APOE* genotypes were included with each assay.

2.2.4 Plasma metabolomics

Plasma was separated from blood by centrifugation at 2500 x *g* for 10 minutes at 4°C, and stored in 200uL aliquots at -80°C until further use. Upon thawing, ice cold 100% methanol solution containing 40nM L-norvaline (internal standard) was added to 80 ul of plasma and kept on ice for 20 minutes with regular vortexing. The solution was then centrifuged for 10 minutes (14,000 rpm, 4°C). Supernatant containing polar metabolites was removed to a new tube and kept at -80°C until prepped for GCMS analysis (additional details in Supplemental Methods).

2.2.5 Mice

Mice expressing human *APOE* display many of the phenotypic characteristics observed in humans including several metabolic variations noted in epidemiological studies (*83-85*). In this "knock-in" model, the mouse *Apoe* locus is targeted and replaced with the various human *APOE* alleles, thereby remaining under control of the endogenous

mouse *Apoe* promoter and resulting in a physiologically relevant pattern and level of human APOE expression (*3, 36, 86-89*). Mice used in this study were homozygous for either the human E3 or E4 alleles, aged 2-4 months (young) and housed in sterile micro-isolator cages (Lab Products, Maywood, NJ), and fed autoclaved food and acidified water ad libitum. Animal protocols were reviewed and approved by the University of Kentucky Institutional Animal Use and Care Committee.

2.2.6 Metabolic phenotyping

Human E3 and E4 mice were evaluated by indirect calorimetry (TSE Systems, Chesterfield, MO). Mouse body composition was measured using EchoMRI (Echo Medical Systems, Houston, TX) the morning prior to being singly housed in the indirect calorimetry system. Mice were acclimated to singly housed cage conditions for one week prior to beginning data recording. After five days on standard chow diet (Teklad Global 18% protein rodent diet; 2018; Teklad, Madison, WI), mice were fasted overnight before being introduced to a high carb diet (Open Source Diets, Control Diet for Ketogenic Diet with Mostly Cocoa Butter, D10070802) for five days. Mice were monitored for O_2 consumption, CO_2 production, movement, and food and water consumption. Chambers were sampled in succession and were reported as the average of 30 minute intervals in reference to an unoccupied chamber. To negate the effects of activity on EE readouts, we chose to only analyze the light cycles of the mice where activity, and feeding, is minimal. The EE then becomes analogous to a "resting" EE similar to the resting period in the human study and differences observed are likely due to basal metabolic rate differences instead of confounding factors such as feeding and activity (*90*).

2.2.7 Cell culture

Primary astrocytes were isolated from postnatal day 0-4 pups of mice homozygous for E3 or E4. The brain was surgically excised and meninges were removed from cortical tissue in cold DMEM. Tissue from pups of the same genotype was pooled and coarsely chopped to encourage suspension. Tissue homogenates were incubated in serum free DMEM with 0.25% trypsin and DNAse for 30 min with gentle shaking. Cell suspension was then filtered through 40 µm strainer and spun for 5 min at 1100 x *g*. Suspended primary cells were then plated in a poly-lysine coated plate and allowed to grow to confluency in Advanced DMEM (Gibco) with 10% FBS. Immortalized astrocytes were derived from targeted replacement mice expressing human *APOE* alleles (kind gift from Dr. David Holtzman). These immortalized cell lines secrete human ApoE in HDL-like particles at equivalent levels to primary astrocytes from targeted replacement *APOE* knock-in mice and have been relied upon for studies of *APOE*'s role in astrocyte metabolism by several groups (*91-93*). Cells were maintained in Advanced DMEM (Gibco) supplemented with 1mM sodium pyruvate, 1X Geneticin, and 10% fetal bovine serum unless otherwise noted.

2.2.8 Statistical analysis

All results are reported as mean +/- SEM unless otherwise stated. For comparisons between two groups, an unpaired two-tailed Student's *t*-test was used. For pair-wise comparison of two time points a paired two-tailed Student's *t*-test was used. One-way analysis of variance (ANOVA) was used for comparing multiple groups followed by Sidak's multiple comparisons test. Two-way ANOVA with repeated measures was used

for time course analysis. Pearson r correlation test was used for correlative analysis. For dependent variables with categorical independent variables we analyzed covariance (ANCOVA) to assess collinearity. $P<0.05$ was considered significant.

2.3 Results

2.3.1 Young female E4 carriers have a lower resting energy expenditure

We first used IC to test the effect of *APOE* on whole body metabolism in a cohort of healthy volunteers (Tables 2.1 and 2.2). Using a mobile metabolic cart designed to measure VO_2 and VCO_2, we assessed volunteers at rest, during a cognitive task, and after a glucose challenge (Fig 2.1A, Fig S1). Blood samples were collected before and after the glucose challenge to determine *APOE* genotype and to quantify metabolite abundance by mass spectrometry (Fig 2.1B, Table S1).

We began each session by assessing the resting energy expenditure (REE) and respiratory exchange ratio (RER) of participants. After a five-minute buffer to achieve steady state (*81, 82*), we recorded REE over a 25 minute period at 15 second intervals and averaged the RER and REE for each individual. There was no *APOE* effect on RER (Fig S2). Consistent with previous studies, we found REE and age to be negatively correlated (Fig 2.1C). However, when we stratified our analysis by E4 status, linear regression revealed significantly different slopes between E4 carriers and non-carriers. While E4 non-carriers fit the overall correlation of age and REE, E4+ individuals did not fit this model and showed no deviation from the zero slope (Fig 2.1D), suggesting an E4-associated confound in the age versus energy expenditure relationship.

To determine if the E4 effect on REE was age dependent, we separated E4+ and E4- individuals into young (<40 years of age) and middle aged (40-65 years of age) cohorts based on previous literature (*3, 61*). To account for known influences on energy expenditure, we performed one-way analysis of covariance (ANCOVA) using average REE values as the dependent variable, E4 status as the independent variable, and age, sex, lean body mass (LBM), and body mass index (BMI) as covariates. After adjusting for the covariates, we observed a significantly lower REE in female E4 carriers compared to non-carriers, particularly in the young cohort (Fig 2.1E). This E4 effect on REE was not significant in males (Fig S3A-B). Together, these data suggest that there is no age-related REE decline in E4 carriers, and that the REE-*APOE* interaction is modified by sex, with female E4 carriers displaying lower REE.

2.3.2 E4 does not alter cognitive energy expenditure

We next tested if a cognitive intervention would reveal further *APOE* genotype-specific differences in EE. To avoid potential confounding readouts of movement, subjects were asked to remain perfectly still while completing a challenging Novel Image Novel Location test (Fig S1C). We observed a significant increase in average EE during the cognitive challenge in all subjects, regardless of age or *APOE* status (Fig 2.1F). To assess cognitive energy expenditure (CEE), we determined the max EE during the cognitive test period and subtracted the average REE for each subject. We found no difference in CEE, nor in test response accuracy, between E4 carriers and non-carriers (Fig 2.1G, Fig S4).

2.3.3 Female E4 carriers have a lower thermic effect of feeding and fail to increase VO_2 after a glucose drink

We next sought to measure the thermic effect of feeding (TEF) - a constituent of EE that indicates the energy used to absorb, digest, and metabolize dietary energy (*94*, *95*). To induce TEF, all participants consumed a high carbohydrate drink in less than two minutes (Fig S1D). Energy expenditure during the dietary challenge increased significantly in all participants (Fig 2.1H). To account for covariates during the glucose period, we performed two-way ANCOVA using time and IC values as dependent variables, E4 status as the independent variable, and age, sex, LBM, and BMI as covariates. TEF was calculated by subtracting the average REE from the maximum of EE after the glucose challenge for each subject. Similar to resting EE, female E4 carriers displayed a significantly lower TEF than non-carriers, particularly in the young cohort (Fig 2.1I).

We next sought to understand if there were *APOE*-dependent alterations in VCO_2 and VO_2 in the response to the glucose challenge. Plotting the time course of EE after participants consumed the glucose drink revealed a dramatically blunted EE response in E4+ subjects (Fig 2.2A). Further stratification by individual genotypes showed a clear stepwise effect of *APOE* (Fig 2.2B). Plotting the VCO_2 values revealed a similar, but non-significant trend of lower CO_2 production in E4 carriers (Fig 2.2C-D). Analyzing the rate of change in VO_2, we observed that while non-carriers significantly increased their oxygen consumption following the glucose drink, E4 carriers did not, as noted by a non-significant slope deviation from zero (Fig 2.2E). Additionally, the AUC of VO_2 showed significant differences by E4 carrier status and individual genotypes (Fig 2.2F).

We found the E4 effect on EE and VO_2 to be significant and independent of age, BMI, and LBM. Interestingly, when we stratified by sex we observed that the covariate-adjusted E4 effect on EE and VO_2 was significant in females but not in males, again suggesting a sex-specific phenomenon (Fig S5). As EE is calculated based on VCO_2 and VO_2 values, these results likely reflect decreased oxidation of the glucose drink in female E4 carriers.

2.3.4 Targeted metabolomics reveals glycolysis as a differentially regulated pathway in E4+ plasma

To determine if the observed *APOE* differences in energy expenditure were reflected in the plasma metabolome, we conducted a targeted metabolomics analysis of human plasma samples before and after the glucose challenge (Table S1). A pathway analysis of the plasma metabolome before the glucose drink highlighted E4-associated differences in glycolysis and pyruvate metabolism (Fig 2.3A). Further analyses of individual metabolites revealed lactate as the metabolite most strongly affected by E4 carriage (Fig 2.3B). Indeed, E4 carriers displayed dramatically higher plasma lactate concentrations before and after the glucose drink (Fig 2.3C; Fig S6). Following the glucose challenge, there was an increase in the number of carbohydrate processing pathways and metabolites that were differentially altered in E4 carriers (Fig 2.3D-E). A pathway enrichment analysis highlighted multiple E4-associated changes, with top hits including “Warburg effect” and “Transfer of acetyl groups into mitochondria” (Fig 2.3F). Together, analysis of the plasma metabolome from cognitively normal young and middle-aged E4+ individuals suggests a preference for aerobic glycolysis compared to non-carriers.

2.3.5 E4 mice fail to increase energy expenditure on a high carbohydrate diet

We next asked if the metabolic effects of *APOE* on EE would translate to a humanized mouse model of *APOE*. Since mouse IC cages allow for a prolonged and controlled assessment of metabolism, we provided a long-term glucose challenge by way of a high carbohydrate diet (HCD). Similar to the decreases observed in E4 humans, young mice carrying the human E4 allele exhibited significantly lower EE, VCO_2, and VO_2 compared to young E3 mice during their inactive period (light cycle) (Fig 2.4A). Following introduction of a HCD, these decreases were exaggerated; E4 mice again showed substantially lower EE, VCO_2, and VO_2 compared to E3 mice (Fig 2.4B).

We next analyzed the HCD-induced change in EE, VCO_2, and VO_2 from baseline (normal chow). We found both genotypes to show significant positive changes except for E4 VO_2 (Fig 2.4C), suggesting that E4 mice fail to increase oxygen consumption in response to excess dietary carbohydrates. These changes occurred independently of differences in activity and food intake, as there was minimal activity or feeding during the light cycle (the period used for analysis) in both groups (Fig S7A-B). Further, ANCOVA revealed dissimilar correlations between body weight and EE between genotypes indicating the variability in EE cannot be explained by body weight (Fig S7C). These data suggest that E4 acts in young mice to lower EE via a mechanism outside of the typical contributions of feeding, body mass, and activity.

2.3.6 Stable isotope resolved metabolomics (SIRM) reveals increased lactate synthesis and decreased entry into the TCA cycle in E4 brains and astrocytes

Given the decreased VO_2 observed in E4 mice and humans and increased plasma lactate concentrations in E4+ subjects, we hypothesized that these individuals were diverting a higher fraction of glucose to aerobic glycolysis as opposed to oxidative phosphorylation. To test this, we employed ^{13}C tracer metabolomics to quantitatively assess glucose utilization in mice and primary astrocytes expressing human *APOE* (Fig 2.5A). Fasted E3 and E4 mice were administered an oral gavage of fully labeled [U-^{13}C] glucose and brain tissue was collected 45 minutes later for mass spectrometry analysis of ^{13}C enrichment in central carbon metabolites. The brains of E4 mice showed significantly higher ^{13}C-lactate (fully labeled, m+3) compared to E3 mice (Fig 2.5B). Additionally, enzyme activity measures of pyruvate dehydrogenase (PDH) – the primary entry point for pyruvate into the TCA cycle via acetyl-CoA – showed a trend toward lower activity in E4 compared to E3 brain tissue, while lactate dehydrogenase (LDH) – the enzyme responsible for interconversion of pyruvate and lactate – showed a trend toward higher activity (Fig 2.5C).

As astrocytes are the primary source of both cerebral lactate (*96*) and ApoE (*89*), we next utilized SIRM to measure glucose utilization *in vitro* in primary astrocytes expressing human *APOE*. E4 astrocytes showed a significant increase in both LDH activity and in ^{13}C-glucose conversion to lactate (Fig 2.5D-E), and as expected, lactate generation was higher in this glycolytic cell type compared to whole brain homogenates (Fig 2.5B). Conversely, E4 astrocytes displayed substantially lower ^{13}C enrichment of TCA intermediates, suggesting decreased glucose entry into the TCA cycle (Fig 2.5F). To

confirm these results, we performed an independent ^{13}C-glucose tracing experiment in immortalized astrocytes expressing human E3 or E4 (*97*) and quantified ^{13}C-lactate production using nuclear magnetic resonance spectroscopy (Fig 2.5G-H). Again, E4 astrocytes showed significantly higher lactate synthesis, as evidenced by increased ^{13}C-lactate both intracellularly and in the media (Fig 2.5I). Together, these data describe an E4-associated increase in glucose flux into late glycolysis at the expense of entry into the TCA cycle for oxidative phosphorylation.

2.3.7 E4 astrocytes exhibit impairments in glucose oxidation

To functionally assess glycolytic flux *in vitro,* we measured the extracellular acidification rate (ECAR, a marker of glycolysis and lactate export) before and after glucose injection (Fig 2.6A). E4 astrocytes displayed significantly higher ECAR after addition of glucose compared to E3 astrocytes, suggesting these cells shunt more glucose to lactate (Fig 2.6A). Furthermore, E4 astrocytes showed a higher glycolytic capacity, as shown by a heightened ECAR response to oligomycin - an inhibitor of mitochondrial respiration (Fig 2.6B). We then measured glucose oxidation by assessing the oxygen consumption rate (OCR). E4 astrocytes displayed significantly lower OCR both before and after addition of glucose to the media, suggesting an inherent reduction in oxidative metabolism in E4 astrocytes relative to E3 (Fig 2.6C-D). Together these results further confirm an E4-associated shift toward glycolysis (Fig 2.6E).

We next measured glucose oxidation by treating astrocytes with radiolabeled ^{14}C-glucose and capturing the oxidative product $^{14}CO_2$. E4 astrocytes oxidized less glucose to CO_2 compared to E3, but only when the radiolabel ([nM]) was given with a substantial

amount of non-labeled glucose ([mM]) (Fig 2.6F). E4 astrocytes also displayed decreased capacity and flexibility in regards to glucose oxidation, as they were relatively unable to increase glucose oxidation when other fuel sources (fatty acids and glutamine) were inhibited (Fig 2.6G). We reasoned that lower rates of glucose oxidation in a glucose rich environment in E4 cells may be due to increased conversion of glucose to lactate, which in turn inhibits downstream oxidative processes (*98*). Therefore, we tested glucose oxidation following lactate supplementation, and found that E4 astrocytes oxidize less glucose in the presence of lactate than E3 astrocytes (Fig 2.6H). Together, these results suggest that E4 astrocytes exhibit increased reliance on aerobic glycolysis and are less flexible and less able to oxidize glucose, a phenotype seemingly exacerbated by a high glucose environment or the presence of lactate.

2.4 Discussion

In the current study, we used indirect calorimetry to show that *APOE4* reduces energy expenditure in a cohort of young cognitively normal females, a phenomenon exacerbated by a dietary glucose challenge. Analysis of the plasma metabolome revealed E4-associated increases in pathways related to carbohydrate processing, specifically aerobic glycolysis, highlighted by higher concentrations of the glycolytic end-product lactate. By applying stable isotope-resolved metabolomics *in vivo* and functional assays of cellular respiration *in vitro*, we discovered that both E4 expressing mouse brains and E4 expressing astrocytes increase glucose flux through aerobic glycolysis at the expense of TCA cycle entry and oxidative phosphorylation. Cumulatively, these data highlight a

novel mechanism whereby E4 lowers energy expenditure in young women and decreases glucose oxidation by redirecting flux through aerobic glycolysis.

Detecting early symptoms of eventual cognitive decline is important for primary prevention of AD (*99*). Drugs advanced as potential AD therapeutics have targeted pathways associated with neuropathology, such as tau anti-sense oligonucleotides and amyloid-directed monoclonal antibodies (*100*). Given the largely disappointing trial outcomes, these therapies may be intervening after a 'point of no return' and thus offer minimal benefit in prognosis (*101*). In order to design therapies for early interventions in those at risk for AD, we must first identify measurable biomarkers whose severity and/or change over time correlate with risk for clinically observable AD. One such early biomarker of eventual AD onset is low cerebral metabolic rates for glucose (CMRglc).

APOE, the strongest genetic risk factor for late-onset AD, is now recognized as a strong modulator of cerebral metabolism, with E4+ individuals demonstrating metabolic alterations congruent with AD patients (*4*). Even cognitively normal E4 carriers demonstrate this pattern of glucose hypometabolism, thereby lending support to decreased CMRglc being an inherent biological feature of E4, rather than simply a byproduct of dementia (*102-104*). Importantly, these metabolic deficits are present decades in advance of AD onset in E4+ individuals, evidenced by reductions in CMRglc observed as early as their 20s (*3*). While lower CMRglc is measurable in young E4 carriers, a need exists for identification of other measurable metabolic alterations associated with *APOE* and glucose metabolism. Impairments in systemic metabolism are also strongly inversely correlated with CMRglc (*105*), suggesting that peripheral and brain metabolism are tightly coupled.

Thus, we hypothesized that whole body energy expenditure (EE) may be a measurable metabolic biomarker of young E4 carriers.

We used IC to assess EE in young and middle-aged volunteers with and without the E4 allele to test for potential prodromal effects of *APOE* on metabolism. While using IC for metabolic studies is common in clinical settings and exercise studies (*106, 107*), to our knowledge the method has not been previously applied to investigate biomarkers of cognitive impairment. Thus, repurposing IC to study the metabolic effects of an AD risk factor such as E4 represents a mobile, simple, and cost-effective new approach. To our knowledge, only two other studies have attempted to utilize IC to quantify the contribution of cerebral activation (i.e. a mental task) to whole body metabolic measures (*108, 109*). While we did not observe an *APOE* effect on IC measures during the cognitive challenge, we did find that IC is a sensitive tool to evaluate metabolic changes due to mental stress, as all participants showed a significant increase in EE. These results support claims that the brain consumes ~20% of EE despite only accounting for ~2% of body mass (*110*).

Although resting EE was significantly lower in E4 carriers at rest, the most striking effect of *APOE* was observed after participants underwent a dietary carbohydrate challenge. There, E4+ individuals failed to increase VO_2, leading to a significantly lower EE compared to non-carriers. In order to study the effect of a long-term high carbohydrate challenge, as well as test the utility of a human *APOE* mouse model, we fed E3 and E4 mice a high carbohydrate diet (HCD). An E4-associated decrease in EE observed on a normal chow was exacerbated over the course of the HCD. Previous studies have shown differences in substrate utilization in these mouse models of human *APOE* (*54, 111*), and our findings now suggest that a HCD exaggerates E4 differences in EE.

Current understanding supports a triad of primary risk factors for the development of late-onset AD: old-age, E4, and female sex. Female study participants that were E4 carriers showed significant decreases in energy expenditure at rest and after the glucose challenge. Studies have shown that females are at a greater risk for developing AD, as 60% of AD patients are female (*60, 112*). Female E4 carriers are also more likely to develop AD than male E4 carriers (*63*) and show increased neuropathology (*113*). Sex specific E4 effects have also been observed in healthy older adults - female E4 carriers displayed greater CSF tau levels than female E4 non-carriers, a finding not observed in males (*114*). Here, we observed metabolic signatures in female E4 carriers that were different from female non-carriers decades prior to cognitive impairment, supporting a synergism of E4 and female sex which increases AD risk.

Aerobic glycolysis refers to the metabolism of glucose to lactate instead of the oxidative TCA cycle, despite the presence of abundant oxygen. This paradoxical phenomenon occurs in young individuals with a peak around five years of age, when 30% of the brain's glucose is processed anaerobically and then steadily declines with age (*115*). Aerobic glycolysis in the brain appears to be cell and region specific, with astrocytes playing a major role in certain regions such as the dorsolateral prefrontal cortex, precuneus, and the posterior cingulate cortex (*116*). Importantly, areas associated with aerobic glycolysis also overlap with areas known to accumulate amyloid β, indicating that the anaerobic metabolism of certain brain regions may possibly predict amyloid burden in later life (*117*). Furthermore, a recent large-scale proteomics study implicated proteins involved in glial sugar metabolism as most significantly associated with AD pathology and cognitive impairment (*118*), while another showed rates of aerobic glycolysis in preclinical AD

predict higher tau deposition (*119*). Here, we observed that E4 carriers exhibit a bioenergetic profile consistent with an active aerobic glycolysis phenotype. When we performed metabolic pathway and enrichment analyses on plasma metabolites extracted from E4 carriers and non-carriers, the most significant pathways altered were "glycolysis" and "Warburg effect", respectively, while the most significantly increased metabolite in E4 subjects was lactate. Together, these changes in the plasma metabolome of young and middle aged E4 carriers point to a role for *APOE* in regulating aerobic glycolysis.

Using metabolic assays and stable isotope-resolved metabolomics *in vivo* and *in vitro*, we identified an E4-associated bioenergetic phenotype of impaired glucose oxidation and increased glycolysis which promotes lactate production. These results are congruent with other E4 and AD studies. For example, a recent study demonstrated that E4 astrocytes have increased lactate production (*120*), and neurons expressing E4 exhibit increased reliance on glycolysis for ATP production with apparent deficits in mitochondrial respiration (*121*). Fibroblasts from AD patients also show a Warburg-type shift from oxidative phosphorylation to glycolysis with increased lactate production (*122*). The potential mechanism underlying how AD and/or E4 alters metabolic efficiency to induce these effects is unclear. It has been proposed that E4 directly causes mitochondrial dysfunction, which is a known metabolic derangement of AD (*123*). E4 has been shown to reduce mitochondrial membrane potential by directly binding to complexes involved in oxidative phosphorylation and decreasing their activity (*124*). Treating naïve fibroblasts with astrocyte conditioned media from the same immortalized E3 and E4-expressing astrocytes we used here induced a decrease in OCR in tandem with an increase in lipid synthesis and lipid droplet formation (*125*). We have also observed this increased lipid

droplet formation in E4 astrocytes (*126*), as have others (*127*). A seminal study on lipid droplets in the brain found that lipid droplet accumulation in glia is *APOE*-dependent and directly linked to neurodegeneration and lactate transport (*128*). The intriguing link between increased lactate and increased lipid droplets in E4 glia remains to be fully elucidated.

Interestingly, recent evidence has shown that lactate is an energy substrate used by the brain (*129*) and a competitive glucose alternative (*130-132*). Lactate has also been shown to decrease FDG-PET signal (*133*). An increase in astrocyte-derived lactate in E4 carriers may compete with glucose as a substrate for brain metabolism and decrease CMRglc. Further, an increase in aerobic glycolysis might also act to lower energy expenditure, as glycolysis produces only 2 moles of ATP compared to the 34 moles of ATP from a mole of glucose metabolized via mitochondrial oxidative phosphorylation. This balance of anaerobic glycolysis versus oxidative phosphorylation behaves reciprocally (*134*). Increased mitochondrial ATP production downregulates glycolysis, while glycolytic ATP synthesis can suppress aerobic respiration (*135*). Given our findings of lower O_2 consumption and increased production of lactate, we speculate that E4 carriers have lower EE due to glycolysis being less energetically costly than downstream pathways.

Our study has several limitations. As a primary goal was to assess individual metabolic responses to glucose, we performed blood draws immediately prior and immediately after the glucose challenge. It may be possible that mental stress during the cognitive challenge (which occurred prior to the first blood draw) altered the plasma metabolome beyond the normal resting state. We did however provide time after completion of the cognitive test for a “post-cog” rest in which participants were asked to

relax and breathe normally, similar to the initial rest period. Another potential confounder is that we provided glucose in the form of a sugary milk drink for the glucose challenge. While we used 50g of sugar based on clinical guidelines for glucose challenges (*136*), milk also includes fats and proteins. However, the high relative content of carbohydrates to other macronutrients ensures that any observed response (particularly at the ~30 minute time point analyzed) can be primarily attributed to carbohydrate metabolism. Indeed, the pathways most altered by the glucose challenge included galactose metabolism, starch and sucrose metabolism, and glycolysis. Finally, while we found E2 to be associated with lower plasma lactate and higher EE relative to non-E2 carriers, the study did not include any homozygous E2 carriers and the low overall allele frequency makes interpretation challenging. Still, these results are intriguing based on E2 being a known protective allele for AD (*59, 61*), and further study of energy expenditure and glucose metabolism in E2 carriers is warranted.

Using primary astrocytes, humanized mouse models, and cognitively unimpaired humans, we demonstrate decreased energy expenditure in young E4+ individuals. This phenomenon was sex-specific, exaggerated following a dietary glucose challenge, and reflected in a decreased rate of glucose oxidation in preference for aerobic glycolysis. While many questions remain, our study highlights novel roles for *APOE* and sex in modulating systemic glucose metabolism and provides a feasible method to assess *APOE*-dependent metabolic signatures in pre-symptomatic young individuals. These findings provide important insights that may help to define dietary and pharmacological approaches to delay or prevent incipient AD in high-risk E4+ individuals.

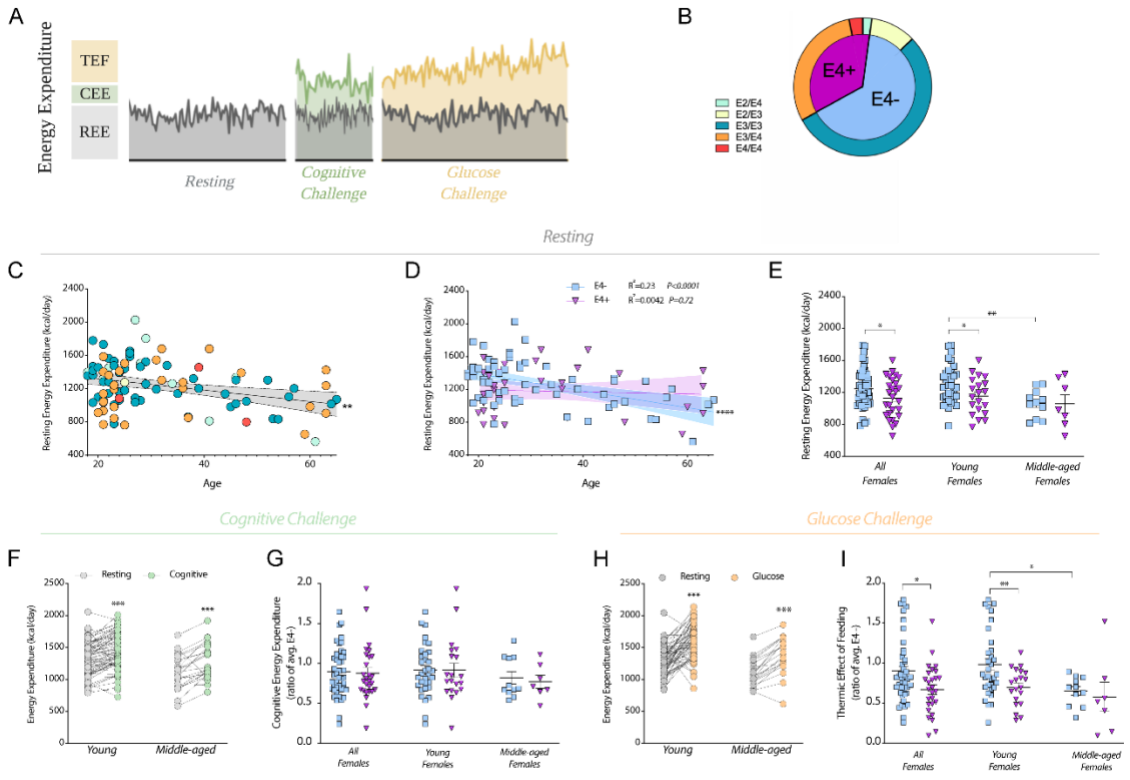

Figure 2.1 Female E4 carriers show lower resting energy expenditure and lower thermic effect of feeding after a glucose challenge.

(A) Experimental design of study. Individual components of energy expenditure were assessed in three distinct periods. Resting energy expenditure (REE) was assessed during the resting period. Cognitive energy expenditure (CEE) was assessed during the cognitive challenge and defined as difference in the area under the curve (AUC) of energy expenditure (EE) during the cognitive challenge and the AUC of EE from the resting period. Thermic effect of feeding (TEF) was assessed during the glucose challenge and calculated as the difference in AUC of EE during the glucose challenge and AUC of REE. (B) APOE genotypes of subjects represented in the study (E4- n=61, E4+ n=33; E2/E4 n=2, E2/E3 n=10, E3/E3 n=51, E3/E4 n=28, E4/E4 n=3). (C) Correlation of average REE with participant age (Pearson correlation R_2=0.11, **P<0.01, n=94). (D) Correlation of average REE and participant age separated by E4 carriers (purple) and non-carriers (blue) (E4- R_2=0.233, ****P<0.0001; E4+ R_2 =0.0042, P=0.719, E4- n=61 and E4+ n=33). Shaded areas refer to 95% confidence intervals. (E) Average REE for all, young, and middle-age E4- (n=44, 33, and 11 respectively) and E4+ females (n=27, 20, and 7 respectively) (*P<0.05, **P<0.01, unpaired t-test, two-tailed). (F) Average EE between resting and cognitive test periods in young (n=71) and middle-aged (n=23) participants. (***P<0.001, paired t-test, two-tailed). (G) CEE for all female participants and for the two age cohorts. (H) Average EE between resting and glucose challenge periods in young and middle-aged participants (***P<0.001, paired t-test, two-tailed). (I) TEF for all females and for the two age cohorts, further separated by E4 carriers and non-carriers. (*P<0.05, unpaired t-test, two-tailed).

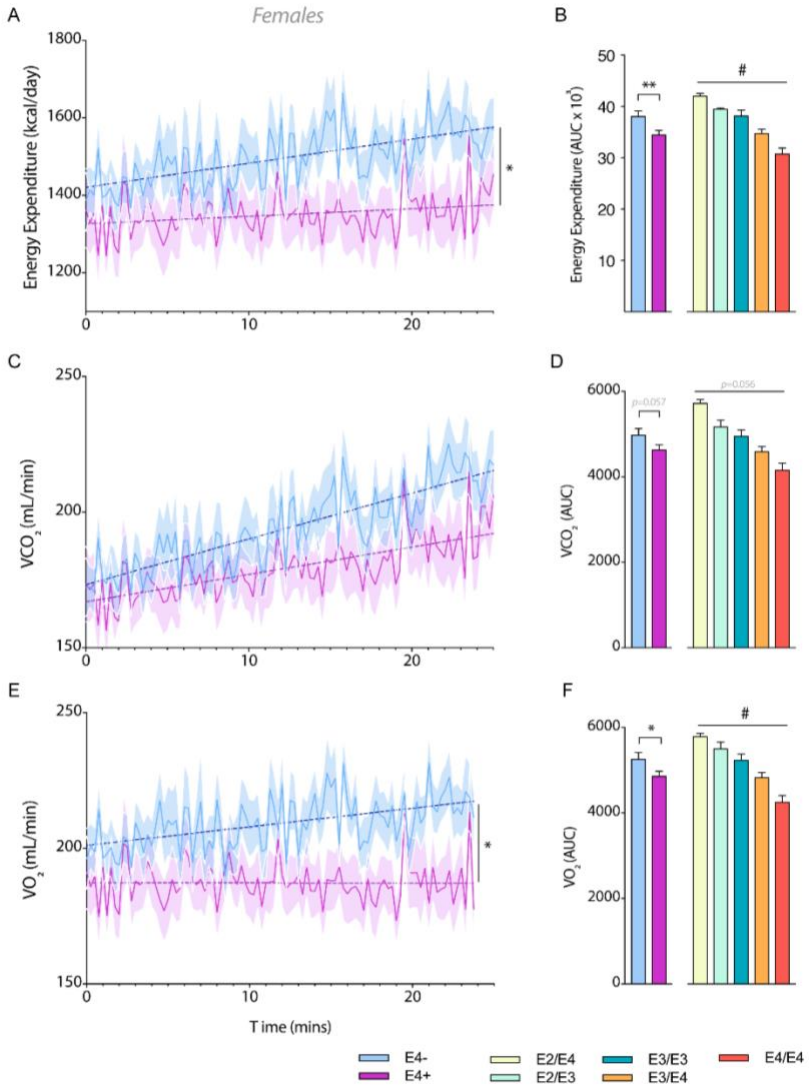

Figure 2.2 Female E4 carriers show lower energy expenditure and lower oxygen consumption after a glucose drink.

(A) Energy expenditure (EE) of female E4 carriers (purple) and E4 non-carriers (blue) during the glucose challenge. Values shown are means (lines) +/- SEM (shaded). (E4- *n*=44, E4+ *n*=27; **P*<0.05, Two-way ANOVA repeated measures) **(B)** Incremental area under the curve (AUC) of EE was determined by E4 carriage and further by respective *APOE* genotypes in all participants. (E4- *n*=61, E4+ *n*=33; E2/E4 *n*=2, E2/E3 *n*=10, E3/E3 *n*=51, E3/E4 *n*=28, E4/E4 *n*=3; ***P*<0.01, unpaired *t*-test, two-tailed; #*P*<0.05 One-way ANOVA,) **(C)** Time course of average VCO_2 values of E4- and E4+ females during the glucose challenge period. Dashed lines refer to linear regression result. **(D)** AUC of VCO_2 for all participants. **(E)** Time course of average female VO_2 during glucose challenge. (**P*<0.05, Two-way ANOVA repeated measures) **(F)** AUC of VO_2 for all participants (**P*<0.05, unpaired *t*-test, two-tailed; #*P*<0.05 One-way ANOVA)

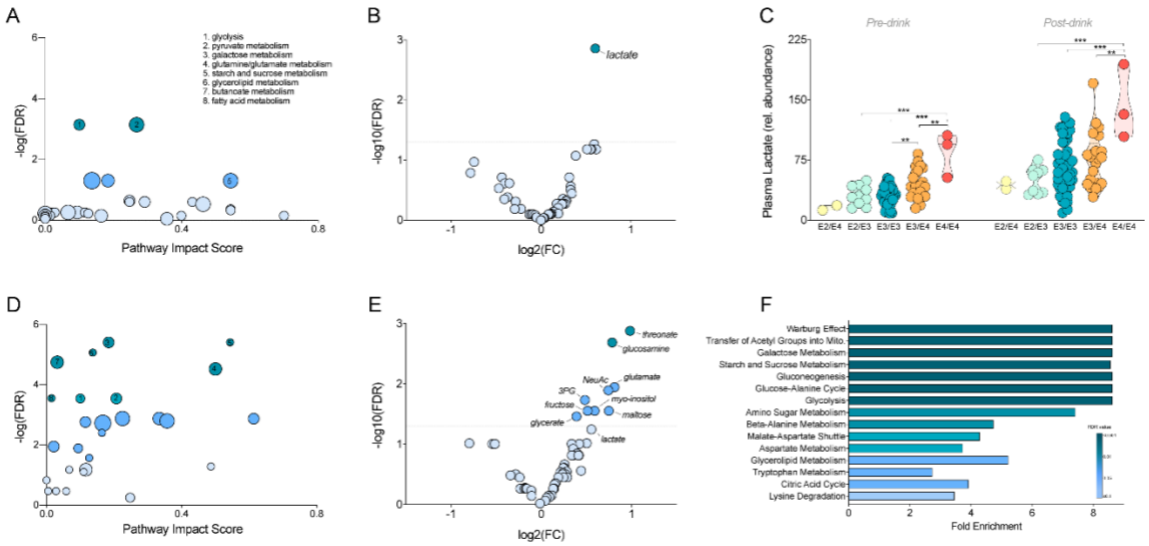

Figure 2.3 Targeted metabolomics reveals lactate as a differentially regulated metabolite in E4+ plasma.

(A,D) Pathway impact analysis highlights pyruvate metabolism and glycolysis as pathways significantly altered by E4 carriage in human plasma at baseline **(A)**, while multiple carbohydrate and lipid processing pathways are altered by E4 carriage following the glucose drink **(D)** (FDR <0.01). **(B,E)** Volcano plots showing changes in plasma metabolites. Lactate was the most significantly altered metabolite by *APOE* genotype at baseline **(B)**, while multiple metabolites differed post-glucose drink **(E)** (ANOVA, FDR <0.05). **(C)** Lactate values in individual subjects as determined by GC-MS analysis. **(F)** Enrichment analysis highlights multiple metabolic pathways as significantly altered by E4 carriage following the glucose drink, including the top hit of 'Warburg effect'. All comparisons are E4+ (*n*=33) vs E4- (*n*=61); A-B, denote analysis of pre-glucose drink plasma samples; D-F, denote post-drink plasma samples.

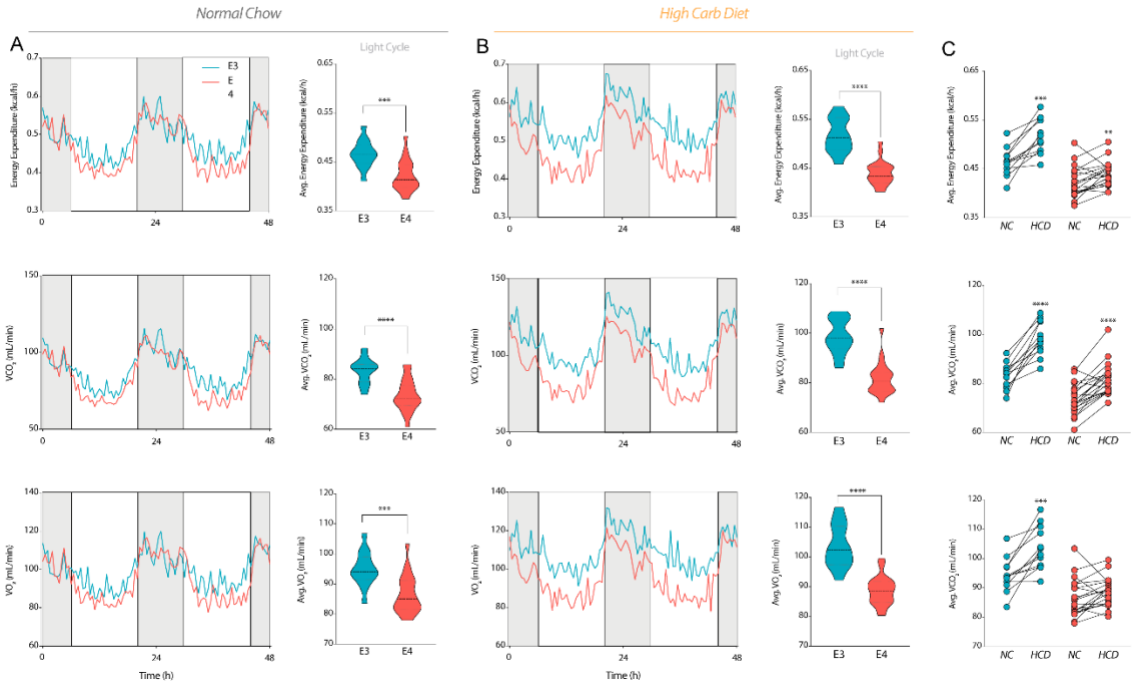

Figure 2.4 E4 mice show lower energy expenditure that is exacerbated by a high carbohydrate diet.

E3 and E4 mice were housed individually for 48 hours with *ad libitum* access to normal chow **(A)** or a high carbohydrate diet (HCD) **(B)**. Dark cycles are indicated in grey with light cycles in white. Light cycles were used for calculating averages of energy expenditure, VCO_2 and VO_2 (shown to the right) (***P<0.0001, ****P<0.00001, unpaired t-test, two-tailed; E3 n=13, E4 n = 20). Violin plot values represent means (black dashed line) and upper and lower quartiles (gray dotted line).

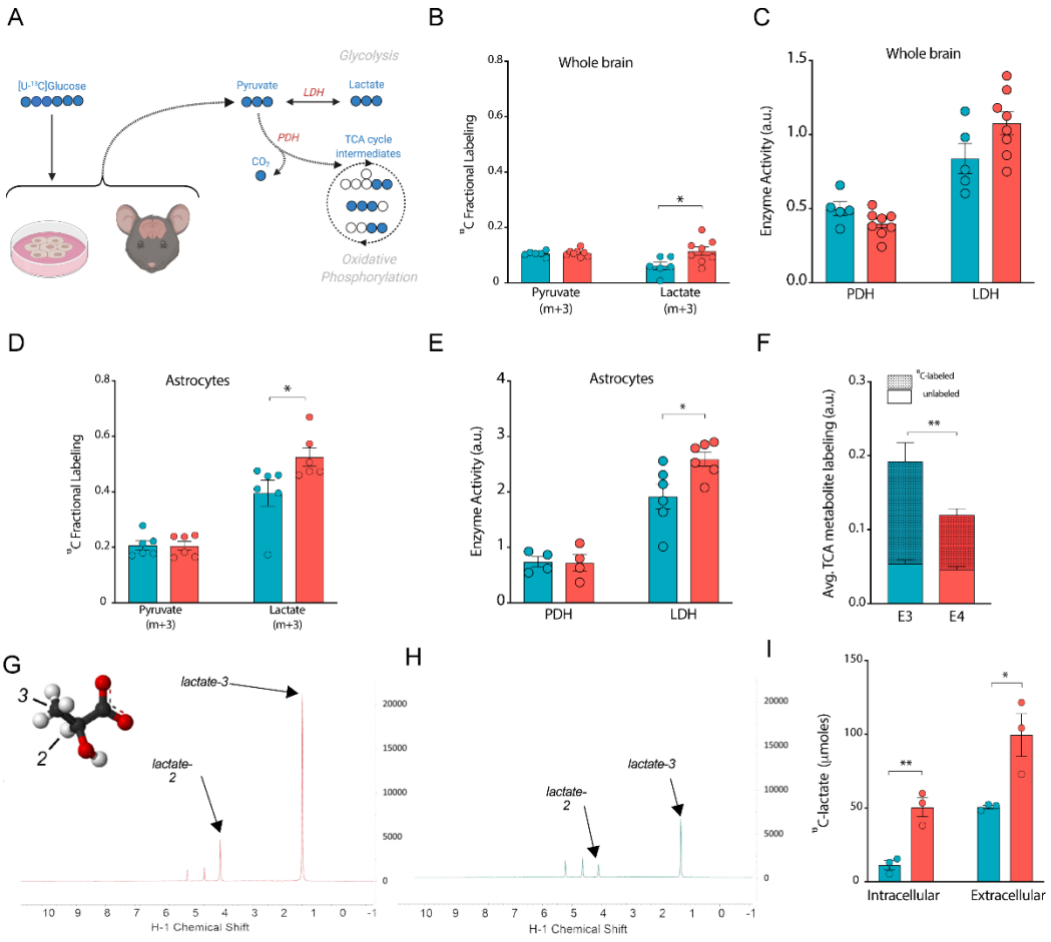

Figure 2.5 Stable isotope resolved metabolomics reveals increased lactate synthesis and decreased entry into TCA cycle in E4 brains and astrocytes.
(A) Experimental design (^{13}C, blue filled circles; ^{12}C, white circles; (m+n, where n is the number of ^{13}C labeled carbons within a metabolite). (B) [U-^{13}C] glucose was administered in vivo to E3 (n=6) and E4 (n=8) mice via oral gavage, brain tissue was collected after 2 hours, and metabolites analyzed for ^{13}C enrichment in pyruvate and lactate. While fully labeled pyruvate is present in similar amounts in E3 and E4 brains, lactate synthesized from ^{13}C-glucose is higher in E4 mouse brains (C) LDH activity is higher in E4 brains as estimated by the ratio of lactate (m+3) / pyruvate (m+3), while glucose entry into the TCA cycle via pyruvate dehydrogenase is decreased in E4 brains as estimated by the citrate (m+2) / pyruvate (m+3) ratio. (D) E3 and E4 expressing astrocytes were cultured in [U-^{13}C] glucose media for 24 hours, media collected, cells washed, and metabolites analyzed for ^{13}C enrichment (n=6). Primary astrocytes expressing E4 show increased ^{13}C enrichment in lactate, (E) higher LDH activity (F) and decreased ^{13}C enrichment in the TCA cycle (average of all detected TCA intermediates) (G-H) Increased lactate synthesis as measured by HSQCAD NMR spectroscopy (n=3). Representative NMR spectra (I) showing E4 astrocytes have increased intracellular ^{13}C-lactate and export more lactate into extracellular media.

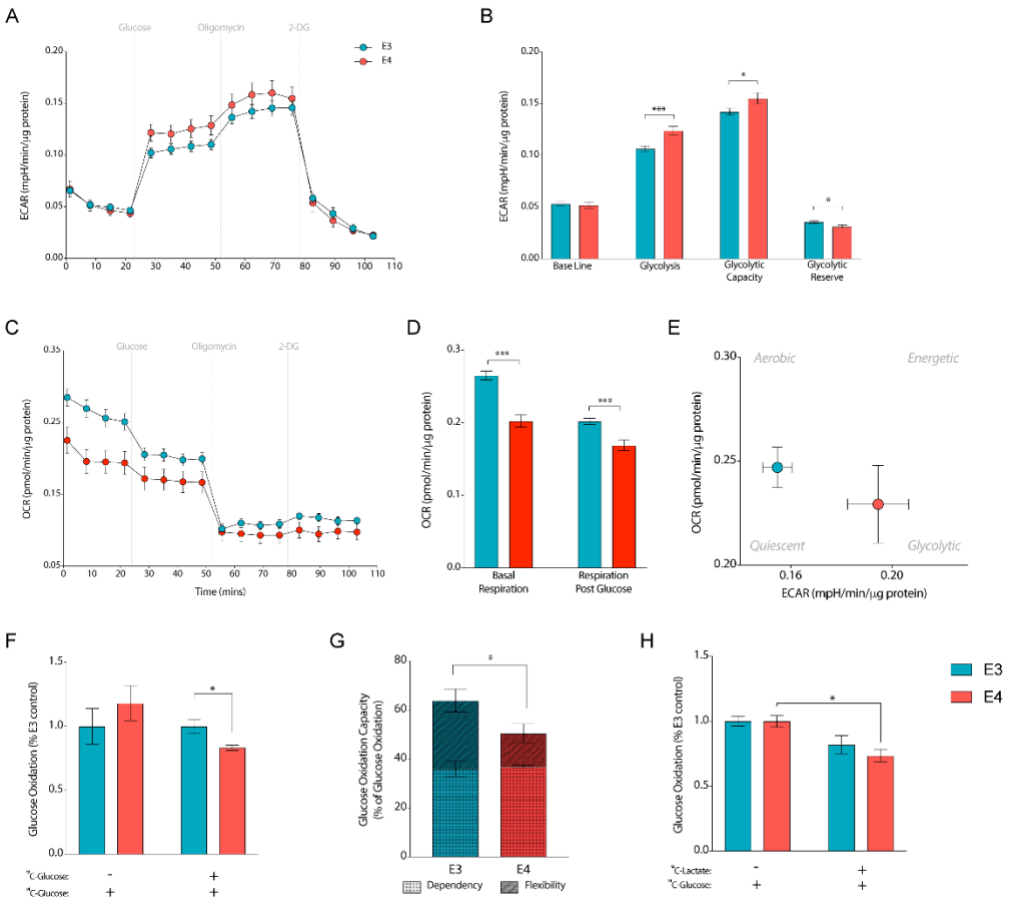

Figure 2.6 E4 astrocytes show increased glycolysis and lower oxidative respiration. **(A)** Extracellular acidification rate (ECAR) of E3 and E4 primary astrocytes shown over time during the glycolysis stress test (n=24 for both groups). **(B)** Contributions to ECAR at baseline, in response to glucose (glycolysis), in response to stress (glycolytic capacity), and un-tapped reserve were calculated and shown. (*P<0.05, ***P<0.001, Unpaired t-test, two tailed) Values represent means +/- SEM. **(C)** Oxygen consumption rate (OCR) during the glycolysis stress test assay was graphed over time and **(D)** represented as average respiration before and after glucose (***P<0.001, ****P<0.0001, unpaired t-test, two tailed). Values represent means +/- SEM. **(E)** Metabolic phenotypes of E3 and E4 astrocytes were characterized by plotting ECAR vs. OCR. **(F)** E3 and E4 astrocytes were incubated in glucose free media (-) or glucose rich media (+) and oxidation of 1.0 µCi/mL ^{14}C-glucose was measured by trapping $^{14}CO_2$ and counting radio activity. (*P<0.05 unpaired t-test, two-tailed, n=4 per genotype) Values represent means of percentages of E3. **(G)** Glucose oxidation capacity, dependency, and flexibility was assessed in E3 and E4 astrocytes via the Mito Fuel Flex Assay. (*P<0.05 Two-way ANOVA, Sidak's multiple comparisons test) Values represent means +/- SEM. **(H)** E3 and E4 astrocytes were incubated in 1.0 µCi/mL ^{14}C-glucose with (+) or without (-) 12.5mM lactate (*P<0.05, unpaired t-test, two-tailed, n=3 per genotype). Values represent mean of percent change from control (no lactate) +/- SEM.

Table 2.1 Age, sex, and APOE genotype of cognitively normal individuals according to E4 carriage and age cohort (young=18-39, middle-aged=40-65).
Values represent means +/- (SD).

	Age		Sex (N)		*APOE* Genotype (N)				
	Average Age (SD)	P	Male	Female	APOE 2/3	APOE 3/3	APOE 2/4	APOE 3/4	APOE 4/4
Young									
E4 Non-carriers (E4-)	24.91 (4.84)	0.486	13	33	8	38	0	0	0
E4 Carriers (E4+)	25.84 (6.08)		5	20	0	0	2	21	2
Middle-age									
E4 Non-carriers (E4-)	51.18 (7.79)	0.233	4	11	2	13	0	0	0
E4 Carriers (E4+)	55.5 (8.78)		1	7	0	0	0	7	1

Table 2.2 Clinical characteristics of cognitively unimpaired individuals according to E4 carriage and age cohort (young=18-39, middle-aged=40-65).
Values represent means +/- (SD). Ca, Caucasian; AA, African American; His, Hispanic; A, Asian; BMI, body mass index.

	Race (N)				Vitals									
	Ca	AA	His	A	BMI (kg/m_2)	P	Waist/ Hip Ratio	P	Systolic (mmHg)	P	Diastolic (mmHg)	P	Lean Body Mass (kg)	P
Young														
E4-	34	4	3	4	25.15 (3.83)	0.93	0.86 (0.1)	0.56	123.2 (21.2)	0.79	72.3 (14.4)	0.9	48.2 (7.3)	0.33
E4+	22	3	0	0	25.06 (4.72)		0.87 (0.1)		121.8 (18.5)		72.1 (12.1)		46.4 (7.2)	
Middle-age														
E4-	12	3	1	0	25.83 -6.07	0.45	0.9 (0.1)	0.14	123.4 (17.6)	0.76	74.2 (8.7)	0.6	47.1 (7.7)	0.63
E4+	7	0	1	0	27.92 -6.73		0.81 (0.2)		126 (23.1)		76.8 (15.9)		48.9 (9.2)	

CHAPTER 3. LIPID DROPLETS IN NEURODEGENERATIVE DISORDERS

[This chapter consists of material adapted from an accepted manuscript: Farmer BC, Walsh AE, Kluemper JC, Johnson LA. Lipid Droplets in Neurodegenerative Disorders. *Frontiers in Neuroscience*. Accepted June 23, 2020. doi: 10.3389/fnins.2020.00742.]

3.1 Introduction

Lipid droplets (LDs) are spherical organelles that store intracellular neutral lipid such as triacylglycerols (TAGs) and cholesteryl esters (CEs) (*137*, *138*). LDs serve as lipid reservoirs for cells by providing substrates for membrane formation and energy metabolism (*139*). Adipose tissue is the most LD-enriched tissue in the body, where fatty acids are stored in times of nutrient excess and then mobilized with increased energy demand (*140*). LDs also affect physiological processes in the periphery beyond simple fatty acid storage and supply, such as in inflammation and insulin signaling. For example, LDs in various immune cell types contain a large pool of intracellular arachidonic acid (AA), which provides a reserve of precursors for eicosanoid synthesis (*141-143*) Enzymes involved in AA processing have been demonstrated to LDs, indicating that these organelles serve as a supply site for inflammation (*144*). Additionally, LDs have been linked to peripheral metabolic dysfunction such as ectopic lipid accumulation (*145*) and insulin resistance (*146*). Overexpression of LD-associated proteins such as Cidea increase fat accumulation in mice, and human expression of LD proteins in adipose correlates with clinical insulin resistance (*147*). These studies therefore suggest a role for LDs in obesity-driven metabolic dysregulation.

Lipid droplets may also affect cellular physiology and function in the central nervous system (CNS). The brain is the second most lipid-rich organ (*148*), storing 20% of the

body's total cholesterol (*149*). Alteration in the lipid composition of CNS cells has been shown to affect cell function and normal neural activity (*150, 151*). Notably, neurodegenerative diseases, including Alzheimer's disease (AD) and Parkinson's disease (PD), share lipid dysregulation as a metabolic feature in disease pathology. In this review, we discuss evolving knowledge and recent advances in understanding the contribution of LDs to pathogenesis of neurodegenerative diseases. Growing knowledge of LDs in the central nervous system is important to the advancement of the field, as these dynamic organelles may reveal common mechanisms and potential therapeutic targets to neurodegenerative disease.

3.2 LD structure, composition, and biogenesis

Hydrophobic molecules such as TAGs, CEs, and retinyl esters constitute the core of a lipid droplet (*152*), while the outer surface is formed by an amphipathic lipid monolayer embedded with LD-associated proteins. (The general structure of an LD is illustrated in Figure 3.1). Additionally, proteins can reside in the LD core depending on the cell type. This unique monolayer distinguishes LDs from organelles of similar size, such as lysosomes and endosomes, as the latter exhibit a lipid bilayer. Of the many LD-associated proteins, members of the perilipin family have been well described for their essential roles in LD metabolic regulation (*153*). The exterior protein components of LDs allow for a variety of unique interactions that may explain the myriad of cellular roles accomplished via LDs in energy homeostasis, cellular communication, and disease.

Lipid droplets arise from the endoplasmic reticulum (ER) by budding off the cytoplasmic leaflet of the ER membrane (*154*). They are comprised of acyl-glycerols that

are synthesized through the action of diacylglycerol transferases (DGATs), which convert acyl-CoA-bound fatty acids and diacylglycerols (DAGs) into the TAGs that fill the LD core (*155*). Cholesterol acyltransferases synthesize CEs which are also incorporated into the core of nascent LDs (*156*). Once separated from the ER membrane, LDs may continue to grow via LD fusion and further TAG incorporation. Fusion of LDs with the aid of members of Cell death-inducing DFF45-like effector (CIDE) family proteins (*157*) coalesce smaller LDs into larger LDs. Re-localization of TAG synthesis enzymes like DGAT2 and GPAT4 from the ER to the LD surface allows direct synthesis of TAGs from cellular lipid sources (*158*), such as fatty acids derived from autophagic phospholipid breakdown (*159*). The incorporation of cellular debris into LDs is commonly seen during periods of stress and starvation and are thought to protect the cells from lipotoxicity (*160*). LDs exhibit a variety of protein and lipid signatures, and these various compositions can help determine LD localization and utilization. For example, perilipin 2 (PLIN2) has relatively low control over lipolysis, so LDs that contain PLIN2 may be more easily broken down. Conversely, PLIN1 and PLIN5 actively promote lipolysis when activated. PLIN1 acts through its release of CGI-58, a co-activator of adipose triglyceride lipase (ATGL) (*161*), while PLIN5 binds directly to ATGL to promote lipolysis (*162*). Therefore, LDs with varying PLIN proteins will behave differently across various tissues and environmental conditions (*153*).

Lipid homeostasis is necessary for maintaining neuronal function and synaptic plasticity (*163*), and dynamic interaction between perilipins and lipases on the LD surface regulate cellular lipid storage, breakdown, and metabolism (*164*). In most cells, the bulk of LD breakdown is accomplished through ATGL, another LD outer layer protein (*165*).

Lipophagy is also a recognized LD breakdown process, in which an LD is taken up into an autophagosome and subsequently fuses with a lysosome to breakdown LD contents mainly through lipid acid lipases (*166*). During times of metabolic stress, lipases cleave triglycerides into FAs, which are then processed in the mitochondria to liberate the energy stored in droplets via beta-oxidation into acetyl-CoA and subsequent TCA cycle activity and oxidative phosphorylation (*167*). LDs have been shown to provide energy substrates (*126, 168*), lipid signaling molecules (*169*), and membrane infrastructure materials (*170*) for various cell types.

3.3 LD formation in cells of the brain

Essentially all brain cell types have been shown to form LDs (Table 3.1 and Figure 3.2**)**. A recent study claimed that the majority of brain LDs (stained with the fluorescent neutral lipid probe BODIPY) were co-localized with ionized calcium binding adaptor molecule 1 (Iba1), a microglia/macrophage-specific protein. This finding implicates microglia as a main harbor of LDs (*171*). These lipid-associated microglia had a unique transcriptomic signature compared to non-LD-laden microglia, suggesting that LDs in microglia are either a cause or result of substantial transcriptional modulations. However, subsequent co-localization using other brain cell-specific markers was not reported in this study, leaving the door open for other cell types to be involved. For example, ependymal cells that line the cerebral ventricular system have been shown to accumulate LDs, along with Glial fibrillary acidic protein (GFAP) positive cells that are closely associated in the ependymal niche (GFAP is a common marker for astrocytes and ependymal cells) (*172*). Lesions to the CNS have also induced LDs in neurons and astrocytes (*173*), and glial cells have been shown to form LDs from phagocytosed myelin fragments (*174*). Finally, a

thorough immunofluorescence study examining cell types that harbor PLIN positive droplets found Iba1+, GFAP+, NeuN+ (a neuron specific antibody), and S100β+ (a calcium binding protein that is localized in astrocytes) to colocalize with droplets (*175*). Together, these studies and others demonstrate that multiple cell types in the brain are capable of forming LDs.

3.4 Anatomic structures associated with LDs in the brain

The subventricular zone (SVZ) has surfaced as a key region for lipid droplets in the brain. The SVZ lines the wall of the lateral ventricles and is composed of neural stem cells that are capable of differentiating into various CNS lineages (*176*). This highly active and heterogeneous cellular region is an energetically needy zone, and it is reasonable to expect ample energy stores are on board in order to meet its energetic needs (*177*). It was first shown that large LDs were found in the ependyma of the SVZ (*178*). This was accomplished using an electron microscopy approach that detailed the associations of various SVZ cell types with confirmatory immunostaining.

Another group found that the LD lipase ATGL, which is encoded by the patatin-like phospholipase domain-containing protein 2 (PNPLA2) gene, is highly active in the SVZ and choroid plexus. Furthermore, mutating PNPLA2 led to a significant increase in LD formation in both areas (*165*). This study was the first to report a function of PNPLA2 in the brain and describe its regional role in maintaining cerebral lipid metabolism. Additionally, knock out of the GTPase regulator associated with focal adhesion kinase-1 (GRAF1) induced LDs in the brains of post-natal day seven pups (*179*). Apart from studies of LDs in the brain arising from genetic alterations, it was found that LDs accumulate in

the SVZ progressively with age; 12-month-old mice showed a nearly two-fold increase in LDs in the SVZ compared to 3-month-old mice (*180*).

The SVZ has also been shown to harbor LDs in the context of Alzheimer's disease (AD). Hamilton and colleagues showed that both an AD mouse model and AD human post-mortem tissue accumulate LDs along the lateral ventricle (*181*). Using tandem mass spectrometry, the LD contents were identified, revealing high concentrations of oleic acid-enriched TAGs (*181*). Interestingly, direct infusion of oleic acid into the lateral ventricle was sufficient to induce LD formation along the SVZ, but insufficient to impair neurogenesis (*181*). Another group found the choroid plexus to have more LDs as AD progressed in human post mortem tissue (*182*). Further studies are needed to clarify the role of LDs in the SVZ in normal aging and neurodegeneration.

Although the SVZ is the most extensively studied brain region with regards to LD formation, other structures such as the frontal cortex, hippocampus, olfactory bulbs, and hypothalamus have been shown to accumulate LDs (Table 3.1). In fact, prior studies on the hypothalamus indicate that LDs may affect certain processes such as satiety (*183*). In this study, Kaushik demonstrates that autophagy during starvation leads to the mobilization of neuronal lipids which can then increase food intake though the upregulation of agouti-regulated peptide. This is just one of many studies which explore the wide variety of brain regions and biological processes which LDs can affect (Table 3.1).

3.5 What causes lipid droplets to form in the brain?

3.5.1 Aging

Lipid droplets appear to accumulate in the brain during the normal process of aging. For example, analysis of microglia from 20-month-old mice revealed an abundance of BODIPY+ cells in comparison to a matched 3-month-old cohort (*171*). Analyses of human tissue (postmortem) also revealed that PLIN2+ Iba1+ microglia were more frequent in an aged (67-years-old) individual than in a young (22-years-old) individual (*171*). A significant increase in LDs has also been observed in the pia mater, cortex, and striatum in 18-month-old mice as compared to middle aged mice (*175*). Furthermore, an electron microscopy analysis of the basement membrane of the blood brain barrier (BBB) in 6-month-old versus 24-month-old mice showed an age-dependent accumulation of LDs which caused significant thickening of the basement membrane (*184*). On the contrary, LDs are more commonly found in perivascular cells in middle age and then seem to shift toward the parenchyma in old age (*175*). Given these findings, age appears to regulate LD accumulation and regional deposition.

3.5.2 Inflammation

From *in vitro* studies of LDs to *ex vivo* brain imaging, inflammation has repeatedly been associated with LD formation as both a cause and as an effect (*143*). Lipopolysaccharide (LPS), a commonly employed pro-inflammatory stimulus, has been shown to increase the number and size of LDs in microglia (*185*). PLIN2 was shown to colocalize with these droplets, providing more evidence that PLIN2 is an LD-associated

protein that can be considered a marker for both LDs and inflammation in the brain. This was repeated recently in microglia-derived BV2 cells and expanded into an *in vivo* model of LPS treatment. That study by Marschallinger and colleagues found that more microglia contained LDs in LPS treated mice when compared to non-treated controls (*171*). To assess how the vasculature might affect LDs in the brain, Lee and colleagues *i.v.* infused triglyceride-rich lipoproteins (TGRL) and lipoprotein lipase into mice and found increased BBB permeability, therefore indicating that hyperlipidemia may increase lipid spill-over into the brain. To test how this treatment affected resident brain cells, they treated normal human astrocytes with the TGRL lipolysis products and found increased LD formation (*186*). Another study found that palmitate treatment of isolated primary astrocytes increased inflammatory markers including TNF-alpha, IL-1 beta, IL-6, and MCP-1 in addition to Oil Red O (a fat-soluble dye) staining and PLIN1 and PLIN2 transcription. Interestingly, treatment of microglia with conditioned media from lipid-loaded astrocytes enhanced microglial chemotaxis through a CCR2-MCP1 mechanism (*187*). These data suggest that LD-associated astrocyte inflammation may subsequently signal to microglia to augment the inflammatory response. However, it remains to be seen whether inflammation causes LDs, LDs cause inflammation, or both.

3.5.3 Oxidative Stress

Intracellular reactive oxygen species (ROS), as well as ectopic treatment with oxidative stressors such as hydrogen peroxide, induce LD formation in various cell types in the periphery (*188-190*). Similarly, increased oxidative stress in the brain appears to drive LD accumulation in a cell-specific manner. For example, neuronal hyperactivity from

trauma or chemogenetic activation increases glial LD accumulation (*173*). These LD-laden glia upregulate genes to neutralize the peroxidated lipids generated by activated neurons. Astrocytes in particular appear to be uniquely suited for ROS management due at least in part to fatty acid binding protein 7 expression (*191*). Liu and colleagues first proposed this neuron-astrocyte metabolic coupling model in which neurons under stress export oxidized lipids to astrocytes as a means of neuroprotection (*128, 192*). LDs in glia may then be viewed as indirect indicators of neuronal damage from oxidative stress. Protective LD formation in glia has also been observed in the SVZ niche, where glia protect neuroblasts from peroxidation and thereby promote neural stem cell proliferation (*193*). Therefore, oxidative stress appears to be a driver of LD formation in the brain both under formative physiological processes during neuronal development, as well as in diseases associated with increased neuronal oxidative stress.

3.6 What neurodegenerative disorders have been linked to lipid droplets?

3.6.1 Amyotrophic Lateral Sclerosis

Amyotrophic lateral sclerosis (ALS) is the most common form of motor neuron disease (*194*). ALS is characterized by the progressive degradation of motor neurons in the CNS, leading to the inability to both initiate and control muscle movement. In addition to genetic mutations, altered metabolic function in ALS has been observed in cellular processes implicated in ALS pathology such as cell stress and energy homeostasis (*195*).

Recent studies interested in lipid metabolism have shed light on connections between LDs and ALS pathology (*196*). For example, it is known that mutations in the human VAMP-associated protein B (hVAPB) cause ALS, although the disease-causing

mechanism itself remains unclear (*197*). Sanhueza and colleagues performed a genome-wide screen in *Drosophila* to identify pathways involved in hVAPB-induced neurotoxicity and found that the list of modifiers was mostly enriched for proteins linked to LD dynamics. One modifier highlighted in this study was acyl-CoA synthetase long-chain (Acsl). Acsl promotes LD biogenesis and its downregulation reduces LD nucleation which decreases the size and number of mature LDs (*198*). Furthermore, another group showed that gain of function mutations in the LD protein seipin contributed to motor neuron disease symptoms in mice (*197, 199*). Together these studies suggest that impaired LD biogenesis may be an important pathological aspect to hVAPB-mediated ALS.

A mutation that contributes to an early onset form of ALS occurs in the gene SPG11 and affects lysosome recycling (*200*). Branchu and colleagues observed intracellular lipid accumulation followed by lipid clearance from lysosomes into droplets in wild-type (WT) mice. However, in Spg11 knockout mice, there was a significantly slower rate of lipid clearance and a decrease in LD size and number. Another study that implicates aberrant lysosomal function as a contributor to ALS reported that the C9orf72 gene plays a key role in metabolic flexibility in times of stress/starvation (*201*). They found that loss of C9orf72 led to an increase in LDs, and that starvation-induced changes in lipid metabolism were mediated by coactivator-associated arginine methyltransferase (CARM-1). Since CARM-1 regulates lysosomal function and lipid metabolism, these results suggest that the dysregulation of lipid metabolism, including the aberrant accumulation of LDs, could contribute to ALS pathology.

Similar to studies linking LDs and peroxidation to Alzheimer's disease, there also appears to be a connection between LDs and cellular stress in ALS. Bailey et al. showed

in *Drosophila* that ROS accumulation increased glial LD content, and that when glia were unable to produce LDs, neuroblasts experienced peroxidative damage (*193*). Additional work by Simpson et al. provided a link between LDs, peroxidation, and ALS by showing a positive correlation between lipid peroxidation markers in ALS patient cerebrospinal fluid and disease burden (*202*). Thus, LD dynamics may contribute to ALS, potentially through a mechanism in which glia are unable to protect neurons through normal lipid accumulation and storage mechanisms (*196*).

3.6.2 Huntington's Disease

Huntington's disease (HD) is a hereditary neurodegenerative disease caused by a mutation in the huntingtin gene (Htt) that then codes for the Htt protein (*203*). Mutant Htt contains an expanse of repeating glutamines at the N terminus, thus causing Htt oligomerization and aggregation that leads to neuronal death. A wide range of metabolic abnormalities characterizes HD, including alterations in autophagy (*204*). Martinez-Vicente et al. found that macroautophagy is compromised in cellular and mouse HD models and in HD patient-derived tissues, as evidenced by the inability to recognize and properly sequester unneeded cellular components (*205*). Autophagosomes in HD models failed to recognize and load excess cargo, thus causing autophagic cytosolic components to have a slower turnover leading to toxic accumulation of lipid in cells. They also observed an increase in LD number and area in fibroblasts, hepatocytes, striatal cells, and primary neurons from a HD mouse model (Qhtt mice). Furthermore, striatal tissue from advanced-stage HD patients had increased oil red O staining density when compared to age-matched

controls (*205*). The authors hypothesized that increased LD content in HD cells could be due to their reduced ability to recognize and degrade excess lipid by macroautophagy.

Aditi and colleagues used transgenic *Drosophila* expressing the mutated form of human Htt in neurons to better understand HD energetics (*206*). They found that when compared to controls, diseased flies exhibited a characteristic pattern of weight change that is correlated with HD progression, as evidenced by altered lipid concentrations over time. Interestingly, and in contrast to the above study by Martinez-Vicente's group, flies had high levels of lipid at disease onset and low levels at the terminal stage in neurons. This finding was also true for abdominal body fat cells, despite only expressing mutant Htt in neurons. LD size mirrored the overall lipid levels, with large LDs being found in 3-7-day-old diseased adults and small lipid droplets forming by days 11-13 in diseased flies. These findings suggest that mutant Htt leads to dysregulated lipid metabolism in addition to neurodegeneration. However, further studies in both mammalian and fly models are needed to fully elucidate the role LDs may play in the onset of HD.

3.6.3 Parkinson's Disease

Parkinson's disease (PD) is caused by a loss of dopaminergic neurons and leads to abnormal brain activity and symptoms such as tremors, bradykinesia, and limb rigidity (*207*). Lewy bodies are pathological hallmarks of PD that are found in pre-synaptic terminals of neurons. These Lewy bodies contain aggregates of the α-synuclein protein which has been shown to accumulate on LD phospholipid surfaces, slowing lipolysis of LDs (*208*). Cole and colleagues also found that two mutant forms of α-synuclein, A30P

and A53T, showed decreased capacity to reduce LD turnover in neurons compared to WT α-synuclein. These results suggest LD turnover in neurons is contingent on proper α-synuclein function, and that LD lipolysis may contribute to PD (*208*). However, these findings are complicated by the work of Outeiro and Lindquist, who found that both WT and A53T α-synuclein caused an accumulation of LDs in yeast, whereas A30P synuclein did not (*209*). These findings suggest that LDs may play a cell-specific role in PD pathology and call for further study in this area.

Integrated genome wide association studies have found that key mechanisms of PD pathogenesis (oxidative stress response, lysosomal function, endoplasmic reticulum stress response and immune response) rely heavily on genes regulating lipid and lipoprotein signaling. For example, Klemann and colleagues found that lipid and lipoprotein signaling is regulated by the same processes involved in dopaminergic neuron death, and found deficient signaling to be associated with increased risk for PD (*210*). Scherzer et al. found that genes related to lipid metabolism and vesicle-mediated transport had the largest effects on increasing α-synuclein toxicity in yeast (*211*). This same group also classified a variety of genes related to α-synuclein expression in *Drosophila*, and again found that lipid-related genes were strongly associated with this process. The authors proposed that dysregulation in lipid processing may be an indicating factor of problems caused by A30P α-synuclein toxicity (*212*).

Additional studies have begun to investigate lipid dyshomeostasis in PD more deeply. For example, suppression of the oleic acid generating enzyme stearoyl-CoA-desaturase (SCD) was recently found to be protective against α-synuclein yeast toxicity, and SCD knockout models in roundworms was shown to prevent dopaminergic neuron

degeneration (*213*). Specific genes related to lipid regulation have also been identified. ATPase cation transporting protein 13A2 (ATP13A2) functions in cation transport within the cell. Mutations to ATP13A2 are associated with PD and overexpression of ATP13A2 showed a decrease in various forms of lipids *in vitro* (*214*). When looking at these findings together, it is evident that LDs and lipid homeostasis play a more significant role in PD than originally thought. This line of thought is supported by Fanning et al., who stated that α-synuclein toxicity and cell trafficking defects have been associated with aberrations in LD content and distribution (*215*). PD has classically been believed to be a "proteinopathy", but with many of the recent discoveries, lipid dyshomeostasis is rapidly becoming one of the fundamental characteristics of this disease (*215*).

3.6.4 Alzheimer's Disease

Alzheimer's disease (AD) is the most common form of dementia worldwide (*216*). When Alois Alzheimer wrote his seminal paper in 1907 describing the case of Auguste Deter, he noted three neuropathological hallmarks. He found "striking changes of the neurofibrils" and "minute milliary foci caused by deposition of a particular substance in the cortex". He also observed glial changes and stated, "many glia include adipose inclusions" (*217, 218*). While the first two findings have been studied extensively by scientists interested in the contribution of tau and amyloid to disease progression, the finding of glial lipid accumulation has largely been overlooked. It wasn't until recently that this phenomenon of increased lipid accumulation in Alzheimer's disease was revisited and examined. Hamilton et.al helped renew interest in this phenomenon in a report describing increased LD formation in the SVZ of both 3xTgAD mice and human AD samples which

correlated with defects in neurogenesis (*181*). Interestingly, acute administration of intracerebral oleic acid mimicked the LD phenotype of the 3xTgAD mice, but did not alter SVZ neuron viability, suggesting that disease-associated LD accumulation is not simply a result of environmental lipid exposure. Derk and colleagues found a highly significant increase in both neutral lipid and diaphanous 1 (DIAPH1) expression in myeloid cells in AD brains (*219*). DIAPH1 mediates signaling for the receptor for advanced glycation end products (RAGE), an inflammatory ROS-producing pathway. This apparent correlation between neutral lipid accumulation and inflammatory signaling suggests that LDs may be key players in cerebral inflammatory responses. A recent study further validated this model, where it was discovered that astrocytes uniquely upregulate ROS management genes, seemingly to manage the import of neuron-derived lipid oxidation products (*173*). This study showed that neuronal hyperactivity alone was sufficient to initiate neuronal lipid peroxidation, neuronal lipoprotein export, and subsequent management and storage of peroxidized lipid as LDs in astrocytes. Further work done by van der Kant and colleagues showed that CE, which can be incorporated into LD cores through normal LD biogenesis, increase the accumulation of phosphorylated tau (p-tau) by reducing proteasome activity (*220*). The study showed that both statins and an allosteric activator of cholesterol 24-hydroxylase (efavirenz) helped lower p-tau levels in human neurons by reducing CE concentrations, thereby providing a potential mechanistic link between LDs and AD neuropathology.

A role for apolipoproteins as shuttles for oxidative waste from neurons has been described in the brain (*128*). Additionally, different isoforms of Apolipoprotein E (ApoE) were shown to have altered efficiency for lipid shuttling. ApoE4-laden lipoproteins

appeared to be less efficacious at the delivery of lipotoxic products to glia than lipoproteins associated with ApoE3.

This is particularly interesting in light of the E4 allele of *APOE* being the strongest genetic risk factor for the development of late onset AD. Our group recently showed that astrocytes expressing E4 preferentially accumulate and utilize LDs for energetic needs (*126*). Additionally, transcriptional profiling of glia derived from human iPSC lines harboring homozygous E4 or E3 alleles showed that the majority of differentially expressed genes in astrocyte-like cells involved lipid metabolism and transport (*221*). This group also found that a phenotype of E4 astrocytes included the accumulation of intracellular and extracellular cholesterol. They hypothesized that since cholesterol is responsible for a wide range of functions in the brain, altered cholesterol metabolism in E4 glia may be associated with pathological phenotypes in neurodegenerative disorders. Conditioned media from E4 astrocytes has been shown to induce LDs in other cell types, suggesting that E4 may also act extracellularly to induce LD formation (*125*). Finally, neutral lipid staining of the choroid plexus in post-mortem AD brains proposed LDs as central hubs of an ApoE-mediated complement-cascade regulation (*182*). The authors found ApoE to bind to complement component 1q (C1q), a protein complex that binds antigen-antibody complexes, on LDs in the choroid plexus. Since C1q protein is involved in the activation of the classical complement pathway, this interaction effectively keeps the complement system of the immune system in check at the CNS/vasculature interface. While all ApoE isoforms showed equal binding affinity for C1q, post-mortem mice and human E4 brains were shown to accumulate LDs more abundantly. Interestingly, these lipid deposits significantly correlated with neuropathological staging of AD, pointing to

APOE regulation of the complement cascade at the choroid plexus niche as a novel hypothesis for AD pathogenesis.

3.6.5 Hereditary Spastic Paraplegia

Hereditary spastic paraplegia (HSP) is a group of inherited neurological disorders that cause muscle weakness and tightness, primarily in the legs, through the degeneration of long corticospinal axons (*222, 223*). Studies of HSP-causing proteins suggest a link between lipid metabolism and the development of disease. For example, DDH2 domain containing protein 2 (DDHD2) is a triglyceride hydrolase in the brain that is implicated in recessive complex HSP. The systemic genetic knockout and pharmacological inhibition of DDH2 resulted in large-scale accumulation of LDs within the CNS, but not elsewhere (*224*). These data indicate a link to TAG metabolism, as the inhibition of DDHD2 affects lipid homeostasis and LD number.

One of the most common genetic mutations involved in HSP occurs in the microtubule severing protein spastin (*200, 225*) . The M1 isoform of spastin contains a LD targeting sequence which contributes to protein targeting to LDs and LD sorting at the ER. Additionally, spastin deficiency in *Drosophila* and *C.elegans* altered LD number and TAG content. This study suggests that LD processing may contribute to the pathogenesis of HSP (*225*). Additionally, a study by Arrabit et al. further identifies spastin as a regulator of LD dispersion and dynamics. This group showed that mutations in the spastin M1 isoform induced ER reorganization in HeLa cells. This reorganization subsequently disrupted spastin's ability to disperse LDs throughout the cell and aberrantly modulated neutral lipids and phospholipids on membranes throughout the muscle and brain (*226*). Furthermore,

embryonic zebrafish cells that were treated with oleic acid (a common method to induce LD formation) indicated that a loss of spastin resulted in a higher number of smaller LDs, therefore suggesting differential generation and/or dispersion of LDs (*226*). In addition to identifying potential new HSP biomarkers, this study also proposes that HSP-causing mutations impacts lipid profiles and LD networks.

Several groups have also forged a connection between the protein spartin and LD regulation. Spartin is a multi-functional unit that associates with LD, and a lack of spartin expression contributes to a HSP form called Troyer syndrome (*227*). In one study by Edwards et al., spartin surrounded LD clusters in oleic acid treated HeLa cells, thus suggesting that spartin is recruited to LDs (*228*). Additionally, in spartin knockout mice, female mice had increased LDs number and higher perilipin protein levels in adipose tissue (*229*). Hooper and colleagues further demonstrated an interaction between spartin and LDs. Their experiments in HeLa cells showed that spartin binds to and recruits the ubiquitin ligase atrophin-1-interacting protein 4 (AIP4) to LD. This interaction subsequently promotes the ubiquitination of PLIN2. Since PLIN2 resides on LD membranes and regulates TAG turnover, spartin may play a role in LD regulation in cells and contribute to Troyer syndrome pathology (*227*). Furthermore, another group reported binding interactions between spartin and protein kinase C interacting proteins (ZIPs) at the surface of LDs. Spartin-expressing HEK-293 cells exhibit co-localization of spartin with ZIP1 and ZIP3 on LDs as shown by superimposition of spartin GFP-tagged fluorescence and Oil Red O fluorescence. (*230*). Interestingly, in the absence of spartin, no ZIP proteins were detected on the LD surface (*230*). These collective findings suggest that impaired LD metabolism might be one mechanism that contributes to Troyer Syndrome.

3.7 Regulation of LDs in the brain

Lipid droplets in the brain may be regulated differently than more traditional LD niches. DDHD2 action in HSP implicates this protein as an important player in CNS lipid metabolism but also shows a dichotomy between peripheral LDs and central LDs. The BBB forms a tight and regulated gate for lipid import and export into the brain, and thus there are separate pools of lipids that constitute the intracellular LDs located in cells in the CNS versus the periphery. Lipid contents of the cell types that make up the BBB appear to regulate its permeability (*184, 231*). Since enzyme mutations of key lipases are manifested differently in the brain and given the existence of lipid-regulatory mechanisms between the periphery and the CNS, it is possible that the two pools are controlled by separate mechanisms. Investigators should be cautious when applying canonical peripheral LD pathways to brain LD biology until more evidence emerges for conserved physiological pathways between the brain and the periphery.

Sex-specific regulation of lipid metabolism and LDs in the brain should also be considered. In one study, neurons of male rats were shown to be more vulnerable to starvation than neurons of female rats, with male neurons exhibiting decreased mitochondrial respiration, increased autophagosome formation, and increased cell death when compared to females (*232*). On the other hand, the same study showed that female tolerance of starvation conditions was associated with increases in fatty acid content and LD formation in order to prolong cell survival. These findings suggest that central LD dynamics may be sex dependent. Potential sex differences should be considered in future studies in order to better understand the contribution of sexually dimorphic features to cerebral LD metabolism and its relevance to disease susceptibility and pathology.

3.8 Future directions and concluding remarks

Several important knowledge gaps remain in our understanding of the role of LD biology in the pathophysiology in neurodegenerative disease. One important future direction for the field is to better understand the full composition of lipids comprising brain LDs – in both healthy and diseased states. A clearer picture would likely be revealed by the precise distribution of lipid classes in distinct brain regions, as well as in specific neurodegenerative diseases. However, their relatively small size and the diversity of LDs by age, cell type, and disease type complicate the compilation of a lipid profile of LDs. Additionally, *in vivo* analysis of lipids in general is challenging, as they are a diverse class of macromolecules and are relatively insoluble (*233*). However, improved techniques in mass spectrometry provide new ways to document the lipid composition in LDs. For example, matrix-assisted laser desorption/ionization imaging mass spectrometry (MALDI-IMS) allows for anatomically-specific direct detection of lipids within membranes through the production of lipid-derived ions (*234*). Since MALDI can detect phospholipids, sphingolipids, and glycerolipids, this technique provides the opportunity for an in depth and spatially-resolved profile of LDs (*235*). The continued use of powerful imaging techniques such as MALDI will be important to providing a better understanding of lipid class distribution in cerebral LDs.

LDs are cellular fuel stores, markers of inflammation, signaling hubs, protective waste reservoirs for hyperactive neurons, products of lysosomal dysregulation, and hallmarks of age. With such a wide array of roles, it is not surprising that LD accumulation has been linked to trauma, neurodegeneration, and aberrant cerebral metabolism. LDs are promising targets for novel investigations of neurological disease diagnosis and therapeutics. Therapeutic treatments could be targeted at restoring lipid balance, decreasing

droplet levels, or improving other aspects of lipid metabolic pathways. Further study on LDs and lipid metabolism will be essential in advancing our knowledge of cerebral metabolism, as well as the multifaceted etiologies of neurological disease.

Table 3.1 Lipid droplet-related literature pertaining to the brain. These papers have been classified by the model organism that was used, area of the brain that was studied, and cell type of focus.

Model Organism	Area of the Interest	Cell Type	Author and Year of Publication	Summary of Findings
Human	Frontal Cortex	Neuron	(*236*)	Large, electron dense LD-like vesicles were visible in some dendrites located in cortical layers that had abundant degeneration.
	Frontal Lobe	Astrocyte	(*237*)	A small amount of sudanophilic LDs were observed in the thalamus of a patient with Nasu-Hakola disease.
	Medial Temporal Cortex	Various	(*219*)	DIAPH1 localized to locations of LD accumulation in myeloid cells.
	Choroid Plexus	Adrenal Cortical	(*238*)	Amyloid inclusions were often associated with LDs in close contact to fibril bundles.
	Whole Brain	Neuron	(*239*)	A brain biopsy found ballooned neurons filled with oligolamellar cytosomes and LDs.
			(*240*)	Demyelination with cuprizone and myelin debris contributed to LD formation. LD volume and number was highest in richly myelinated corpus callosum.

Rat	Cerebral Cortex	Neuron	(*241*)	Injection of squalene led to accumulation of LDs in the myelin sheaths of neurons.
	Hippocampus	Neuron	(*242*)	Exposure to excess oxygen caused neuronal necrosis and was more severe in young rats. Neurons accumulated electron dense LDs.
			(*208*)	The protein alpha-synuclein was less effective at regulating triacylglycerides turnover and showed variable distribution on LDs.
	Median Eminence	Tanycyte	(*243*)	As rats aged, the number and size of LDs increased. Degenerate bodies also developed with age and were interspersed with large LDs.
	Olfactory Bulbs	Neurons	(*244*)	LDs are manifestations of cell response to injury.
	Perineurium	Perineurial Glia	(*245*)	LD formation was found to be an early reactive change to ischemia in perineurial, endothelial, and Schwann cells.
	Pineal Gland	Pinealocyte	(Johnson, 1980)	Removal of the hypophysis led to a significant loss of LDs in the pineal gland.
	Pituitary Gland	Folliculostellate	(*246*)	Following the withdrawal of estrogen from estrogen primed male rats, folliculo-stellate cells became packed with LDs.
		Neuron	(*247*)	Supraopticus and paraventricularis neurons showed an increased number of LDs following ischemia.

Rat (cont.)	Striatum	Neuron	(*248*)	LDs were observed in neurons of rats injected with kainic acid to simulate HD.
	Whole Brain	Glia	(*249*)	Macrophages and astrocytes played important roles in lipid metabolism.
			(*250*)	LDs reached a maximum at 7 days following middle cerebral artery occlusion and were localized mainly within microglia in the ischemic core and within astrocytes in the penumbra.
Mouse	Choroid Plexus	Astrocyte	(*251*)	LD-like droplets were frequently found in several brain regions of senescence-accelerated mice.
		Macrophage	(*252*)	About half of the macrophages in the brains studied were distended due to excess LDs or foamy aggregations.
		Various	(*253*)	LDs appeared in the choroid plexus with increased age.
	Cortex	Astrocyte	(*254*)	Inhibition of diacylglycerol acyltransferase blocked oleic acid induced LD accumulation and lipotoxic cell death in astrocytes.
		Autolysosome	(*255*)	Lipid species were elevated in an AD mouse model and impeded macroautophagy and clearance of lipids.
	Hippocampus	Neuron, glia	(*256*)	Neuronal loss and glial cell proliferation was associated with changes in lipid related transcripts.
			(*173*)	Neurons expelled fatty acids in association with ApoE-positive lipid particles. Nearby astrocytes

Mouse (cont.)				then engulfed them and stored them as LDs.
		Microglia	(*171*)	A LD-accumulating subset of microglia were defective in phagocytosis, produced high levels of ROS, and secreted pro-inflammatory cytokines.
	Hypothalamus	Astrocyte	(*187*)	Hypothalamic astrocytes accumulated LDs and had increased astrogliosis markers along with increased levels of inflammatory cytokines.
		Tanycyte	(*257*)	LD signal in the tanycyte layer was higher in high fat diet mice and returned to normal under telmisartan treatment.
			(*258*)	A high fat diet increased the number and size of LDs in tanycytes.
	Mesencephalon	Neuron	(*259*)	Lipid dysregulation in PD involved upregulated expression of Plin4, increased intracellular LD deposition, and loss of neurons.
	Neostriatum	Various	(*260*)	Pericytes contained LDs in the neostriatum, indusium griseum, and anterior commissure at varying ages.
	Supraoptic Nucleus	Neuron	(*261*)	Neurons stimulated with CDP-choline displayed LDs in their cytoplasm.
	Subventricular Zone	Neuronal stem	(*180*)	Cells with increased numbers of large LDs showed heighted signs of quiescence and metabolic disturbance
			(*181*)	Impaired fatty acid metabolism suppressed neural stem cell activity while oleic acid signaling

Mouse (cont.)				interference rescued stem cell regenerative function
	White Matter	Various	(*262*)	Macrophages in mice Creutzfeldt-Jakob disease were filled with LDs.
	Whole Brain	Glia	(*263*)	Mice fed high fat diets had increased LDs and cells with more LDs were more likely to be senescent. Clearing senescent cells from restored neurogenesis and alleviated anxiety related behavior.
	Whole Brain	Neuron	(*264*)	Postmortem AD brains and 3xTg mice were shown to accumulate neutral lipids in ependymal cells.
		Various	(*175*)	Cerebral lipid loaded cells displayed a variety of distinct phenotypes based on their location in the brain. Lipid loaded cell numbers increased with age.
	Cortex	Glia	(*265*)	ND23 knockdown in glial cells created massive LD accumulation and induced brain degeneration.
Fly	Cortex	Glia	(*266*)	LDs were localized in glial cells and were enriched in the cortex.
	Whole brain	Neuronal stem	(*267*)	LDs played an antioxidant role in neural stem cells by reducing ROS and protecting against peroxidation.
	Hypothalamus	Neuron	(*268*)	Large LDs were found in CSF contacting neurons.
	Various	Glia	(*192*)	ROS and neuronal mitochondrial dysfunction contributed to LD accumulation prior to the onset of neurodegeneration.

Other	Various	Neuron	(*269*)	Air pollution caused ApoE-positive LDs to be deposited in smooth muscle cells and pericytes.
In vitro	In vitro	Glia	(*179*)	GRAF1a was found on LDs in primary glial cells that were fed oleic acid. Overexpression of GRAF1a promoted LD clustering and perturbed lipolysis.
			(*185*)	LPS treated microglia accumulated LDs and Plin2 colocalized with droplets.
			(*186*)	TGRL lipolysis increased the BBB transfer coefficient, induced droplet formation in astrocytes, activated cell stress pathways, and increased inflammatory cytokine levels.
			(*126*)	E4 astrocytes have increased lipid content compared to E3 astrocytes. LDs provide energy substrates.
		HeLa	(*208*)	PD mutations in a-synuclein showed less variable LD distribution and less effective TG turnover. Synuclein formed oligomers within cells and associated with droplets.
		N41	(*270*)	Cells treated with LPL accumulated lipid into droplets.

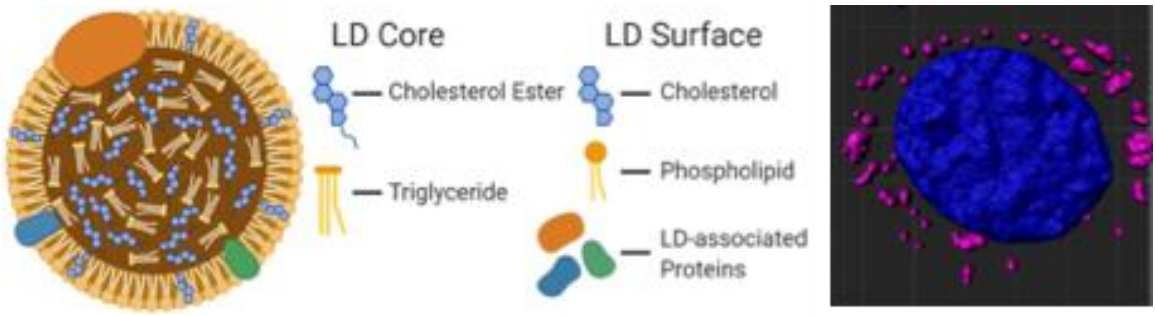

Figure 3.1 A diagram of the molecular structure of a standard lipid droplet (LD) along with a software reconstruction of a microscopic image of astrocytes *in vitro* containing LDs (highlighted in pink; LipidSpost) surrounding a nucleaus (in blue; DAPI).

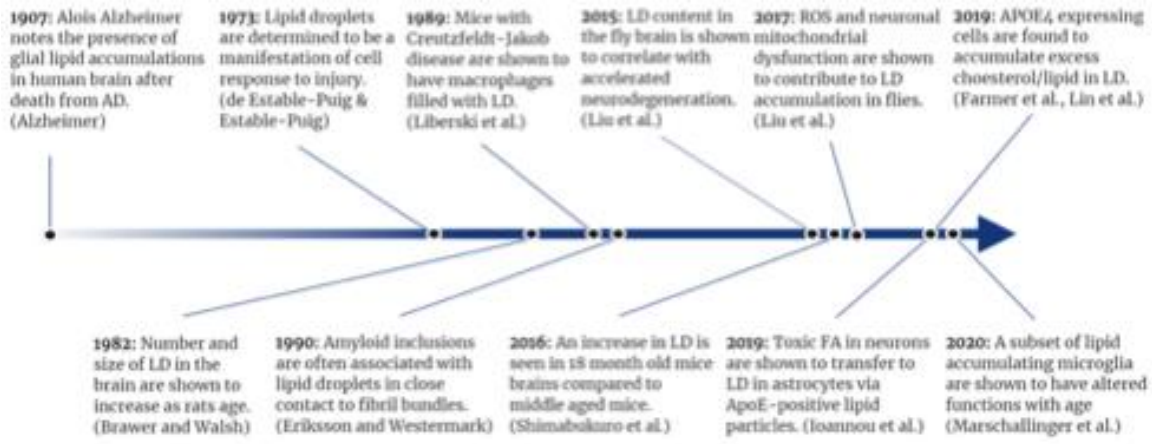

Figure 3.2 A timeline of selected lipid droplet discoveries as they relate to neurodegenerative disease

CHAPTER 4. APOE4 ALTERS FATTY ACID METABOLISM AND INCREASES LIPID DROPLET FORMATION IN ASTROCYTES

[This chapter consists of material adapted from a published manuscript: **Farmer BC**, Kluemper JC, Johnson LA. Apolipoprotein E4 Alters Astrocyte Fatty Acid Metabolism and Lipid Droplet Formation. *Cells*. 2019 Feb. PMID: 30791549. For supplementary materials pertaining to this chapter, see appendix 1.]

ABSTRACT

Lipid droplets (LDs) serve as energy rich reservoirs and have been associated with apolipoprotein E (*APOE)* and neurodegeneration. The E4 allele of *APOE* (E4) is the strongest genetic risk factor for the development of late onset Alzheimer's disease (AD). Since both E4 carriers and individuals with AD exhibit a state of cerebral lipid dyshomeostasis, we hypothesized that *APOE* may play a role in regulating LD metabolism. We found that astrocytes expressing E4 accumulate significantly more and smaller LDs compared to E3 astrocytes. Accordingly, expression of perilipin-2, an essential LD protein component, was higher in E4 astrocytes. We then probed fatty acid (FA) metabolism and found E4 astrocytes to exhibit decreased uptake of palmitate, and decreased oxidation of exogenously supplied oleate and palmitate. We then measured oxygen consumption rate, and found E4 astrocytes to consume more oxygen for endogenous FA oxidation and accumulate more LD-derived metabolites due to incomplete oxidation. Lastly, we found that E4 astrocytes are more sensitive to carnitine palmitoyltransferase-1 inhibition than E3 astrocytes. These findings offer the potential for further studies investigating the link between astrocyte lipid storage, utilization, and neurodegenerative disease as a function of *APOE* genotype.

4.1 Introduction

Apolipoprotein E (apoE) is associated with circulating lipoproteins, specifically very low-density lipoproteins and high-density lipoproteins **(*271*)**. The polymorphic *APOE* gene encodes for three isoforms, E2, E3, and E4, with frequencies of 8%, 77%, and 15%, respectively, in the general US population **(*59*)**. E4 is the strongest genetic risk factor for late onset Alzheimer's disease (AD) **(*59*)**. In addition to established effects on AD neuropathology, *APOE* genotype is also recognized as a strong modulator of cerebral metabolism (*4, 68, 272, 273*). In fact, cognitively normal E4+ individuals demonstrate alterations in cerebral fatty acid (FA) and carbohydrate metabolism congruent with AD patients (*3, 4*). Understanding the metabolic effects of apoE in the brain may be a critical step in discovering the underlying mechanism(s) of E4-driven AD risk.

The brain is one of the largest site of apoE synthesis, second to the liver **(*274*)**. The majority of brain apoE is astrocyte derived, though under certain conditions such as trauma, neurons and microglia also synthesize apoE **(*275*)**. ApoE binds to receptors of the low-density lipoprotein receptor family, which are expressed on astrocytes as well as neurons **(*276*)**. Astrocytes aid in shuttling lipids from the blood-brain barrier (BBB) to neurons by both binding and internalizing BBB permeable FAs from the endothelial cells, and loading lipid-free apoE with cargo through action of the ATP-binding cassette transporters such as ABCA-1 **(*277, 278*)**. Therefore, astrocytes are key players in the lipid uptake-apoE-lipidation axis, and are vital to maintaining brain lipid homeostasis and proper neuronal function. Not only are astrocytes critical for uptake and export of FAs and lipid-loaded lipoproteins, they also are the main cell population mediating β-oxidation of FAs in the brain **(*279, 280*)**. Astrocytes contain a higher relative density of mitochondria than the

surrounding neuropil, giving them superior machinery to oxidize FA **(*281*)**. Furthermore, carnitine palmitoyltransferase-1 (CPT-1), an essential enzyme for the beta-oxidation of long chain FA, is preferentially expressed in astrocytes compared to neurons, microglia, and oligodendrocytes **(*282*)**. Recent studies clearly show that the brain does in fact utilize a significant amount of FAs, with some reports estimating FAs are responsible for up to 20% of cerebral ATP generation **(*280, 283*)**.

Lipid droplets (LD) are organelles containing triacylglycerols and cholesterol esters surrounded by a layer of amphipathic lipids and associated proteins. Once thought to be inert cellular depots of fat, lipid droplets are now considered to be dynamic organelles that play a role in various metabolic diseases **(*139, 284*)**. Indeed, the overaccumulation of LDs has been linked to atherosclerosis, metabolic syndrome, cancer, and diabetes **(*285, 286*)**. However, only recently have studies begun to address the potential pathological consequences of abnormal LD accumulation in the brain **(*284*)**. Although low amounts of LD are observed in the brain under normal conditions **(*165*)**, studies have noted increased LD content in neurodegenerative conditions such as Parkinson's **(*208*)** and AD **(*181, 219*)**. Interestingly, Alois Alzheimer noted glial lipid accumulation in his first description of AD pathology **(*218*)**, but this has gone relatively unstudied apart from a few reports linking LDs and AD **(*128, 181*)**. Recent findings suggest that glial cells within the brain form LD as a function of neuronal stress, and in the fly brain this process is apoE dependent **(*128*)**. Astrocyte derived E4 has been shown to promote LD formation in fibroblasts **(*287*)**, and iPSC-derived astrocytes expressing E4 exhibit increased lipid storage in the form of cholesterol (*34*). E4 astrocytes also show varied expression of numerous genes associated with lipid metabolism and transport, compared to those expressing E3 (*34*). However,

apoE-isoform specific modulation of LD accumulation and FA metabolism in astrocytes has not been previously described.

In this study, we characterize an increase in lipid droplet formation and endogenous FA utilization in E4 astrocytes, as well as decreased uptake and oxidation of exogenous FAs. These lipid metabolism events influenced by *APOE* offer both targets for future late onset AD therapies and potential for more studies analyzing the metabolic effects of *APOE* in the brain.

4.2 Methods

4.2.1 Cell Culture

E3 and E4 expressing astrocytes were derived from targeted replacement mice expressing human *APOE3* or *APOE4* (kind gift from Dr. David Holtzman). These cell lines secrete apoE in high density lipoprotein-like particles at equivalent levels to primary astrocytes from targeted replacement APOE knock-in mice and have been relied upon for studies of APOE's role in astrocyte metabolism by many groups **(*91-93, 97*)**. Cells were maintained in Advanced Dulbecco's Modified Eagle Medium (DMEM) (Gibco, Carlsbad, CA, USA) supplemented with 1 mM sodium pyruvate, 1× Geneticin, and 10% fetal bovine serum. For imaging experiments, cells were grown on sterilized coverslips in 6-well plates pre-treated with poly-L. For lipid loading experiments, 250 µM oleate pre-conjugated to bovine serum albumin (BSA) (Sigma, St. Louis, MO, USA) was added to the media 24 h prior for lipid droplet induction as previously described **(*288*)**.

4.2.2 Western Blotting

Cells were lysed on ice using radioimmunoprecipitation assay Buffer (Thermo Fisher Scientific, Waltham, MA, USA) with 1× proteinase inhibitor (Sigma, St. Louis, MO, USA). Protein concentration was determined by Pierce bicinchoninic acid (BCA) protein assay (Thermo Fisher Scientific, Waltham, MA, USA). 20–30 µg of protein was diluted with 2× Laemmli Sample Buffer (Bio-Rad Laboratories, Hercules, CA, USA) and heated at 100 °C for 10 min. Protein samples were then loaded on 4–20% PROTEAN TGX gels (Bio-Rad Laboratories, Hercules, CA, USA) for SDS-PAGE. Gels were transferred using a Trans-Blot Turbo Transfer system (Bio-Rad Laboratories, Hercules, CA, USA) onto polyvinylidene fluoride membrane. Membranes were then blocked for 2 h in 1% casein and then incubated overnight in primary antibody solution (1:1000 PLIN-2 (Novus Biologicals, Centennial, CO, USA); 1:1000 APOE (Abcam Inc., Cambridge, MA, USA); 1:1000 β-actin (Novus)) at 4 °C. Membranes were then washed three times for five minutes each with PBS, pH 7.4, 0.05% Tween-20, and then incubated with secondary antibody solution (1:10,000 Goat α rabbit IR 680 (LI-COR, Lincoln, NE, USA); 1:5000 goat α mouse IR 800 (LI-COR)) for 2 h at room temperature. Membranes were then washed as before, with an additional two 10 min washes in PBS. Images were acquired on a LI-COR Odyssey Infrared Scanner. Resulting images were exported to ImageJ for blot densitometry and quantification.

4.2.3 Lipid Droplet Imaging

After lipid incubation, coverslips were lifted from the wells and cells were fixed for 15 min in 4% PFA, washed 1× with PBS, and incubated for 30 min in 1:1000 LipidSpot

(Biotium, Fremont, CA, USA). Coverslips were then mounted onto slides using Fluoroshield mounting media with DAPI (Abcam). Slides were kept at 4 °C. Wide field images were obtained on a Nikon Ti2 microscope using a 20× objective. Single cell images were obtained on a Nikon A1R Laser Scanning Confocal Microscope (Nikon, Tokyo, Japan) using an oil immersed 100× objective. Astrocytes were selected in the 405 channel (DAPI-stained nuclei) and then the 610 channel was added (LipidSpot-stained LDs) and the images were captured. Z-stacks were taken in a range of 10 µM, 40 images per stack. 3-D reconstructions were processed in Imaris 9.2 software using the surfaces module to obtain statistics for lipid droplets. Experimenter was blind to slide identity and slides were processed in random order under identical microscope settings.

4.2.4 Fatty Acid Uptake Assay

Astrocytes were plated at 50,000 cells/well in CytoStar T plates (Perkin Elmer, Waltham, MA, USA) and allowed to grow to confluency. Media was aspirated, and new glucose free media supplemented with either 0.5 µCi/mL ^{14}C-palmitate or ^{14}C-oleate (Perkin Elmer) was added to the wells. Scintillation bead technology in the wells emitted light proportionate to the cellular uptake of the FA **(*289*)**. Radioactivity counts were read on a Microbeta 2 Microplate Counter (Perkin Elmer) and normalized to protein content in the well using a BCA assay (Thermo Fisher Scientific, Waltham, MA, USA).

4.2.5 Fatty Acid Oxidation Assay

Astrocytes were plated in a 24-well plate at 300,000 cells/well and allowed to grow to confluency for 24 h. Using a previously published protocol **(*290*)**, cells were then incubated with 0.5 µCi/mL [1-^{14}C] palmitate or 0.5 µCi/mL [1-^{14}C] oleate for 24 or 3 h.

For the pulse experiment (exogenously supplied FA) radiolabeled FAs were added in nutrient depleted media (Glucose Free DMEM; 5% FBS) for 3 h. Buffered $^{14}CO_2$ in the media was then liberated by addition of 1 M hydrochloric acid and captured on a filter paper disc pre-soaked with 1N sodium hydroxide. For the pulse chase experiment (endogenous FA), radiolabeled FAs were added in nutrient rich media (25 mM Glucose; 10% FBS) for 24 h, then aspirated and nutrient depleted media was added to promote oxidation of fatty acid from intracellular lipid pools. Radioactivity of the filter paper was measured in a Microbeta 2 Microplate Counter after addition of 3 mL Ultima-Gold Scintillation Fluid. Acid soluble metabolites, which represent incomplete oxidation of the fatty acids, were extracted from the media and cellular fractions. Total protein from each well was assayed using a BCA assay (Thermo) and all radioactivity measures were normalized to protein content.

4.2.6 Seahorse Extracellular Flux Analysis

Astrocytes expressing E3 or E4 were seeded in a 96-well microplate at 50,000 cells/well and left to form a monolayer overnight. Media was aspirated and 135 µL of limited nutrient running media (DMEM; 5 mM glucose, 2.5 mM carnitine, 5 mM 4-(2-hydroxyethyl)-1-piperazineethanesulfonic acid) was added to each well and allowed to incubate for 1 h. Then 30 µL of 1 mM sodium palmitate complexed to BSA (6:1 molar ratio) or BSA alone was added to wells according to group assignment, at which point the oxygen consumption rate (OCR) was determined by a Seahorse Extracelluar Flux Analyzer xF96 (Agilent, Santa Clara, CA). At each successive 18 min, an injection of 200 µM etomoxir, 1 µM oligomycin, or 1 µM Rotenone | Antimycin was added to each well to inhibit carnitine palmitoyltransferase-1 (CPT-1), ATP synthetase, or complex I and III

respectively. OCR was measured every 6 min. Values were normalized to protein content in each well by a BCA Assay (Thermo). OCR from endogenous FA oxidation was determined by calculating the average etomoxir effect in BSA treated astrocytes (Equation (1)).

$$\overline{OCR}_{Endo\ FAO} = \overline{OCR}_{Pre-Eto\ Control} - \overline{OCR}_{Post-Eto\ Control} \quad (1)$$

OCR from exogenous FA oxidation was determined by calculating the average difference in basal OCR in the palmitate treated astrocytes versus the basal OCR in BSA treated astrocytes (Equation (2)).

$$\overline{OCR}_{Exo\ FAO} = \overline{OCR}_{Pre-Eto\ PA} - \overline{OCR}_{Pre-Eto\ Control} \quad (2)$$

4.2.7 Statistical Analysis

All data are expressed as mean ± standard error. Comparisons between two groups were analyzed by *t*-test. Multiple groups and/or multiple time points were analyzed using ANOVAs (Prism, Graphpad, San Diego, CA, USA), or repeated measures ANOVA (time × groups) (SPSS). Statistical significance was determined using an error probability level of $p < 0.05$ corrected by a false discovery rate (FDR) analysis (Benjamini Hochberg method).

4.3 Results

4.3.1 E4 Astrocytes Display Increased LD Count, Increased Cellular LD Volume, Decreased LD Size

We first asked if APOE influences lipid storage within astrocytes. To answer this, we lipid-loaded E3 and E4 astrocytes with 250 μM oleate for 24 h, stained for neutral LDs (Figures 1A and S3A), and quantified LDs per cell (Figures 1B and S3B). E4 astrocytes showed a significant increase in the number of LDs, both at basal levels and in a FA-rich environment, compared to E3. (Figure 4.1B) Total LD volumes within the cell were also analyzed, and E4 astrocytes held significantly more lipid volume under lipid loaded conditions compared to E3. (Figure 4.1C). Furthermore, expression of perilipin-2 (PLIN-2), a LD associated protein, was increased in E4 astrocytes in an FA-rich environment compared to E3. (Figure 4.1D–E; Appendix 2.1).

To determine LD size and distribution, LDs in individual cells were rendered using Imaris software under control and lipid-loaded conditions (Figure 4.2A), and volumes were quantified (Figure 4.2B–D) and binned using 0.1 μm as a bin size. It was found that E4 astrocyte LDs were on average 54.8% smaller on a volume per droplet basis than E3s under control conditions, and 33.7% smaller when lipid-loaded. Together, these results suggest that E4 astrocytes form more LDs than E3 astrocytes regardless of FA exposure, as reflected in increased expression of PLIN-2 and an increased LD count.

4.3.2 E4 Astrocytes Take Up Less Palmitate

Hypothesizing that an increase in lipid storage may be a result of increased uptake of FAs, we next sought to determine if APOE regulates astrocyte FA uptake. Using a scintillation proximity assay and treating with ^{14}C-labeled FAs, we found E4 astrocytes to take up significantly less palmitate (Figure 4.3A–B), with no significant difference in oleate uptake (Figure 4.3C). Conversely, there was a trend toward increased oleate uptake in E4 astrocytes, with cumulative uptake slightly higher when expressed as the area under curve despite lacking statistical significance. (Figure 4.3D) These data suggest that *APOE* isoforms may modulate FA uptake in astrocytes dependent on the FA species.

4.3.3 E4 Astrocytes Oxidize Less Exogenous Fatty Acids

We next examined how APOE might regulate FA oxidation in astrocytes. We first assessed how E3 and E4 astrocytes oxidize exogenously supplied FA. We treated cells with radiolabeled palmitate or oleate for 3 h in a nutrient depleted media, and captured the oxidation product CO_2, as well as incompletely oxidized products of FA metabolism in the form of acid soluble metabolites (ASM). (Figure 4.4A). We found that E4 astrocytes oxidize significantly less exogenously supplied oleate and palmitate than E3 astrocytes (Figure 4.4B), and instead accumulate significantly more metabolites that are acid soluble (Figure 4.4C–D); these ASM include ketone bodies, acyl carnitines, citric acid cycle intermediates, and FA less than six carbons in length (*290*). We found an increased concentration of these ASM inside E4 cells (Figure 4.4C). We also found an increased concentration of ASM in the media (Figure 4.4D), suggesting that E4 astrocytes may export more FA metabolites than E3s. Using Seahorse Extracellular Flux Analysis, we then measured the oxygen consumption rate (OCR) before and after inhibition of CPT-1 in E3 and E4 astrocytes supplied with palmitate in the media (Figure 4.4E). We found E4

astrocytes to exhibit a lower OCR compared to E3 at all time points (Figure 4.4E). This lower OCR is likely primarily due to a decreased rate of glucose oxidation, as E4 is strongly associated with a phenotype of glucose hypometabolism (*4*, *48*). When we specifically calculated the contribution of FA oxidation to OCR by comparing basal OCR in palmitate treated versus BSA treated astrocytes, we found that E4 astrocytes utilize significantly less exogenously supplied FA as part of their basal respiration. (Figure 4.4F)

Since E4 astrocytes showed a significant increase in LD accumulation, we next studied how APOE modulates FA oxidation from intracellular FA pools. Knowing that incubation with oleate for 24 h induces LD formation, we "pulsed" E3 and E4 astrocytes with radiolabeled FAs for 24 h to incorporate the radiolabel into LDs (Figure 4.5A). We then aspirated the media, washed with PBS, and captured oxidation and non-oxidation products of the intracellular FAs after a 4 h "chase". Interestingly, in contrast to the oxidation of exogenously supplied FA, E3 and E4 astrocytes showed no difference in CO_2 production from intracellular pools of oleate or palmitate (Figure 4.5B). Quantification of ASMs of intracellular palmitate and oleate revealed that E4 astrocytes once again exported significantly more ASM into the media (Figure 4.5C), and have similar levels within the cells (Figure 5D). We next quantified OCR using Seahorse in E3 and E4 astrocytes that were incubated in serum free media and not supplied with exogenous FA (Figure 4.5E), assuming the only source of FA would be from intracellular LDs. We found that the OCR in E4 astrocytes that could be attributed to oxidation of endogenous FA was significantly higher than E3 astrocytes, suggesting that while CO_2 production is similar between genotypes, E4 astrocytes seem to consume more oxygen from the metabolism of intracellular FAs (Figure 4.5F). Together these data suggest that APOE alters FA oxidation

in astrocytes, and that these effects differ depending on the source of FAs (endogenously stored as LD vs exogenously supplied in media)

4.3.4 E4 Astrocytes Are More Sensitive to CPT-1 Inhibition

Since CPT-1 is the rate-limiting enzyme of fatty acid oxidation, we hypothesized that E3 and E4 astrocytes may exhibit varying responsiveness to CPT-1 inhibition. Using Seahorse, we measured OCR before and after CPT-1 inhibition with etomoxir and assessed the percent change in OCR from baseline in E3 and E4 astrocytes pretreated with palmitate and the non-pretreated control cells (Figure 4.6A). We found that E4 astrocytes have a significantly larger drop in OCR after CPT-1 inhibition compared to E3 astrocytes in both pretreated and control cells, suggesting an increased reliance on FA oxidation for overall OCR (Figure 4.6A).

To determine if CPT-1 inhibition results in APOE genotype specific effects on palmitate and oleate oxidation, we used a $^{14}CO_2$ trap approach and found E4 astrocytes to exhibit a greater fold change in oxidation of palmitate from the baseline after CPT-1 inhibition (Figure 4.6B). However, we saw no differences between genotypes with regards to the etomoxir effect on oleate oxidation (Figure 4.6B), again suggesting these APOE effects may be specific to certain FA species.

4.4 Discussion

Lipid droplets in astrocytes serve to both sequester fatty acids that would otherwise be cytotoxic if free in the cytoplasm and to offer an energy rich and accessible pool for

cellular metabolic needs in times of starvation and stress. Recent studies of AD brain tissue have demonstrated an increase in LDs (*181, 219*). ApoE is an important component of peripheral and central nervous system lipoproteins, which share many biochemical features with LDs (*139*). The E4 allele of *APOE* is a critical genetic risk factor for late onset AD, and is strongly associated with a number of metabolic abnormalities (*4, 34, 42, 47*). However, the link between E4 and LD biology has not been widely explored. In the current study, we characterized a number of apoE isoform specific differences in LD formation and FA utilization in astrocytes.

We found that E4 astrocytes form many small LDs compared to the few large LDs observed in E3 astrocytes. The structural makeup of LDs could be a contributor to overall LD size. Surfactant lipids such as phosphotidylcholine (PC) are known to stabilize LD emulsions, while more fusogenic lipids, such as phosphatidic acid, promote LD coalescence (*139, 291*). Our group previously showed that E4 mice brains differ in various lipid concentrations using an unbiased metabolomics approach(*51*). Interestingly, Heinsinger et al. recently showed that the apoE isoforms are associated with varying sizes of CNS lipoproteins, with E4 individuals and astrocytes synthesizing smaller apoE-associated lipoprotein particles (*292*). As the structure and makeup of LDs and lipoproteins are similar, it is possible that E4 promotes smaller spherical lipid carriers whether that be inside or outside the cell. Overall isoform specific effects on FA metabolism could also be a result of differing total concentrations of apoE. E4 astrocytes are known to secrete less apoE into the media and have less intracellular apoE (Figure S2) (*97*), and E4 brains from targeted replacement mice have less apoE (*293*). Whether the lower quantity of apoE4 in E4 carriers is related to disease pathogenesis is unknown.

LD associated proteins, such as perilipins, serve to stabilize the LD from excessive lipolysis. Loss of perilipin-2 has been associated with an increase in endogenous fatty acid oxidation (*294*). We found that E4 astrocytes exhibit increased expression of perilipin-2, decreased exogenous FA oxidation, and increased oxygen consumption from endogenous fatty acid oxidation. Overexpression of PLIN2 has been liked to a decrease in glucose uptake by LD sequestration of key regulators of glucose transporters (*295*). In unpublished work, our group found that E4 down-regulates astrocyte glucose metabolism, much like the effects reported in neuronal models of apoE overexpression (*47*). It may be that the energetic needs of an E4 astrocyte in the absence of robust glucose metabolism overpower the inhibitory effect of PLIN2 on LD lipolysis. The overexpression of PLIN2 has also been shown to increase LD formation in various cell types (*190, 296, 297*). This is congruent with our findings in regards to E4 astrocytes, where an increase in LD number paralleled with increased PLIN2 expression. In hepatocytes, increased levels of reactive oxygen species (ROS) prompt increased *PLIN2* expression subsequent LD formation (*190*). ROS has been linked to LDs in glia in a Drosophila model as well, and this process was found to be apoE dependent (*128, 192*). Oxidative stress as an inducer of LDs in astrocytes as a function of *APOE* deserves further investigation in light of the poor anti-oxidant capacity of E4 (*298*). Alternatively, the presence of many small droplets as opposed to larger droplets could be a result of increased FA oxidation resulting from LD turnover. More studies are needed in CNS in vitro models to define LD metabolism and how it may differ from peripheral LD metabolism.

E4 carriage in humans seems to promote an “accelerated AD” status, particularly in terms of cerebral glucose metabolism (*4*). Namely, as individuals transition through mild

cognitive impairment to AD, glucose metabolism progressively decreases in several distinct brain regions (*299, 300*). E4 individuals, however, show a state of glucose hypometabolism in these same regions even in the absence of cognitive impairment, and as early as the third decade of life (*3*). LDs are known to increase in cerebral density with age and are found in GFAP+ cells (*175*). E4 carriers show an accelerated development of AD neuropathology and cognitive symptoms, and astrocytes have been shown to play a key role in E4-driven AD pathogenesis (*301*). Perhaps this accelerated AD phenotype in E4 individuals extends to cerebral LD accumulation as well.

It has been proposed that E4 carriers may be at risk for cognitive decline because of an E4-driven disruption in FA metabolism (*302, 303*). Here we showed that APOE regulates fatty acid metabolism in the astrocyte depending on the saturation status of the fatty acid. We observed marked decrease in uptake of the fully saturated fatty acid palmitate in E4 astrocytes compared to E3 astrocytes while no difference was observed in oleate uptake. When we treated with etomoxir, we saw drastic reduction in oleate oxidation in both genotypes, but much less of a reduction in oxidation in E3 astrocyte palmitate oxidation compared to E4. These data may shed light on a phenomenon seen in epidemiological studies where E4 carriers respond well to an acute high fat meal (by cognitive measures and plasma AD biomarkers), while non-E4 carriers responded poorly (*10*). This may be due to a lower uptake of saturated fatty acids. Conversely, E4 carriers have been shown to exhibit increased uptake of unsaturated fatty acids, specifically docosahexaenoic acid (*304*). This could be related to the preventative effect of a Nordic diet rich in fish, fruits, and vegetables on cognitive decline in E4 individuals (*23*). Indeed, apoE isoform specific effects on lipid usage have been characterized systemically, wherein

E4 mice show a metabolic preference for oxidizing FAs (*111*). Related FA disturbances have been characterized in humans carrying E4. For instance, E4 carriers show greater uptake, brain incorporation, and whole-body β-oxidation of docosahexaenoic acid compared to non-E4 carriers (*28, 304*). In the current study, our data using ^{14}C-labeled FAs support the idea that E4 alters the flux of metabolites into the TCA cycle and because of this, decreases CO_2 production and increases metabolites that are acid soluble. Our group previously showed that E4 alters numerous pathways within the cerebral metabolome (*51*), and others have shown changes in TCA specific metabolites in the brain (*305*).

4.5 Conclusion

In this study we showed that E4 astrocytes display an increase in LD formation compared to E3 astrocytes. Specifically, E4 astrocytes have a higher number of smaller LD and increased expression of the LD marker PLIN2. We also observed increased oxygen consumption rates from endogenous fatty acid oxidation, decreased rates of exogenous fatty acid oxidation, and an increased sensitivity to CPT-1 inhibition in E4, compared to E3, astrocytes. While a number of important questions remain, we hope these initial findings will serve as a basis for the further study of APOE-associated alterations in astrocyte metabolism and future treatments of AD and other neurodegenerative diseases.

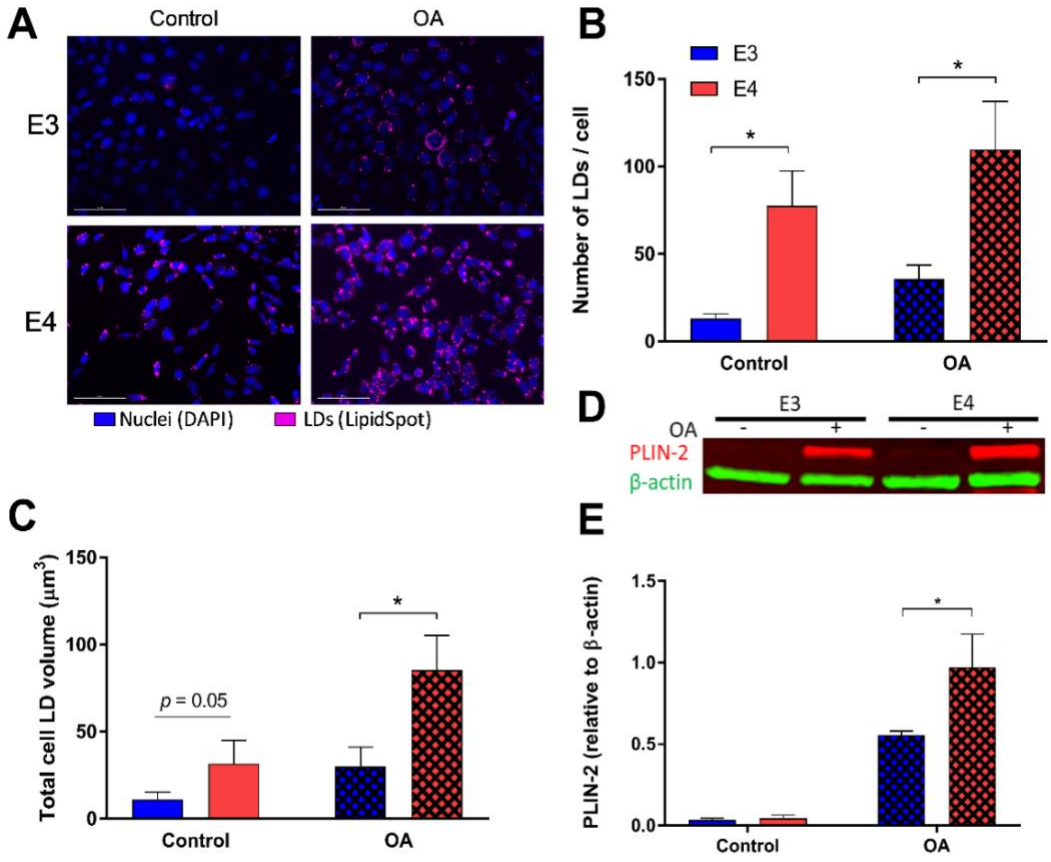

Figure 4.1 E4 astrocytes have increased lipid droplet (LD) count, LD volume, and LD associated protein.

(**A**) Astrocytes expressing either E3 or E4 were stained with LipidSpot to quantify lipid content under control conditions (left), and after 24 h oleic acid (OA) supplementation ("lipid-loaded"; right). The number of LDs per individual cell (**B**) and total LD volume per cell (**C**) were quantified. Values represented are means +/− SEM (n = 10). Data were analyzed by t-test for specific comparisons between means; * p <0.05. (**D**) Representiative image of the total expression of perilipin-2 (PLIN2) and β-actin in control or lipid-loaded E3 and E4 astrocytes was determined by SDS-PAGE and Western blotting and quantified (**E**). Values represent mean +/− SEM (n = 3). Data were analyzed by by t-test; * p <0.05. Scale bar = 100µm.

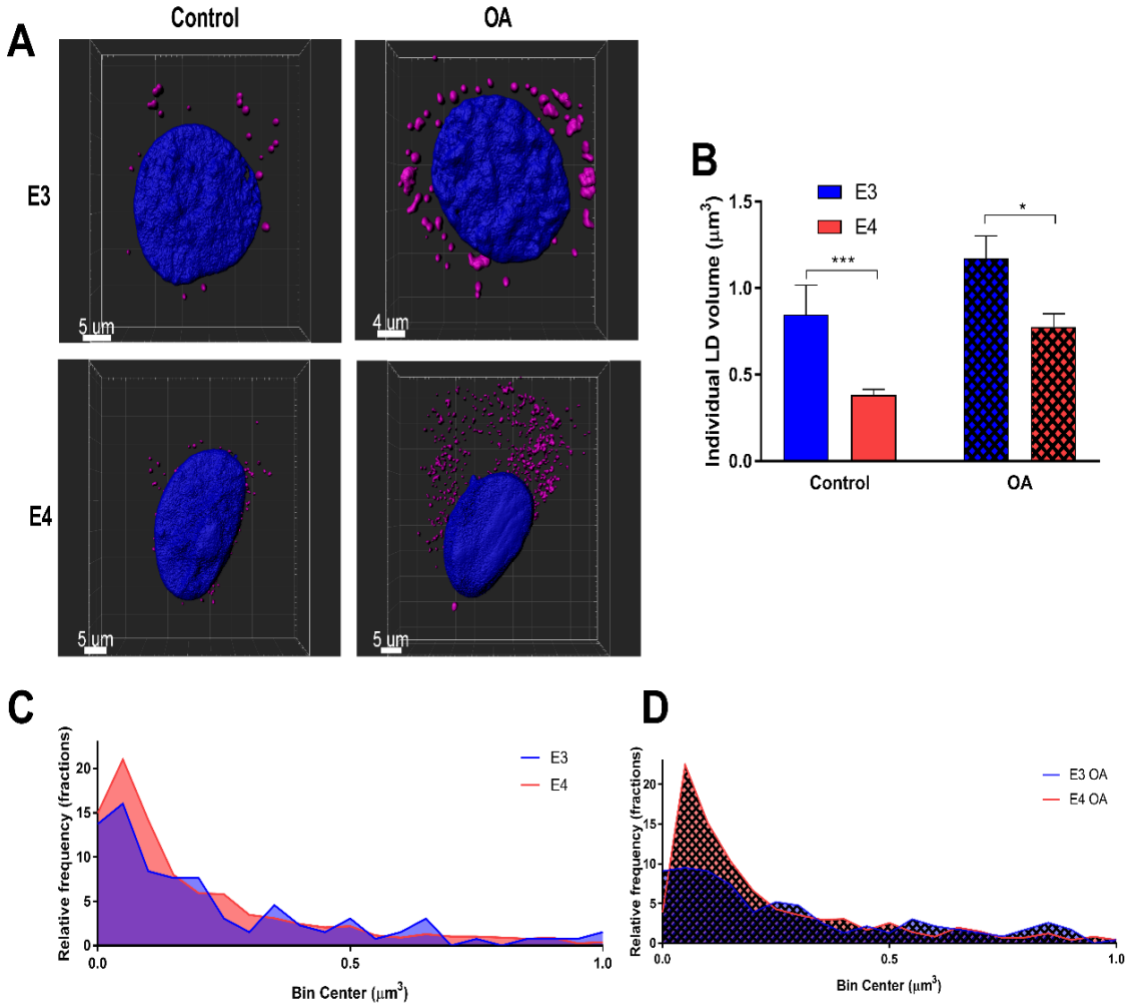

Figure 4.2 E4 astrocytes have smaller lipid droplets.
(**A**) Representative 3D renderings of E3 and E4 astrocytes stained with LipidSpot and DAPI under control and lipid-loaded conditions. (**B**) Individual lipid droplet (LD) volume was quantified under control and lipid-loaded conditions. Values represented are means +/− SEM. Data were analyzed by unpaired t-test; *** p <0.001, * p <0.05. (**C**) Relative frequencies of LD volumes were binned between 0 and 1 µm3 under control and (**D**) lipid loaded conditions. Bin size = 0.1 µm3. E3 control LDs (n = 131); E4 control LDs (n = 775); E3 OA LDs (n = 231); E4 OA LDs (n = 1208).

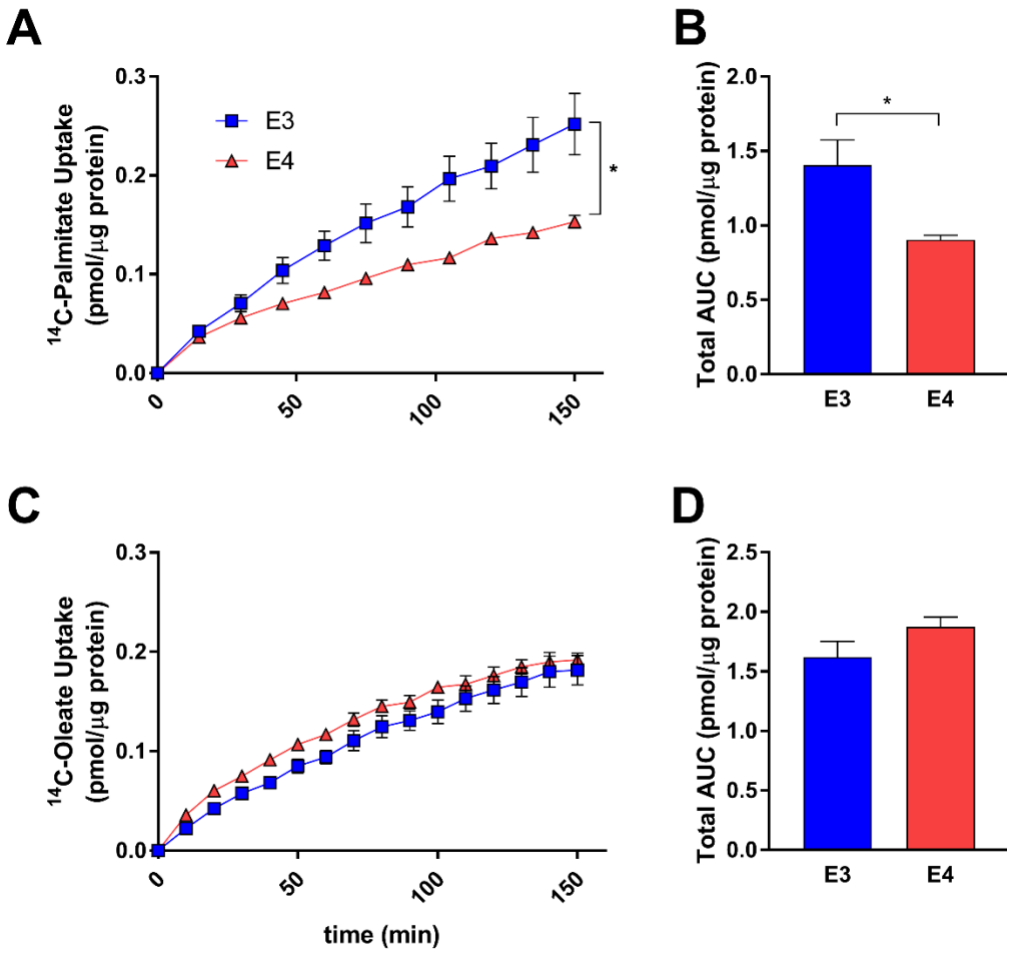

Figure 4.3 E4 astrocytes uptake less palmitate, but not oleate.
E3 and E4 astrocytes were treated with 0.5 µCi/mL [1-^{14}C] palmitate (**A**,**B**) or (**C**) [1-^{14}C] oleate (**C**,**D**) and uptake was measured over 150 min by a scintillation proximity assay. Values represent mean +/− SEM (n = 6). Data were analyzed by two-way ANOVA of repeated measures (**A**,**C**) or t-test (**B**,**D**); * p <0.05. Total area under the curve (AUC) was determined for palmitate (**B**) and oleate (**D**).

.

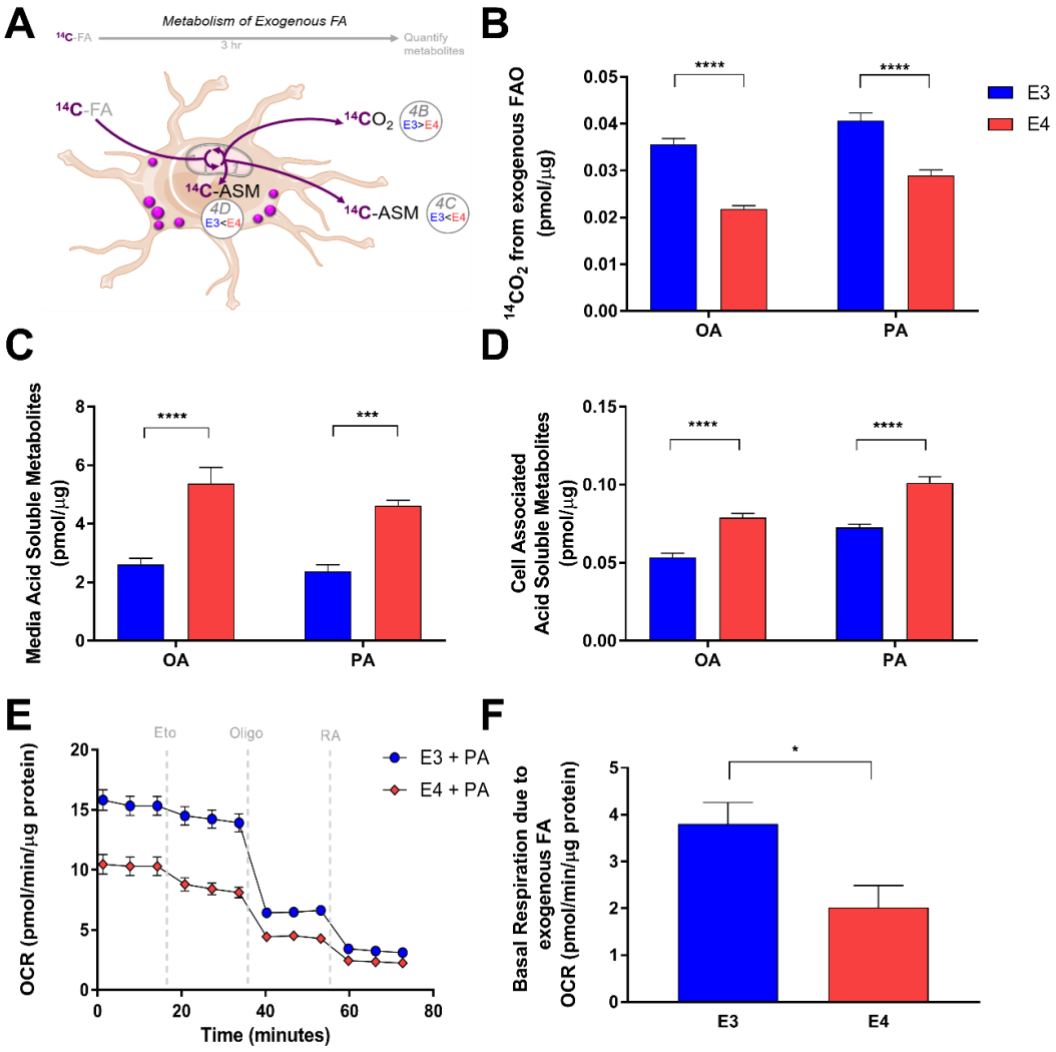

Figure 4.4 E4 astrocytes oxidize less exogenously supplied fatty acids.
(**A**) Schematic and summary of pulse experiment to determine oxidation of exogenously supplied fatty acids. (**B**) E3 and E4 astrocytes were treated with [1-^{14}C] oleate (OA) or [1-^{14}C] palmitate (PA) and oxidation was measured over 3 h by a CO_2 trap assay. Acid soluble metabolites were quantified in media (**C**) and intracellular (**D**) fractions. Values represent mean +/− SEM (n = 6). Data were analyzed by t-test;*** $p < 0.001$, **** $p < 0.0001$. (**E**) E3 and E4 astrocytes were pretreated for 1 h with palmitate and subjected to a Seahorse Extracellular Flux Fatty Acid Oxidation Assay. Vertical gray dashes indicate time points of pharmacological injections of etomoxir (Eto), oligomycin (Oligo), or Rotenone and Antimycin (RA). (**F**) Oxygen consumption due to FA oxidation of exogenously supplied palmitate was determined (see methods) and graphed. Values represent means +/− SEM (n = 3–4). Data were analyzed by unpaired t-test; * $p < 0.05$.

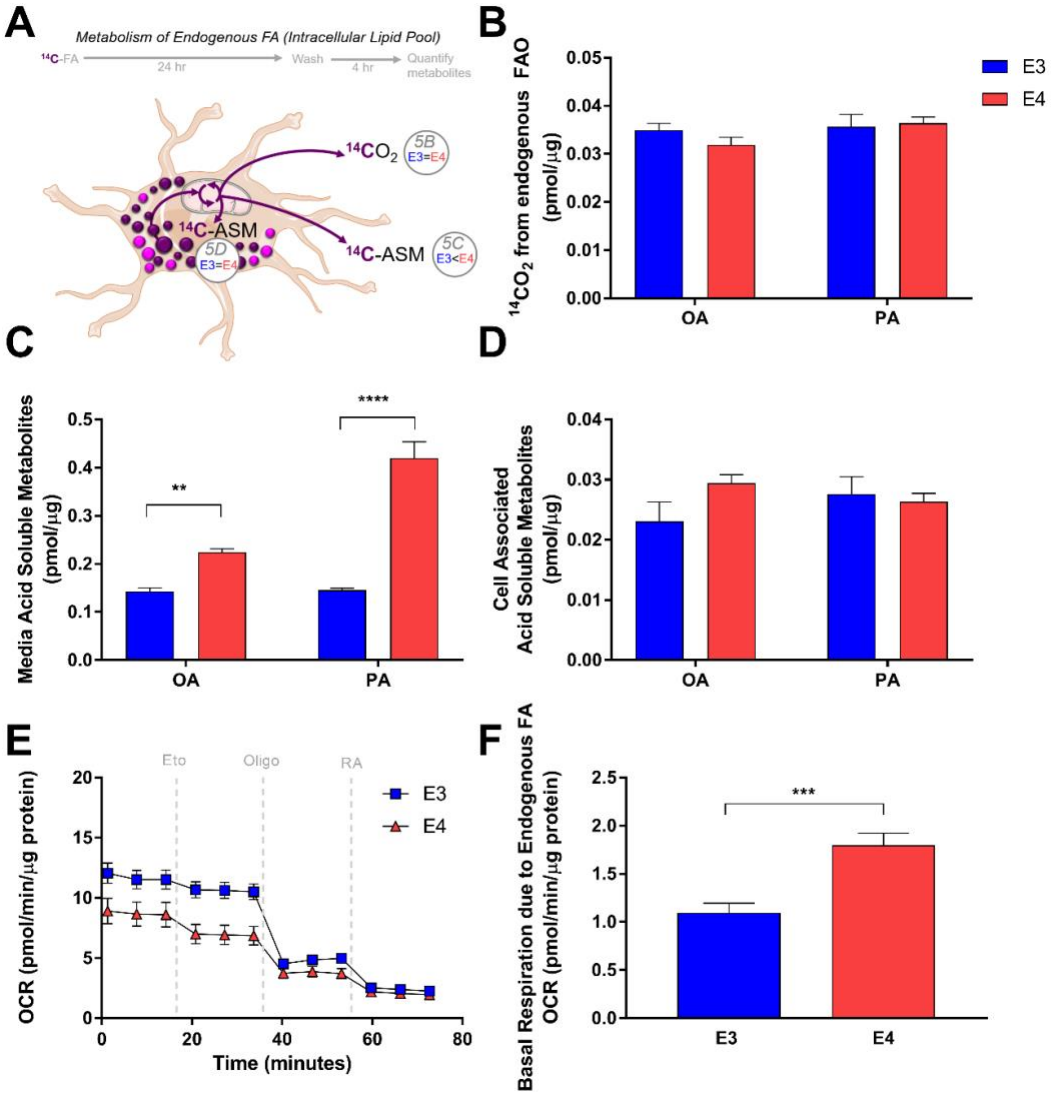

Figure 4.5 E4 astrocytes oxidize more endogenous fatty acids.
(**A**) Schematic and time-course of pulse-chase experiment to determine oxidation of endogenous fatty acids.. (**B**) E3 and E4 astrocytes were treated with 1 μCi/mL [1-^{14}C] oleate (OA) or [1-^{14}C] palmitate (PA) combined with non-labelled isotopes to 200 μM in Advanced DMEM for 24 h, washed with PBS, and then oxidation was measured over 4 h in a nutrient depleted media by a CO_2 trap assay. Acid soluble metabolites were quantified in media (**C**) and intracellular (**D**) fractions. Values represent mean +/− SEM (n = 6). Data were analyzed by t-test; ** $p < 0.01$, *** $p < 0.001$; **** $p < 0.0001$. (**E**) E3 and E4 astrocytes were pretreated for 1 h with bovine serum albumin supplemented media and subjected to a Seahorse Extracellular Flux Fatty Acid Oxidation Assay. Vertical gray dashes indicate time points of pharmacological injections of etomoxir (Eto), oligomycin (Oligo), or Rotenone and Antimycin (RA). (**F**) Oxygen consumption due to intracellular FA oxidation was determined (see methods) Results were normalized to protein content. Values represent means +/− SEM (n = 3–4). Data were analyzed by unpaired t-test; *** $p < 0.0005$.

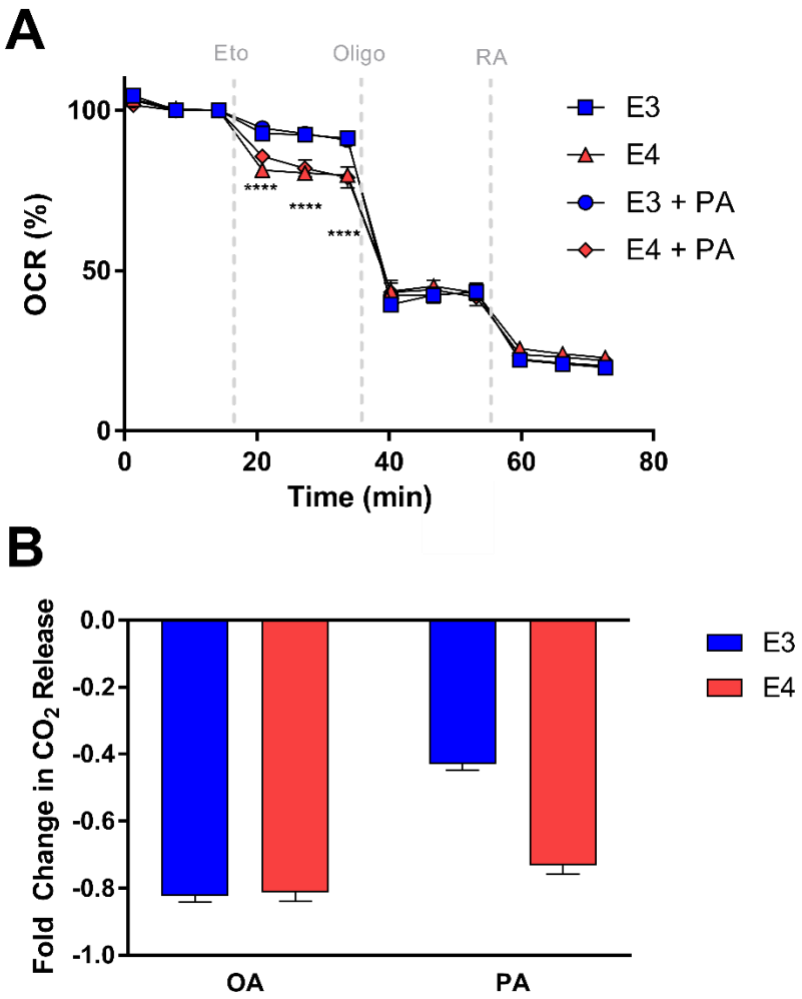

Figure 4.6 E4 astrocytes are more sensitive to CPT-1 inhibition.
(A) Percent change in OCR for E3 and E4 astrocytes pretreated with BSA or palmitate-BSA. Data represent mean of replicate wells +/− SEM (n = 3–4). Data were analyzed by two-way ANOVA, repeated measures; **** p <0.0001. (**B**) Fold change in oxidation of oleate (OA) or (PA) due to carnitine palmitoyltransferase 1 (CPT-1) inhibition was determined by CO_2 trap assays and represented as mean of replicate wells +/− SEM (OA: n = 4; PA: n = 3). Data were analyzed by t-test; **** p <0.0001.

CHAPTER 5. DISCUSSION AND EXPERT OPINION

5.1 Summary of dissertation

This dissertation work leverages human data, humanized mice models, and cutting edge *in vitro* assays of metabolism to detail a role for the gene *APOE* as a metabolic regulator at the cellular and organismal level. *APOE* has been studied extensively in the context of neurodegeneration and neuropathology, peripheral lipid transport, and cardiovascular disease (*306*). Here, *APOE* genotype is revealed to glucose flux through central carbon pathways in astrocytes, manifesting at the systemic level by decreasing energy expenditure in E4 carriers – a phenomenon which can be measured via indirect calorimetry. Furthermore, a role for *APOE* in lipid droplet formation and utilization is detailed in astrocytes. The literature and field of *APOE* metabolism regulation in the brain and beyond is growing, and this body of work contributes substantially to our budding understanding of this crucial gene.

5.2 *APOE* in human health

The polymorphic *APOE* gene encodes for three alleles in humans: E2, E3, and E4 (*307*). E3 has the highest allelic representation in the human population with 78% of individuals carrying at least one copy of E3. E2 represents the smallest percentage of the population at 8%. E4 carriers constitute 14% of the global population (*1*). Though *APOE* alleles differ by single polymorphisms at two genetic loci, the alleles confer a range of pleiotropic phenotypes. E4 is the strongest genetic risk factor for the development of late onset Alzheimer's disease, while E2 offers protection and is associated with longevity (*59*). The E2 allele differs from the E4 allele by two amino acids (at AA 112 and AA 158) yet

according to recent estimates lowers the odds ratio of developing late onset Alzheimer's disease by nearly hundredfold (*308*). A step wise progression of increased risk to decreased risk with allelic dose (E4>E3>=E2) is seen in multiple diseases of the central nervous system including dementia with Lewy bodies, frontotemporal lobar degeneration, Parkinson's disease, ischemic stroke, and vascular dementia (*58*). Furthermore, E4 increases the risk of diseases commonly thought of as diseases of the periphery, such as hypercholesterolemia, coronary artery disease, atherosclerosis, and metabolic syndrome (*307, 309*). The range of diseases, central and peripheral, associated with *APOE* suggests that *APOE* plays a multifaceted role in human health.

5.3 Antagonistic pleiotropy as an explanation for *APOE4* population frequency

A common question regarding the genetic frequency of *APOE4* is: if E4 drives so much disease risk, how could it still be selected for evolutionarily in our population? This is likely answered by the increase in human life expectancy across history (*310*). We now live longer than ever before as humans, which may be revealing age-dependent genetic effects which may have conferred advantages in our youth (and in ancestors with shorter lifespans) but be pathogenic in old age. This concept is known as antagonist pleiotropy and is supported by advantageous characteristics of young E4 carriers which are lost with age (*311, 312*).

5.3.1 *APOE4* as the ancestral allele

To consider *APOE* and its relevance to human health it is useful to phylogenetically trace the gene's evolution, which is now feasible based on advances in molecular genetics and anthropology. *APOE* is genetically conserved across mammalian and non-mammalian

species, reflecting an ancient entry of *APOE* as a component of organismal genomes (*313*). Mice possess an *Apoe* gene with a similar amino acids at AA 112 and AA 158 as human *APOE4,* yet the protein behaves functionally similar to human ApoE3 since it does not bear the domain-interaction observed in the protein structure of ApoE4 (*314*). Interestingly, this shared sequence of *APOE4* between humans and lower vertebrates, including non-human primates, gives support for the theory that *APOE4* is the ancestral allele, and that the other alleles arose from evolutionary selection (*315*). This is also supported by the geographical distribution of the alleles across the continents; *APOE4* has a much higher population frequency in the indigenous populations of Central Africa (40% in Aka Pygmies, 38% in Tutsis, 33% in Zairians, and 29% in Fon), Oceania (49% in the Hui population of New Guinea), and Australia (26% in the Mowanjum aboriginal tribe) relative to its worldwide frequency (*316, 317*). Therefore it appears that *APOE4* was the original allele in our ancient ancestors.

5.3.2 Unique human *APOE* polymorphisms

The polymorphic nature of *APOE* in humans is unique (*318*). No other species known to date has multiple common alleles for the *APOE* gene. Therefore, if we assume that *APOE4* was the ancestral allele and evolutionary pressures gave rise to *APOE3* and *APOE2,* it would seem that these evolutionary pressures were unique upon the human species. If a global event had occurred that would have selected for mutations in the *APOE4* common ancestral allele, more species would likely share the polymorphic *APOE* as seen in humans.

5.3.3 Historical shift in human feeding patterns

In the course of human history it has been necessary to metabolically adapt to our environmental energy supply apart from other species. Ancient humans likely were stationary until resources were depleted relative to the population size, which then required humans to compete for resources (*319*). With territorial disputes and large-migrations away from resources, human metabolism was challenged to adapt due to food scarcity. Pre-historic hunter gatherers were accustomed to a "feast and then fast" dietary program and required metabolic adaptations to fuel the body in times of starvation to adequately store energy during times of energy availability to permit survival. Extended foraging distances required endurance and conversion of bodily energy stores into usable energy substrates critical to maintain energy homeostasis (*320*). As the body begins a period of fasting, energy stores are tapped, releasing non-esterified fatty acids from lipolysis of triglyceride adipose reservoirs, glucose from glycogen stores and gluconeogenesis, and amino peptides from proteolysis. Importantly, genes that promoted energy pool tapping and utilization would have been selected for in the gene pool during this period of human evolution. Conversely, genes that are associated with impairments or inefficiencies in energy utilization would likely be negatively selected. This may help explain why *APOE,* a gene associated with mobilization of fatty acids for energy, is polymorphic in humans alone. It may be that E3 and E2 conferred metabolic advantages over the E4 allele in our human ancestors that resulted in the current population frequencies millennia later. It is also possible that E4 was the advantageous allele for the hunter gatherer population due to its "thrifty" nature allowing extended lipoprotein circulation and increased storage (*317*).

5.3.4 Modern day feeding on the background of inherited ancestral genetics

Shifting to the present, we are now accustomed to an excess of caloric availability and modern humans typically follow a “feast and then feast” diet. Therefore, processes of energy management and efficiency are relatively less active in modern humans consuming excess calories compared to our ancestors. The increase in caloric consumption and our increased life expectancy has occurred relatively rapidly. Yet, our species carries the genetic profile of humans in a world where energy was scarce, feeding was rare, and life expectancy was shorter.

This drastic shift in our energy availability and consumption has occurred in parallel with a rise in the incidence of diseases of metabolic dysfunction including type 2 diabetes, metabolic syndrome, and obesity. These diseases of metabolic dysfunction increase the risk of dementia and share several pathological characteristics with Alzheimer’s disease (AD), such as inflammation, increases in oxidative stress and vascular dysfunction (*321*, *322*). Metabolic disorders also increase in incidence with age, (*323*) and a rapidly aging demographic means the number of individuals suffering from both metabolic disorders and AD is expanding precipitously. While diet has been proven to play a role in the rise of these diseases, the influence of diet-by-gene interactions on disease risk is just beginning to be understood.

5.4 *APOE*, astrocytes, and cerebral metabolic flexibility

Normal brain function requires a multitude of energy-intensive processes, and a complex and intricately linked interplay between neurons and supporting glia is necessary to maintain efficient energy metabolism. Astrocytes in particular play a critical role in brain

homeostasis, regulating both local energy metabolism and defense against oxidative stress, two aspects of great importance to neuronal viability and function (*96, 324*). Being the specialized metabolic neighbors of neurons, astrocytes bridge the distance between the vasculature and the energetically needy synaptic parenchyma. In contrast to neurons, astrocytes are highly glycolytic but also able to β-oxidize fatty acids (*325, 326*). This unique ability of fuel switching from primarily carbohydrate metabolism to fatty acid oxidation is vital for neuronal health in times of variable energy supply as in our ancestors' environments. Metabolic inflexibility, that is the inability to utilize other substrates in the context of substrate deprivation, occurs in situations of caloric oversupply as a result of mitochondrial indecision (*327*). Essentially a traffic jam occurs at the key nodes of central carbon metabolism leading to metabolic gridlock instead of normal flux and energy production. This is detrimental in the brain where tight metabolic coupling between astrocytes and neurons depends on cooperative and smooth metabolic networks to sustain cerebral viability. Since astrocytes are the primary cell type in the brain to produce ApoE, and are key suppliers of metabolites to neurons, we chose to utilize *in vitro* astrocyte models to study the *APOE* genotype-specific alterations in fatty acid and glucose metabolism.

5.4.1 Glucose hypometabolism as a shared feature of AD and E4 brains

E4 carriers and individuals with AD both display an underutilization of glucose as a brain fuel source, seen early in AD disease progression and even in young and healthy E4 carriers (*4*). Even non-demented, cognitively normal E4 carriers demonstrate this pattern of glucose hypometabolism, thereby lending support to this being an inherent biological feature of E4, rather than simply a byproduct of dementia (*3*). Importantly,

glucose hypometabolism is considered the earliest detectable change in the AD brain regardless of *APOE* genotype, reflecting a pre-symptomatic biomarker and potential nidus for incipient AD (*328*).

5.5 Metabolic inflexibility as a unifying mechanism to explain E4-associated antagonistic pleiotropy and disease risk

It is possible that E4 drives glucose hypometabolism due to the metabolic gridlock associated with over consumption of energy substrates that is common in our modern era. While E4 conferred a survival advantage in hunter gathers when resources were scarce and energy storage was more important than energy utilization, today E4's advantage is overcome by the carbohydrate rich diets of Western civilization which give E4 carriers an energy surplus that they are not adapted for. This metabolic indecision would occur at the level of the mitochondria, leading to overall decreases in ATP production, fuel oxidation, and glucose uptake due to negative feedback mechanisms.

E4 as a driver of metabolic inflexibility would explain why in chapter 2 we observed increased lactate production in human, mice, and astrocytes fed glucose since the glucose is fluxed through aerobic glycolysis rather than the high energy yielding oxidative phosphorylation. We observed that deficits in oxidation and energy expenditure at baseline were exacerbated after a glucose challenge, implying that energy substrate supply (at least in terms of carbohydrates) worsens the E4 effect on metabolism. Previous work by our group demonstrated that mice fed a high fat diet also show exacerbated glucose metabolic impairments and worsened outcomes of cognition (*43*). Lactate has been shown to compete with glucose for uptake and oxidation, as shown in chapter 2. Therefore, metabolic inflexibility is doubly problematic since energy oversupply leads to suppressed

glucose oxidation resulting in increased lactate which then also acts to impair glucose oxidation.

Mitochondrial inflexibility would also explain why when we inhibited glutamine metabolism and fatty acid oxidation in E4 astrocytes, they were significantly less flexible at upregulating glucose oxidation relative to E3 astrocytes. It is important to note, however, that the energy substrates (glucose, fatty acids, glutamine) were all present during this experiment, and only pharmacological inhibitors were used to shut down metabolic pathways. This is distinct from a true "starvation" environment in which energy substrates would be absent.

Regarding chapter 4, the E4 astrocytes were shown to increase storage of LDs and increase oxidation of the LD pools, but only when they were starved of glucose. That is, only when we removed the nutrient-dense media did we observe an increase in fatty acid oxidation from the LD pool over in E4 astrocytes relative to E3 astrocytes. This is consistent with the 'thrifty' gene hypothesis since E4 astrocytes showed an advantage in times of nutrient scarcity, and were shown to increase storage of energy substrates in times of nutrient abundance.

Regarding chapter 1, many dietary interventions have been tried in E4 carriers with minimal success. Perhaps the repeated failures of dietary interventions can be explained by the nature of the dietary interventions, that is, the E4 carriers were still consuming an abundance of calories regardless of the type of diet. Dieting may not be the answer to mitigating E4 risk. Instead, I would advocate for a feeding regimen similar to our human ancestors. A diet with restricted feeding and intermittent fasting. To date, there has been no evidence based clinical study showing a beneficial (or non-beneficial) effect of

intermittent fasting in E4 carriers. However, a recent case report of a ketogenic diet intervention in a morbidly obese 68 year old male E4 carrier with mild AD and type 2 diabetes showed promise (*329*). The patient was screened at baseline via the Montreal Cognitive Assessment (MoCA) test and comprehensive diabetic and lipid tests. The patient was prescribed a ketogenic diet over a 10-week period with intermittent fasting on an 8 hour time-restricted feeding window for 3 days per week. The patient showed remarkable improvement from baseline in HgA1c levels (from diabetic to normal range), fasting insulin (85% reduction), body weight (5.5% reduction), and HDL levels (35.7% improvement). Furthermore, MoCA revealed an improvement in cognition with the patient scoring in the mild-AD range at baseline (23/30) and normative range post-intervention (29/30). While this is only a case report (n=1), the study begs the question; are the metabolic derangements driven by E4 mitigated by simply restricting feeding? Future studies are needed in *APOE* mice models and humans to address this fundamental gap in our knowledge.

The metabolism hypothesis of AD states that the primary pathogenic driver of disease progression is altered brain metabolism (*330*). This hypothesis is supported by a number of studies that reflect AD-associated impairments in mitochondrial respiration and aberrant upregulation of glycolysis. For example, fibroblasts taken from LOAD patients show inherent decreased glucose oxidation, diminished mitochondrial membrane potential, increased oxidative stress, and a Warburg-type effect that is unrelated to the age of the patient (*331, 332*). Recent proteomic profiling of over 2000 AD brain samples revealed that changes in expression of proteins involved in glial metabolism is the most significant module associated with AD pathology and cognitive decline (*118*). Increased expression

of enzymes in this module included lactate dehydrogenase, pyruvate kinase, and glyceraldehyde-3-phosphate dehydrogenase, all of which are elevated in aerobic glycolysis/Warburg phenotypes. Laser microdissection of neurons from the posterior cingulate of AD postmortem samples has revealed reduced expression of electron transport genes (*333*). AD-related reduction in ETC activity may also explain findings from Terada and colleagues who used a novel FDG probe that binds to mitochondrial complex 1 to show oxidative metabolic failure in parahippocampal regions of living early stage AD brains (*334*). As stated previously, AD brains show lower FDG PET uptake and this is considered one of the earliest biomarkers of disease (*328, 335*). FDG-PET is able to differentiate AD from other types of dementia with a high degree of specificity due to specific regional signaling patterns.(*336*) Detectable AD symptoms essentially never occur without lower FDG-PET signal, and the degree of FDG-PET signal loss is strongly correlated with the severity of clinical symptoms (*337-339*). Interestingly, analysis of CSF samples from 32 confirmed AD patients showed a significant correlation between increased CSF lactate and reduced glucose uptake (by FDG PET) in parahippocampal areas, the medial prefrontal cortex, and the left orbitofrontal cortex. Imaging studies in live AD patients via magnetic resonance spectroscopy have shown elevated lactate levels in the posterior cingulate/precuneus region compared to controls (*340*). Elevated brain lactate correlates strongly with mild cognitive impairment progression (*341*), and in a mouse model of AD correlates well with interstitial amyloid beta levels.

Based on the data shown in this dissertation, I believe that E4 may be a causative driver of AD based on its effect on metabolic flexibility and subsequent lactate production. Specifically, I hypothesize that E4 carriers consuming high-caloric diets have greater risk

for developing AD because of the increased flux of glucose through aerobic glycolysis to lactate. This lactate then serves to suppress glucose uptake in the brain and drive traditional AD pathology through mechanisms yet to be determined.

5.6 Future studies

Discovering early biological signs that forecast future disease is critical in primary prevention of disease. With the elderly population predicted to increase significantly in the coming decades, early detection and intervention will be critical to lower healthcare burden in the treatment and care of AD patients. Young female E4 carriers offer a unique sample population as being at high risk for development of late onset AD, yet with no age-related AD symptomology. Similar to the seminal finding that young E4 carriers show FDG-PET imaging congruent with AD patients (*3*), we show here that young female E4 carriers show a resting energy expenditure profile congruent with aged individuals. It is unclear if whole body energy expenditure is altered in AD (*342*) and future studies aiming to validate indirect calorimetry as a screen for AD risk should confirm EE alterations in the AD population.

5.7 Conclusion

In summary, I have shown that *APOE* regulates fatty acid metabolism in astrocytes, whole body response to glucose challenges in humans and mice, and central carbon pathways in mice brains and astrocytes. These data show the metabolic effects of E4 in the central nervous system but also show peripheral mechanisms for *APOE* regulation of metabolism. While questions remain, these findings inform the field of neurometabolism and shed light on how the E4 allele contributes to AD risk.

APPENDICES

5.8 APPENDIX 1 – CHAPTER 2 SUPPLEMENTARY MATERIALS

Supplementary Table 1 – Ratios of plasma metabolite abundances in human participants with or without the E4 allele.

(all comparisons shown are E4+ vs E4-)		Pre-glucose challenge		Post-glucose challenge	
Metabolite	**HMDB ID**	**Ratio**	**FDR**	**Ratio**	**FDR**
beta-alanine	HMDB0000056	1.059	0.797	1.179	0.314
cholesterol	HMDB0000067	1.176	0.541	1.084	0.699
citrate	HMDB0000094	1.258	0.273	1.276	0.152
GABA	HMDB0000112	1.203	0.532	1.419	0.096
glyoxylic acid	HMDB0000119	0.822	0.489	0.891	0.542
glycine	HMDB0000123	1.102	0.717	1.098	0.546
glycerol 3-phosphate	HMDB0000126	1.002	0.994	0.853	0.542
fumaric acid	HMDB0000134	0.940	0.797	0.822	0.314
glyceric acid	HMDB0000139	1.243	0.193	1.310	**0.034**
glutamic acid	HMDB0000148	1.427	0.066	1.757	**0.011**
ethanolamine	HMDB0000149	1.141	0.532	1.160	0.291
tyrosine	HMDB0000158	1.072	0.797	1.331	0.153
phenylalanine	HMDB0000159	0.999	0.994	1.141	0.354
maltose	HMDB0000163	1.143	0.775	1.681	**0.028**
threonine	HMDB0000167	0.597	0.107	0.897	0.546
isoleucine	HMDB0000172	1.063	0.798	1.183	0.299
lysine	HMDB0000182	0.929	0.797	1.197	0.216
lactose	HMDB0000186	1.218	0.466	1.471	0.057

serine	HMDB0000187	1.025	0.919	1.277	0.118
lactate	HMDB0000190	1.519	**0.001**	1.264	**0.013**
oleic acid	HMDB0000207	0.722	0.294	0.991	0.957
α-ketoglutarate	HMDB0000208	1.084	0.775	1.057	0.715
myo-inositol	HMDB0000211	1.149	0.532	1.508	**0.028**
n-acetylgalactosamine	HMDB0000212	1.507	0.054	1.359	0.275
palmitic acid (polar lipids)	HMDB0000220	1.074	0.797	1.341	0.098
n-acetyl-neuraminic acid	HMDB0000230	1.026	0.919	1.676	**0.013**
pyruvate	HMDB0000243	1.128	0.532	1.108	0.464
sucrose	HMDB0000258	0.817	0.649	0.791	0.326
serotonin	HMDB0000259	0.757	0.242	1.032	0.861
pyroglutamic acid	HMDB0000267	1.256	0.312	1.336	0.153
ribose	HMDB0000283	0.9659	0.894	1.102	0.546
urea	HMDB0000294	1.1415	0.621	1.117	0.441
creatinine	HMDB0000562	0.7535	0.445	0.701	0.098
fructose	HMDB0000660	1.212	0.489	1.429	**0.028**
linoleic acid polar	HMDB0000673	0.914	0.797	1.066	0.750
methionine	HMDB0000696	1.268	0.358	1.205	0.313
homoserine	HMDB0000719	0.857	0.647	0.688	0.098
malic acid	HMDB0000744	1.185	0.441	1.185	0.247
3-phosphoglyceric acid	HMDB0000807	1.306	0.0843	1.398	**0.018**
stearic acid	HMDB0000827	1.156	0.532	1.317	0.143
valine	HMDB0000883	1.174	0.533	1.217	0.284
tryptophan	HMDB0000929	0.957	0.822	1.105	0.54
threonic acid	HMDB0000943	1.464	0.065	1.977	**0.0013**
F16BP	HMDB0001058	0.783	0.242	0.927	0.584
glucosamine-1-phosphate	HMDB0001109	0.739	0.193	0.883	0.527

alanine	HMDB0001310	1.018	0.919	1.192	0.244
guanosine-5-phosphate	HMDB0001397	1.063	0.797	0.848	0.353
glucosamine	HMDB0001514	1.531	0.066	1.724	**0.002**
oxalic acid	HMDB0002329	1.024	0.919	0.929	0.715
threose	HMDB0002649	0.772	0.414	1.043	0.772
n-acetyl-tryptophan	HMDB0013713	1.076	0.797	1.220	0.354
acetohydroxamic acid	HMDB0014691	1.186	0.532	1.187	0.353
aspartyl-glutamate	HMDB0028752	0.581	0.162	0.576	0.096
leucine	HMDB00687	1.077	0.797	1.265	0.152

Supplementary Table 2. Pre-screening checklist. A response of "yes" to any of the following resulted in exclusion from the study.

Pre-Existing Symptoms Checklist	**INSTRUCTIONS:** Review this list at each visit. If any symptom is present at Baseline, be sure to report it on the ***on medical history***	
Symptom	___Yes ___No	Comments
1. pregnant or breastfeeding	___Yes ___No	
2. have a bleeding disorder	___Yes ___No	
3. allergy to the local anesthetic lidocaine	___Yes ___No	
4. history of stroke, seizures, Parkinson's disease, history of head injury with loss of consciousness, or other dementing disorder	___Yes ___No	
5. history of alcoholism or drug abuse	___Yes ___No	
6. History of schizophrenia or currently suffer from bipolar disorder or major depression.	___Yes ___No	
7. vision or hearing loss severe enough to interfere with cognitive testing	___Yes ___No	
8. Taking Beta Blockers (ex. Sectral, Tenormin, Zebeta, Lopressor, Corgard, Bystolic, Inderal LA, InnoPran XL)	___Yes ___No	
9. Taking Neuroleptics (ex. Clozaril, Saphris, Zeprexa, Seroquel)	___Yes ___No	
10. Taking Narcotic Analgesics (ex. Codeine, Zohydro ER, Oxycodone, Methadone, Hydromorphone, Morphine, Fentanyl)	___Yes ___No	
11. Taking Anti-Parkinsonian Agents (ex. Sinemet, Symmetrel, Artane, Cogentin, Elderpryl, Azliect, Comtan)	___Yes ___No	
12. Taking CNS-Active antihypertensive agents (ex. Catapres, Kapvay, Intuniv, Tenex)	___Yes ___No	
Information obtained by:		

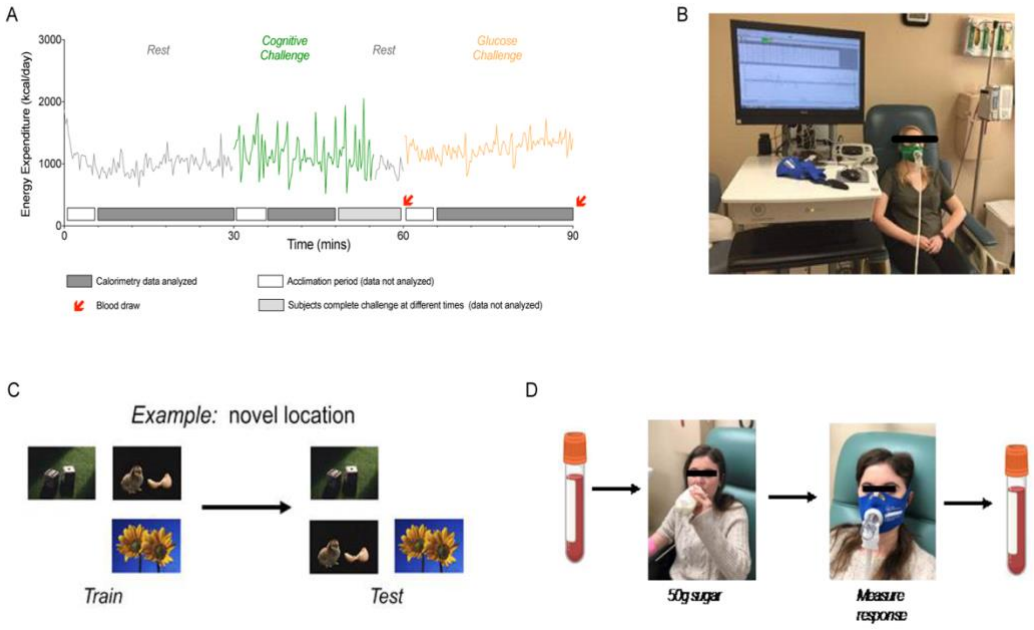

Fig. S1. Human indirect calorimetry study design

(A) Representative time course of energy expenditure (EE) measures during the three periods of the study (rest in gray, cognitive challenge in green, and glucose challenge in orange). Data was only analyzed during the last 25 minutes of the resting and glucose periods and during a common 5-15 minute span during the cognitive challenge in which all 100 subjects were actively engaged in the task – denoted by grey bar on x axis. Blood was drawn immediately prior and after the glucose challenge. **(B)** Representative photo of a participant during the resting challenge connected to the Ultima MGX indirect calorimetry (IC) system. **(C)** Example slides from the Novel Image Novel Location test used as a cognitive challenge. **(D)** The glucose challenge consisted of a blood draw, followed by ingestion of the 50g sugar drink (all subjects consumed drink within 90 seconds), followed by IC measurement, and a second blood draw.

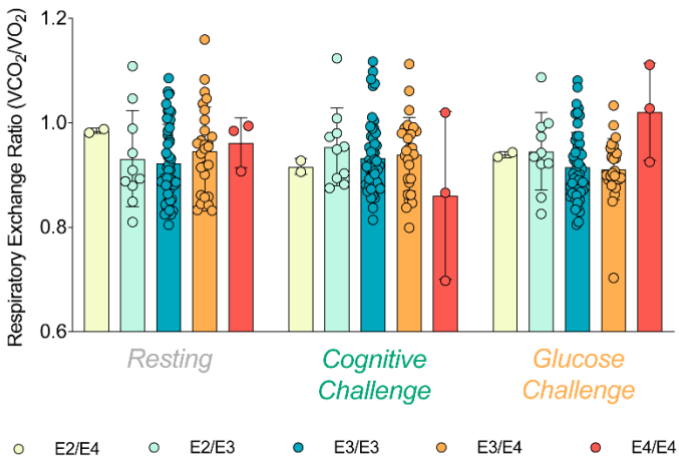

Fig. S2. Respiratory Exchange Ratio (RER) does not differ by *APOE* genotype.

Respiratory exchange ratio (RER) (VCO_2/VO_2) was not significantly different between *APOE* genotypes across any of the three periods tested.

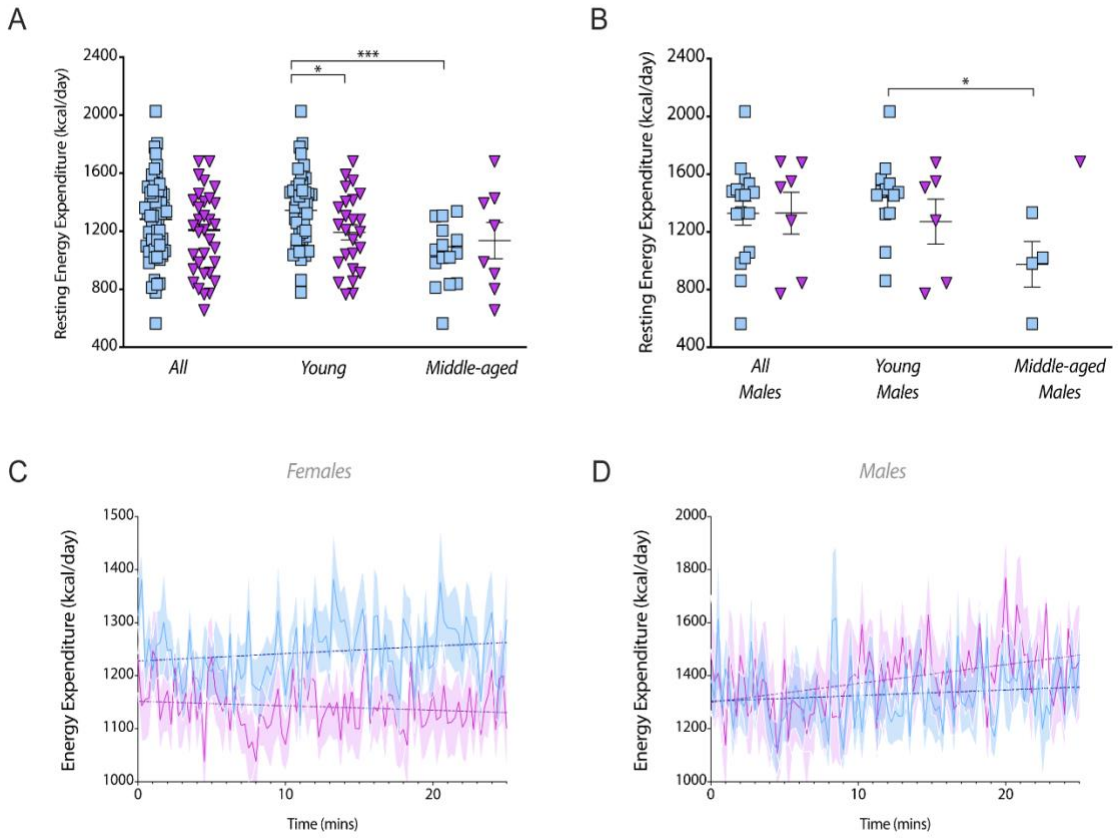

Fig. S3. E4 effect on resting energy expenditure

(A) E4 non-carriers' (blue) and E4 carriers' (purple) average resting energy expenditures were determined and stratified by young and middle-aged. (*P<0.05, ***P<0.001, unpaired t-test, two-tailed)**(B)** This was repeated for only male participants (*P<0.05, unpaired t-test, two-tailed). **(C)** Average EE was plotted over the resting period for females and **(D)** males. Dotted lines indicate liner regression results and shaded area are SEMs.

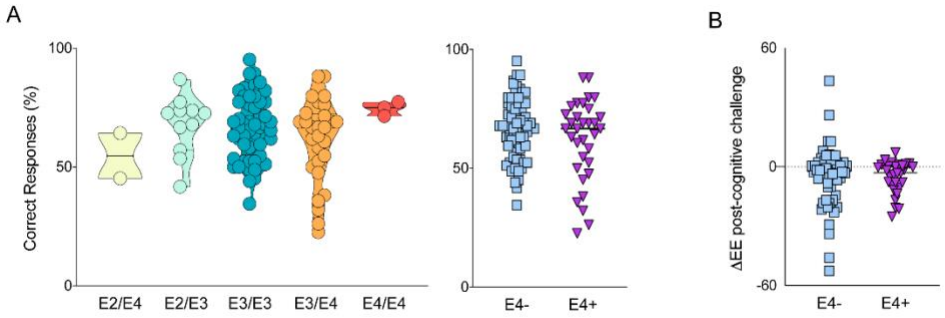

Fig. S4. Novel image novel location object recognition test response accuracy by APOE genotype.

(A) The novel-image-novel-location (NINL) object recognition test contains 7 sets of 12 slides. Each slide has 3 images and 4 possible locations. Each slide is viewed for eight seconds in the order as follows: See Set A, See Set B. Test Set A, See Set C, Test Set B, See Set D, Test Set C, etc. To be considered correct, subjects must identify both the type of change and in which quadrant the change has occurred. The test is designed so that on average subjects answer 60-80% of questions correctly. Total percent correct was calculated for each genotype **(B)** and stratified by E4 carriage. **(C)** Individual slopes of EE after the cognitive challenge showing an average decrease in EE after the challenge.

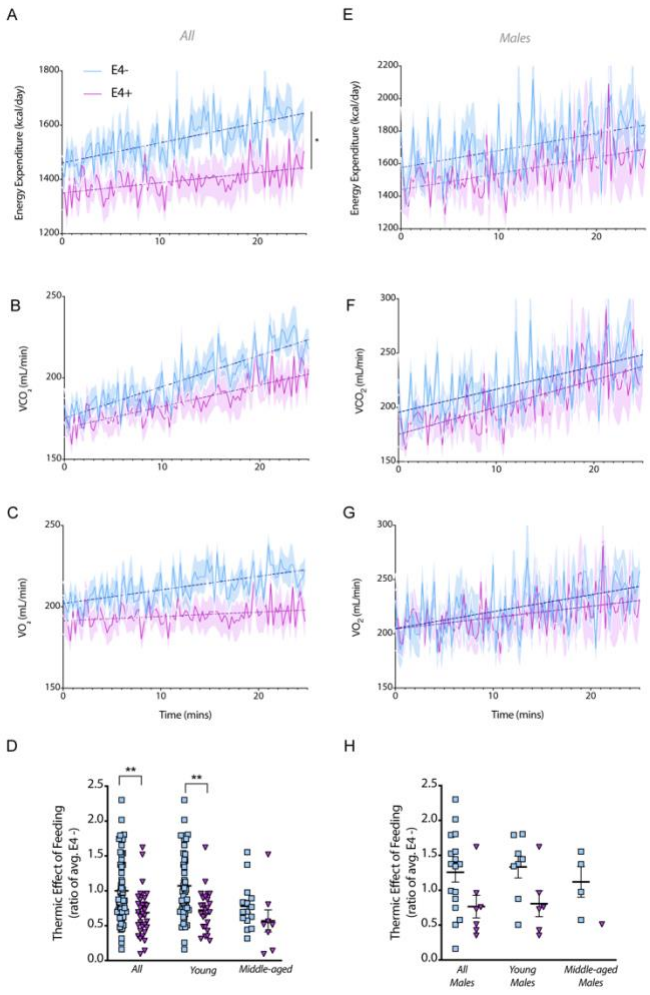

Fig. S5. E4 effect on energy expenditure during glucose challenge

(A) Energy expenditure **(B)** VCO_2 and **(C)** VO_2 was plotted over the glucose challenge period in all E4- (blue) and E4+ (purple) participants. (*P<0.05, Two-way ANOVA repeated measures). **(D)** Thermic effect of feeding was determined as a ratio of E4 non-carriers in all, young, and middle-aged participants. (**P<0.01, unpaired t-test, two-tailed) (E) Energy expenditure **(F)** VCO_2 and **(G)** VO_2 was plotted over the glucose challenge period in male participants. Dotted lines show linear regression trend line, shaded areas refer to SEM. **(H)** Thermic effect of feeding was determined as a ratio of E4 non-carriers in all, young, and middle-aged male participants.

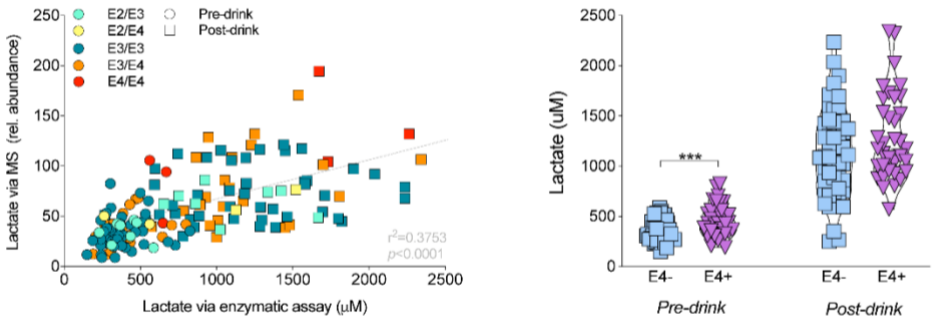

Fig. S6. Plasma lactate assessed via enzymatic assay.

(A) Lactate values quantified by GCMS (relative abundance, y-axis) strongly correlate with lactate values (uM) assessed via enzymatic assay. **(B)** E4 carriers had higher plasma lactate pre-drink and a trend toward higher lactate post-drink (p=0.09) compared to non-carriers, as measured via enzymatic assay.

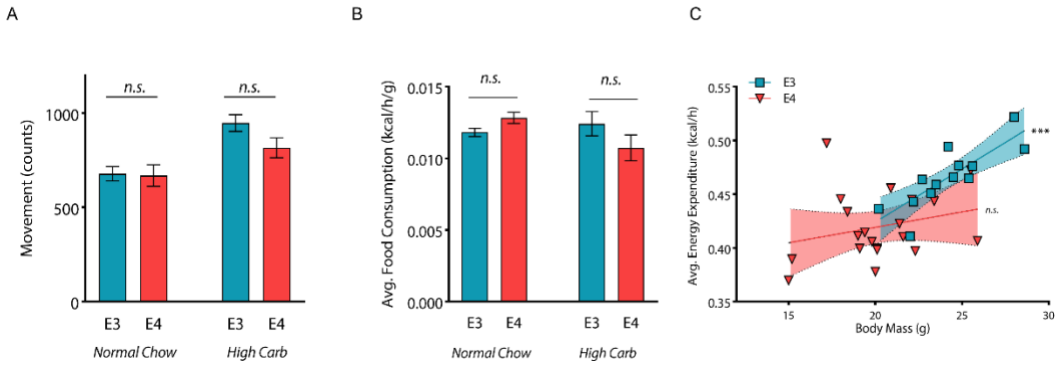

Fig. S7. Activity, food consumption, and age comparisons from mice indirect calorimetry

(A) Activity and **(B)** food consumption during light cycles were averaged for E3 and E4 mice. **(C)** Analysis of covariance was performed by separately correlating average EE and body weight for E3 and E4 mice. (Spearman correlation r=0.86, ***P<0.001).

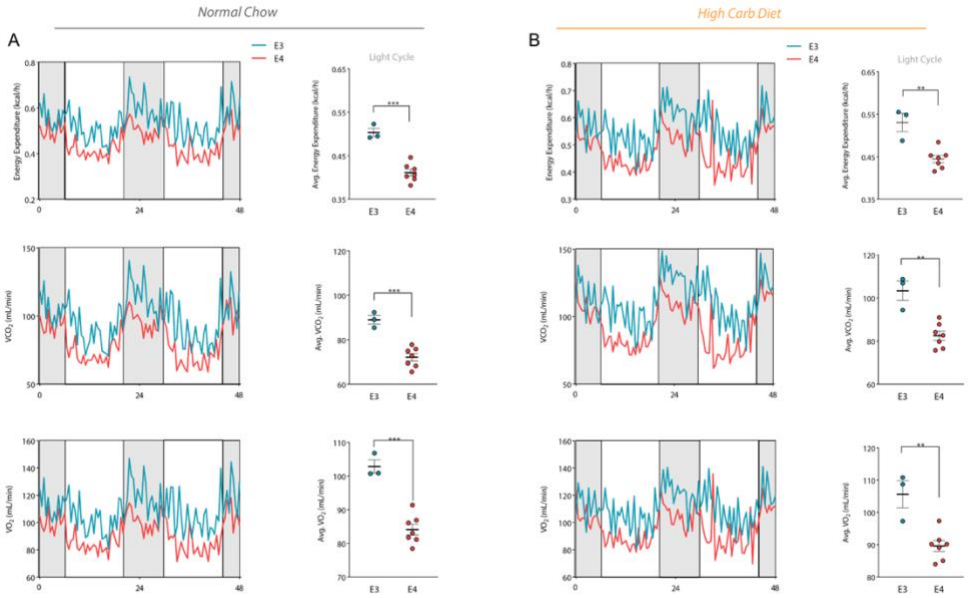

Fig S8. Indirect calorimetry data from male mice

(A) Normal chow and **(B)** high carbohydrate data from male mice only corresponding to Fig 4.

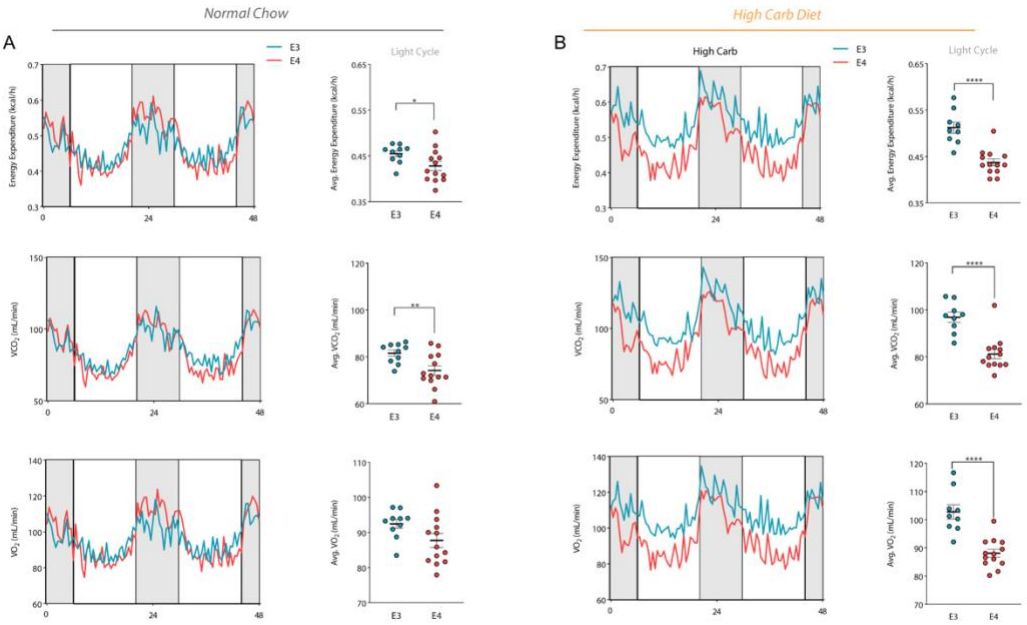

Fig S9. Indirect calorimetry data from female mice

(A) Normal chow and **(B)** high carbohydrate data from female mice only corresponding to Fig 4.

Supplementary Materials and Methods

Glucose metabolism assays

For glucose oxidation assays, astrocytes were plated in a 24-well plate at 300,000 cells/well with 500 µL of maintenance media (Advanced DMEM, 10% FBS, 1% sodium pyruvate, 0.4% Geneticin) and incubated at 5% CO_2 and 37°C and allowed to grow to confluency for 24 hours. Using a previously published protocol (*290*), cells were then incubated with 1 µCi/mL [U-^{14}C] glucose in maintenance media (25mM glucose) or starvation media (same as maintenance except 0mM glucose) for 3 hours. Buffered $^{14}CO_2$ in the media was then liberated by addition of 1 M perchloric acid and captured on a filter paper disc pre-soaked with 1N sodium hydroxide using airtight acidification vials. Radioactivity of the filter paper was measured in a Microbeta 2 Scintillation Counter (Perkin Elmer) after addition of 3 mL Ultima-Gold Scintillation Fluid.

For glucose tracing in primary astrocytes, cells were plated in a 6-well plate at 600,000 cell/well in astrocyte growth media (Advanced DMEM, 10% FBS, 1% sodium pyruvate, 1% penicillin-streptomycin) and incubated at 5% CO_2 and 37°C. After 48 hours, growth media was replaced with tracer media (Glucose-free DMEM containing 10% dialyzed FBS, 10mM [U-^{13}C] glucose) and incubated under previous conditions for 24 hours at which time quenching and metabolite extraction were carried out as follows: Plates were retrieved from incubator and placed on ice, tracer media removed and wells washed once with ice-cold PBS. Immediately following washing, 1 mL of ice-cold extraction buffer (50% MeOH, 20nM norvaline) was added to quench enzymatic activity and plates were placed at -20°C for 10 min. Cellular contents were then scraped with a cell-scraper in extraction buffer and collected into 1.5 mL and tubes placed on ice for 20 min with regular

vortexing. Samples were then centrifuged at 14,000 rpm, 10 min, 4°C after which supernatant containing polar metabolites were removed to a new tube and frozen at -80°C until prepped for GCMS analysis. The resulting pellet was re-suspended in RIPA buffer (Sigma) and protein concentration was measured with BCA kit (Pierce) for normalization.

Glucose tracing *in vivo*

Female TR mice homozygous for E3 or E4 (12-13 mo) were fasted for 2-3 hours then, via oral gavage, administered 250 uL [U-^{13}C] glucose solution at a concentration of 2 g/kg of body weight based on average cohort bodyweight. 45 minutes following gavage, mice were euthanized by cervical dislocation, brains were removed and quickly washed twice in PBS, once in H_2O then frozen in liquid N_2. Tissues were kept at -80°C until ground under liquid N_2 using a Freezer/Mill Cryogenic Grinder (SPEX SamplePrep model 9875D). Approximately 60 mg of tissue was placed in a 1.5 mL tube then 1 mL extraction buffer (50% MeOH, 20nM norvaline) was added followed by a brief vortex and placed on ice for 20 min, briefly vortexed every 5 min. Samples were then centrifuged at 14,000 rpm, 4°C for 10 min. The supernatant containing polar metabolites was removed to a new tube and kept at -80°C until prepped for GCMS. The resulting pellet was re-suspended in RIPA buffer (Sigma) and protein concentration was measured with BCA kit (Pierce) for normalization.

GCMS Sample Preparation

Polar metabolites were thawed on ice then dried under vacuum. Dried pellet dissolved in 50 uL methoxyamine HCl-pyridine (20 mg/ml) solution and heated 60 minutes at 60°C. Following heating, samples were transferred to v-shaped glass chromatography vials and 80 ul of MTSFA + 1% TMCS (Thermo Scientific) was added. Samples then heated for 60 minutes at 60°C then allowed to cool to room temperature and analyzed via GCMS with parameters as previously described (*343*). Briefly, a GC temperature gradient of 130°C was held for 4 minutes, rising at 6°C/min to 243°C, rising at 60°C/min to 280°C and held for two minutes. Electron ionization energy was set to 70 eV. Scan and full scan mode used for metabolite analysis, spectra were translated to relative abundance using the Automated Mass Spectral Deconvolution and Identification System (AMDIS) software with retention time and fragmentation pattern matched to FiehnLib library with a confidence score of >80. Chromatograms were quantified using Data Extraction for Stable Isotope-labelled metabolites (DExSI) with a primary ion and two or more matching qualifying ions. Metabolite quantification was normalized to relative abundance of internal standard (L-norvaline), brain and cell data also normalized to protein concentration. Metabolomics data was analyzed using the web-based data processing tool Metaboanalyst (*344*). Metabolites significantly altered by *APOE* genotype and/or time point were defined by ANOVA and subsequent false discovery rate cutoff of < 0.05. All identified metabolites for which >75% of participants had a measurable concentration were included, and missing values were estimated with an optimized random forest method (*345*). For the pathway impact analysis, the parameters were set to 'global test' and 'Relative-betweenness Centrality', a node centrality measure which reflects metabolic pathway 'hub' importance. For enrichment analyses, parameters were set to "Pathway-associated metabolite sets

(SMPDB)", a library that contains 99 metabolite sets based on normal human metabolism. For both pathway and impact analyses, only metabolic pathways with 3+ metabolites represented in our data set were included, and a false discovery rate cutoff of <0.05 was utilized.

Mitochondrial respiration assays

Astrocytes were plated at 40,000 cells/well in maintenance media and grown to confluency for 24 hours. The following day media was replaced with assay running media (Seahorse XF Base Medium, 1mM pyruvate, 2mM glutamine, and 10mM glucose) and after 1 hour oxygen Consumption rate (OCR) and extracellular acidification rate (ECAR) were measured using a Seahorse 96XF instrument as previously described (*126*). Manufacturer protocols were followed for the glycolysis stress test assay and Mito fuel flex assay. Briefly, the glycolysis stress test assesses the ability of cells to respond to challenging conditions by increase the rate of glycolytic activity. Glycolytic capacity refers to the glycolytic response to energetic demand from stress (Glycolytic capacity = ECAR post-oligomycin – Baseline ECAR) while glycolytic reserve refers to the capacity available to utilize glycolysis beyond the basal rate (Glycolytic reserve = ECAR post-oligomycin – ECAR post-glucose). The Mito Fuel Flex assay assesses mitochondrial energy consumption by measuring respiration in the presence or absence of fuel pathway inhibitors. The following equations were used in the calculations of mitochondrial flexibility parameters: Dependency (%) = [(Baseline OCR - Target inhibitor OCR)/ (Baseline OCR - All inhibitors of OCR)] x 100%. Capacity (%) = 1 / [(Baseline OCR -

Other two inhibitors of OCR)/(Baseline OCR - All inhibitors of OCR)] x 100%. Flexibility (%) = Capacity (%) - Dependency (%).

5.9 APPENDIX 2 – CHAPTER 4 SUPPLEMENTARY MATERIALS

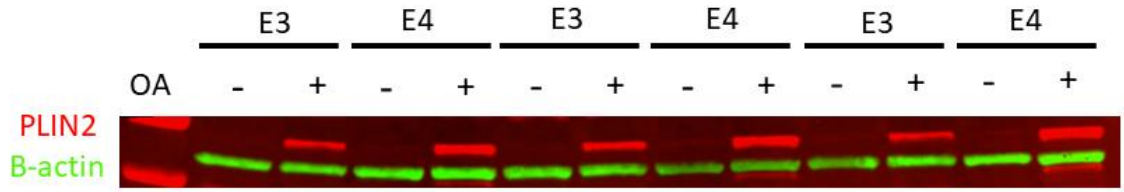

Supplementary Figure 1 - E4 astrocytes express more perilipin-2

E3 and E4 astrocytes were incubated in Advanced DMEM with or without 250 µM oleic acid (OA) conjugated to BSA. Protein was extracted by RIPA lysis and 20µg was loaded for immunoblot analysis of perilipin-2 (PLIN2 with β-actin as a loading control.

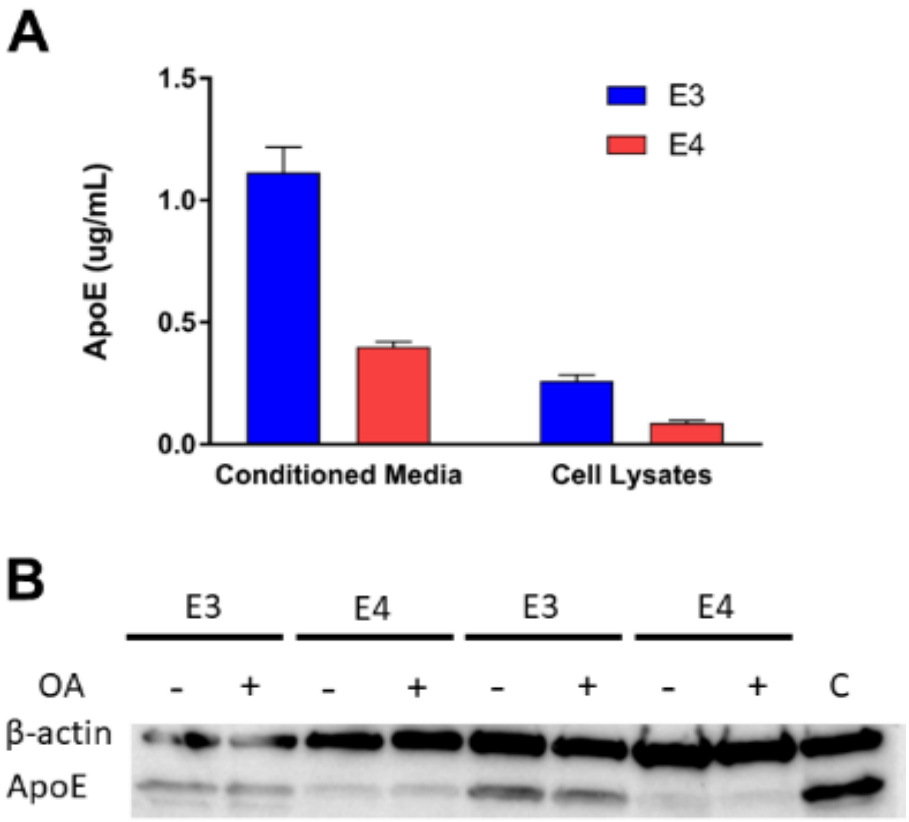

Supplementary Figure 2 - E4 astrocytes secrete less ApoE into the media and have less intracellular ApoE
(A) Media and cell lysates from E3 and E4 astrocyte cell cultures were isolated. Samples were assayed for ApoE using Abcam Human ApoE ELISA kit as previously described (*346*). (B) E3 and E4 cell lysates were separated using SDS-PAGE and immunoblotted for total human ApoE and β-actin as loading control.

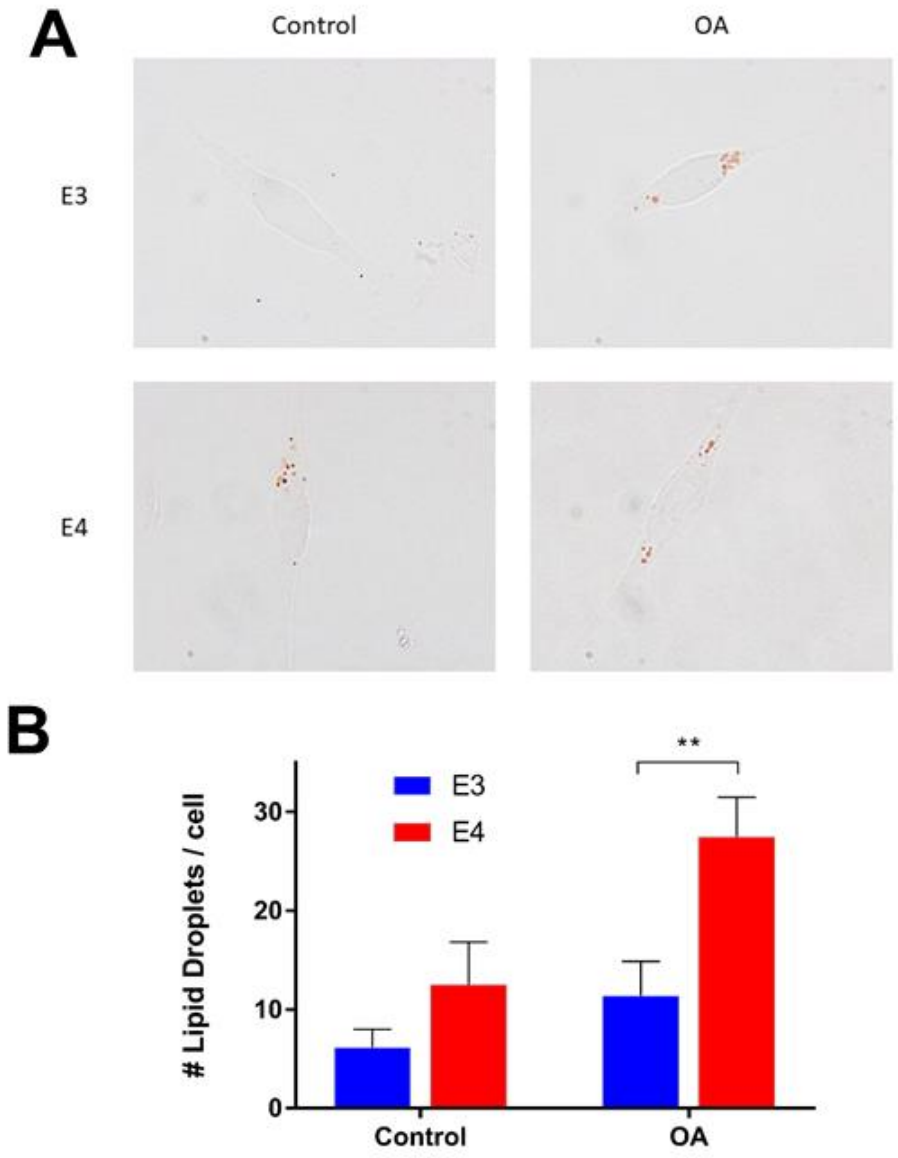

Supplementary Figure 3 – E4 astrocytes form more lipid droplets

(A) E3 and E4 expressing astrocytes were lipid loaded for 24 hours in control or oleic acid supplemented media. Cells were fixed and incubated with oil red O to stain lipid droplets. (B) Oil red O stained LDs were quantified using image J. Values represent means +/- SEM from 8 images. Data was analyzed by t-test. ** $p<0.005$

Supplementary Methods

Oil Red O Histology

Oil Red O staining was performed as previously described (*346*). Astrocytes were plated on TissueTek chamber slides. After lipid incubation, media was aspirated and slides were washed 2X with sterile PBS. 4% PFA was added for 30 min at 37 C to fix the cells, followed by a PBS wash. 60% isopropanol was added to the chamber wells for 5 min for permeabilization. Isopropanol was aspirated and the cells were dried. Oil red O was then added to the chamber wells for 20 min followed by 3 washes in ddH_2O. Chambers were removed from the slides and then coverslips were mounted. Images were acquired at 100X on a phase contrast Nikon microscope under oil immersion.

BIBLIOGRAPHY

1. C. C. Liu, T. Kanekiyo, H. Xu, G. Bu, Apolipoprotein E and Alzheimer disease: risk, mechanisms and therapy. *Nature reviews. Neurology* **9**, 106-118 (2013).
2. R. W. Mahley, Y. Huang, K. H. Weisgraber, Detrimental effects of apolipoprotein E4: potential therapeutic targets in Alzheimer's disease. *Current Alzheimer research* **4**, 537-540 (2007).
3. E. M. Reiman *et al.*, Functional brain abnormalities in young adults at genetic risk for late-onset Alzheimer's dementia. *Proc Natl Acad Sci U S A* **101**, 284-289 (2004).
4. J. A. Brandon, B. C. Farmer, H. C. Williams, L. A. Johnson, APOE and Alzheimer's Disease: Neuroimaging of Metabolic and Cerebrovascular Dysfunction. *Frontiers in aging neuroscience* **10**, 180 (2018).
5. K. Gustaw-Rothenberg, Dietary patterns associated with Alzheimer's disease: population based study. *Int J Environ Res Public Health* **6**, 1335-1340 (2009).
6. V. Solfrizzi *et al.*, Diet and Alzheimer's disease risk factors or prevention: the current evidence. *Expert review of neurotherapeutics* **11**, 677-708 (2011).
7. T. L. Huang *et al.*, Benefits of fatty fish on dementia risk are stronger for those without APOE epsilon4. *Neurology* **65**, 1409-1414 (2005).
8. P. Barberger-Gateau, C. Samieri, C. Feart, M. Plourde, Dietary omega 3 polyunsaturated fatty acids and Alzheimer's disease: interaction with apolipoprotein E genotype. *Current Alzheimer research* **8**, 479-491 (2011).
9. M. Kivipelto *et al.*, Apolipoprotein E epsilon4 magnifies lifestyle risks for dementia: a population-based study. *Journal of cellular and molecular medicine* **12**, 2762-2771 (2008).
10. A. J. Hanson *et al.*, Differential Effects of Meal Challenges on Cognition, Metabolism, and Biomarkers for Apolipoprotein E varepsilon4 Carriers and Adults with Mild Cognitive Impairment. *J Alzheimers Dis* **48**, 205-218 (2015).
11. J. Fan, J. Donkin, C. Wellington, Greasing the wheels of Abeta clearance in Alzheimer's disease: the role of lipids and apolipoprotein E. *Biofactors* **35**, 239-248 (2009).
12. A. J. Hanson, S. Craft, W. A. Banks, The APOE genotype: modification of therapeutic responses in Alzheimer's disease. *Current pharmaceutical design* **21**, 114-120 (2015).
13. B. Cholerton, L. D. Baker, S. Craft, Insulin resistance and pathological brain ageing. *Diabetic medicine : a journal of the British Diabetic Association* **28**, 1463-1475 (2011).
14. S. Craft *et al.*, Cerebrospinal fluid and plasma insulin levels in Alzheimer's disease: relationship to severity of dementia and apolipoprotein E genotype. *Neurology* **50**, 164-168 (1998).
15. J. Dumurgier *et al.*, CSF Abeta1-42 Levels and Glucose Metabolism in Alzheimer's Disease. *Journal of Alzheimer's disease : JAD*, (2011).
16. K. Talbot *et al.*, Demonstrated brain insulin resistance in Alzheimer's disease patients is associated with IGF-1 resistance, IRS-1 dysregulation, and cognitive decline. *The Journal of clinical investigation*, (2012).

17. S. Craft *et al.*, Insulin effects on glucose metabolism, memory, and plasma amyloid precursor protein in Alzheimer's disease differ according to apolipoprotein-E genotype. *Ann N Y Acad Sci* **903**, 222-228 (2000).
18. G. Tsivgoulis *et al.*, Adherence to a Mediterranean diet and risk of incident cognitive impairment. *Neurology* **80**, 1684-1692 (2013).
19. A. Pelletier *et al.*, Mediterranean diet and preserved brain structural connectivity in older subjects. *Alzheimer's & dementia : the journal of the Alzheimer's Association* **11**, 1023-1031 (2015).
20. M. Vassilaki *et al.*, Mediterranean Diet, Its Components, and Amyloid Imaging Biomarkers. *Journal of Alzheimer's disease : JAD* **64**, 281-290 (2018).
21. N. Scarmeas *et al.*, Mediterranean diet and mild cognitive impairment. *Archives of neurology* **66**, 216-225 (2009).
22. T. Ngandu *et al.*, A 2 year multidomain intervention of diet, exercise, cognitive training, and vascular risk monitoring versus control to prevent cognitive decline in at-risk elderly people (FINGER): a randomised controlled trial. *Lancet* **385**, 2255-2263 (2015).
23. A. Solomon *et al.*, Effect of the Apolipoprotein E Genotype on Cognitive Change During a Multidomain Lifestyle Intervention: A Subgroup Analysis of a Randomized Clinical Trial. *JAMA neurology* **75**, 462-470 (2018).
24. M. C. Morris *et al.*, MIND diet associated with reduced incidence of Alzheimer's disease. *Alzheimer's & dementia : the journal of the Alzheimer's Association* **11**, 1007-1014 (2015).
25. O. van de Rest *et al.*, APOE epsilon4 and the associations of seafood and long-chain omega-3 fatty acids with cognitive decline. *Neurology* **86**, 2063-2070 (2016).
26. J. F. Quinn *et al.*, Docosahexaenoic acid supplementation and cognitive decline in Alzheimer disease: a randomized trial. *JAMA : the journal of the American Medical Association* **304**, 1903-1911 (2010).
27. C. Samieri *et al.*, Relationship between diet and plasma long-chain n-3 PUFAs in older people: impact of apolipoprotein E genotype. *Journal of lipid research* **54**, 2559-2567 (2013).
28. R. Chouinard-Watkins *et al.*, Disturbance in uniformly 13C-labelled DHA metabolism in elderly human subjects carrying the apoE epsilon4 allele. *The British journal of nutrition* **110**, 1751-1759 (2013).
29. S. Cunnane *et al.*, Brain fuel metabolism, aging, and Alzheimer's disease. *Nutrition* **27**, 3-20 (2011).
30. S. T. Henderson *et al.*, Study of the ketogenic agent AC-1202 in mild to moderate Alzheimer's disease: a randomized, double-blind, placebo-controlled, multicenter trial. *Nutrition & metabolism* **6**, 31 (2009).
31. S. Patil, C. Chan, Palmitic and stearic fatty acids induce Alzheimer-like hyperphosphorylation of tau in primary rat cortical neurons. *Neuroscience letters* **384**, 288-293 (2005).
32. J. M. Cacicedo, S. Benjachareowong, E. Chou, N. B. Ruderman, Y. Ido, Palmitate-induced apoptosis in cultured bovine retinal pericytes: roles of NAD(P)H oxidase, oxidant stress, and ceramide. *Diabetes* **54**, 1838-1845 (2005).

33. A. A. Pendse, J. M. Arbones-Mainar, L. A. Johnson, M. K. Altenburg, N. Maeda, Apolipoprotein E knock-out and knock-in mice: atherosclerosis, metabolic syndrome, and beyond. *J Lipid Res* **50 Suppl**, S178-182 (2009).
34. Y. T. Lin *et al.*, APOE4 Causes Widespread Molecular and Cellular Alterations Associated with Alzheimer's Disease Phenotypes in Human iPSC-Derived Brain Cell Types. *Neuron* **98**, 1141-1154.e1147 (2018).
35. P. M. Sullivan *et al.*, Targeted Replacement of the Mouse Apolipoprotein E Gene with the Common Human APOE3 Allele Enhances Diet-induced Hypercholesterolemia and Atherosclerosis. *Journal of Biological Chemistry* **272**, 17972-17980 (1997).
36. C. Knouff *et al.*, Apo E structure determines VLDL clearance and atherosclerosis risk in mice. *The Journal of Clinical Investigation* **103**, 1579-1586 (1999).
37. M. T. Venzi, Miklós; Häggkvist, Jenny; Bogstedt, Anna; Rachalski, Adeline; Mattsson, Anna; Frumento, Paolod; Farde, Lars, Differential Effect of APOE Alleles on Brain Glucose Metabolism in Targeted Replacement Mice: An [18F]FDG-µPET Study. *Journal of Alzheimer's Disease Reports* **1**, 169-180 (2017).
38. M. J. Grothe, S. Villeneuve, M. Dyrba, D. Bartres-Faz, M. Wirth, Multimodal characterization of older APOE2 carriers reveals selective reduction of amyloid load. *Neurology* **88**, 569-576 (2017).
39. P. M. Sullivan *et al.*, Reduced levels of human apoE4 protein in an animal model of cognitive impairment. *Neurobiol Aging* **32**, 791-801 (2011).
40. J. M. Arbones-Mainar, L. A. Johnson, M. K. Altenburg, H. S. Kim, N. Maeda, Impaired adipogenic response to thiazolidinediones in mice expressing human apolipoproteinE4. *Faseb j* **24**, 3809-3818 (2010).
41. G. A. Rodriguez, M. P. Burns, E. J. Weeber, G. W. Rebeck, Young APOE4 targeted replacement mice exhibit poor spatial learning and memory, with reduced dendritic spine density in the medial entorhinal cortex. *Learning & memory (Cold Spring Harbor, N.Y.)* **20**, 256-266 (2013).
42. A. L. Lin *et al.*, Rapamycin rescues vascular, metabolic and learning deficits in apolipoprotein E4 transgenic mice with pre-symptomatic Alzheimer's disease. *Journal of cerebral blood flow and metabolism : official journal of the International Society of Cerebral Blood Flow and Metabolism* **37**, 217-226 (2017).
43. L. A. Johnson *et al.*, Apolipoprotein E4 mediates insulin resistance-associated cerebrovascular dysfunction and the post-prandial response. *Journal of cerebral blood flow and metabolism : official journal of the International Society of Cerebral Blood Flow and Metabolism*, 271678x17746186 (2017).
44. W. Alata, Y. Ye, I. St-Amour, M. Vandal, F. Calon, Human apolipoprotein E varepsilon4 expression impairs cerebral vascularization and blood-brain barrier function in mice. *J Cereb Blood Flow Metab* **35**, 86-94 (2015).
45. J. M. Castellano *et al.*, Human apoE isoforms differentially regulate brain amyloid-beta peptide clearance. *Science translational medicine* **3**, 89ra57 (2011).
46. A. J. Hanson *et al.*, Effect of Apolipoprotein E Genotype and Diet on Apolipoprotein E Lipidation and Amyloid Peptides: Randomized Clinical Trial. *JAMA neurology*, 1-9 (2013).
47. J. T. Keeney, S. Ibrahimi, L. Zhao, Human ApoE Isoforms Differentially Modulate Glucose and Amyloid Metabolic Pathways in Female Brain: Evidence of the

Mechanism of Neuroprotection by ApoE2 and Implications for Alzheimer's Disease Prevention and Early Intervention. *J Alzheimers Dis* **48**, 411-424 (2015).
48. L. Wu, X. Zhang, L. Zhao, Human ApoE Isoforms Differentially Modulate Brain Glucose and Ketone Body Metabolism: Implications for Alzheimer's Disease Risk Reduction and Early Intervention. *The Journal of neuroscience : the official journal of the Society for Neuroscience* **38**, 6665-6681 (2018).
49. N. Zhao *et al.*, Apolipoprotein E4 Impairs Neuronal Insulin Signaling by Trapping Insulin Receptor in the Endosomes. *Neuron* **96**, 115-129.e115 (2017).
50. A. W. To, E. M. Ribe, T. T. Chuang, J. E. Schroeder, S. Lovestone, The epsilon3 and epsilon4 alleles of human APOE differentially affect tau phosphorylation in hyperinsulinemic and pioglitazone treated mice. *PLoS One* **6**, e16991 (2011).
51. L. A. Johnson, E. R. S. Torres, S. Impey, J. F. Stevens, J. Raber, Apolipoprotein E4 and Insulin Resistance Interact to Impair Cognition and Alter the Epigenome and Metabolome. *Scientific Reports* **7**, 43701 (2017).
52. K. N. Nam *et al.*, Integrated approach reveals diet, APOE genotype and sex affect immune response in APP mice. *Biochimica et biophysica acta. Molecular basis of disease* **1864**, 152-161 (2018).
53. V. A. Moser, C. J. Pike, Obesity Accelerates Alzheimer-Related Pathology in APOE4 but not APOE3 Mice. *eneuro* **4**, (2017).
54. P. Huebbe *et al.*, Apolipoprotein E (APOE) genotype regulates body weight and fatty acid utilization-Studies in gene-targeted replacement mice. *Molecular nutrition & food research* **59**, 334-343 (2015).
55. J. Raber *et al.*, Isoform-specific effects of human apolipoprotein E on brain function revealed in ApoE knockout mice: increased susceptibility of females. *Proc Natl Acad Sci U S A* **95**, 10914-10919 (1998).
56. C. C. Liu *et al.*, ApoE4 Accelerates Early Seeding of Amyloid Pathology. *Neuron* **96**, 1024-1032.e1023 (2017).
57. M. Haddadi, U. Nongthomba, S. R. Jahromi, S. R. Ramesh, Transgenic Drosophila model to study apolipoprotein E4-induced neurodegeneration. *Behav Brain Res* **301**, 10-18 (2016).
58. M. E. Belloy, V. Napolioni, M. D. Greicius, A Quarter Century of APOE and Alzheimer's Disease: Progress to Date and the Path Forward. *Neuron* **101**, 820-838 (2019).
59. C.-C. Liu, T. Kanekiyo, H. Xu, G. Bu, Apolipoprotein E and Alzheimer disease: risk, mechanisms, and therapy. *Nature reviews. Neurology* **9**, 106-118 (2013).
60. B. C. Riedel, P. M. Thompson, R. D. Brinton, Age, APOE and sex: Triad of risk of Alzheimer's disease. *The Journal of steroid biochemistry and molecular biology* **160**, 134-147 (2016).
61. L. A. Farrer *et al.*, Effects of age, sex, and ethnicity on the association between apolipoprotein E genotype and Alzheimer disease. A meta-analysis. APOE and Alzheimer Disease Meta Analysis Consortium. *Jama* **278**, 1349-1356 (1997).
62. H. Payami *et al.*, Alzheimer's disease, apolipoprotein E4, and gender. *Jama* **271**, 1316-1317 (1994).
63. A. Altmann, L. Tian, V. W. Henderson, M. D. Greicius, Sex modifies the APOE-related risk of developing Alzheimer disease. *Annals of neurology* **75**, 563-573 (2014).

64. T. J. Hohman *et al.*, Sex-Specific Association of Apolipoprotein E With Cerebrospinal Fluid Levels of Tau. *JAMA neurology* **75**, 989-998 (2018).
65. A. Fleisher *et al.*, Sex, apolipoprotein E epsilon 4 status, and hippocampal volume in mild cognitive impairment. *Archives of neurology* **62**, 953-957 (2005).
66. C.-C. Liu *et al.*, ApoE4 Accelerates Early Seeding of Amyloid Pathology. *Neuron* **96**, 1024-1032.e1023 (2017).
67. E. Kok *et al.*, Apolipoprotein E–dependent accumulation of Alzheimer disease–related lesions begins in middle age. *Annals of Neurology* **65**, 650-657 (2009).
68. Y. Shi *et al.*, ApoE4 markedly exacerbates tau-mediated neurodegeneration in a mouse model of tauopathy. *Nature* **549**, 523-527 (2017).
69. J. M. Farfel, L. Yu, P. L. De Jager, J. A. Schneider, D. A. Bennett, Association of APOE with tau-tangle pathology with and without β-amyloid. *Neurobiology of aging* **37**, 19-25 (2016).
70. L. Mosconi *et al.*, Multicenter standardized 18F-FDG PET diagnosis of mild cognitive impairment, Alzheimer's disease, and other dementias. *J Nucl Med* **49**, 390-398 (2008).
71. G. W. Small *et al.*, Cerebral metabolic and cognitive decline in persons at genetic risk for Alzheimer's disease. *Proc Natl Acad Sci U S A* **97**, 6037-6042 (2000).
72. M. D. Paranjpe *et al.*, The effect of ApoE ε4 on longitudinal brain region-specific glucose metabolism in patients with mild cognitive impairment: a FDG-PET study. *NeuroImage: Clinical* **22**, 101795 (2019).
73. H. D. Protas *et al.*, Posterior cingulate glucose metabolism, hippocampal glucose metabolism, and hippocampal volume in cognitively normal, late-middle-aged persons at 3 levels of genetic risk for Alzheimer disease. *JAMA neurology* **70**, 320-325 (2013).
74. A. B. Martínez-Martínez *et al.*, Beyond the CNS: The many peripheral roles of APOE. *Neurobiology of Disease* **138**, 104809 (2020).
75. B. C. Farmer, L. A. Johnson, A. J. Hanson, Effects of apolipoprotein E on nutritional metabolism in dementia. *Curr Opin Lipidol* **30**, 10-15 (2019).
76. J. A. Levine, Measurement of energy expenditure. *Public Health Nutr* **8**, 1123-1132 (2005).
77. J. B. D. B. Weir, New methods for calculating metabolic rate with special reference to protein metabolism. *The Journal of physiology* **109**, 1-9 (1949).
78. C. Scott, Misconceptions about Aerobic and Anaerobic Energy Expenditure. *J Int Soc Sports Nutr* **2**, 32-37 (2005).
79. C. B. Scott, Contribution of anaerobic energy expenditure to whole body thermogenesis. *Nutrition & Metabolism* **2**, 14 (2005).
80. F. Berteau-Pavy, B. Park, J. Raber, Effects of sex and APOE ε4 on object recognition and spatial navigation in the elderly. *Neuroscience* **147**, 6-17 (2007).
81. N. K. Horner *et al.*, Indirect calorimetry protocol development for measuring resting metabolic rate as a component of total energy expenditure in free-living postmenopausal women. *J Nutr* **131**, 2215-2218 (2001).
82. C. J. Popp, J. J. Tisch, K. E. Sakarcan, W. C. Bridges, E. D. Jesch, Approximate Time to Steady-state Resting Energy Expenditure Using Indirect Calorimetry in Young, Healthy Adults. *Frontiers in nutrition* **3**, 49 (2016).

83. B. S. Duman, M. Ozturk, S. Yilmazer, H. Hatemi, Apolipoprotein E polymorphism in Turkish subjects with Type 2 diabetes mellitus: allele frequency and relation to serum lipid concentrations. *Diabetes Nutr Metab* **17**, 267-274 (2004).
84. R. Elosua *et al.*, Obesity modulates the association among APOE genotype, insulin, and glucose in men. *Obes Res* **11**, 1502-1508 (2003).
85. J. M. Arbones-Mainar, L. A. Johnson, M. K. Altenburg, N. Maeda, Differential modulation of diet-induced obesity and adipocyte functionality by human apolipoprotein E3 and E4 in mice. *International journal of obesity (2005)* **32**, 1595-1605 (2008).
86. L. A. Johnson *et al.*, Apolipoprotein E-low density lipoprotein receptor interaction affects spatial memory retention and brain ApoE levels in an isoform-dependent manner. *Neurobiol Dis* **64**, 150-162 (2014).
87. P. M. Sullivan *et al.*, Targeted replacement of the mouse apolipoprotein E gene with the common human APOE3 allele enhances diet-induced hypercholesterolemia and atherosclerosis. *J Biol Chem* **272**, 17972-17980 (1997).
88. P. M. Sullivan, H. Mezdour, S. H. Quarfordt, N. Maeda, Type III hyperlipoproteinemia and spontaneous atherosclerosis in mice resulting from gene replacement of mouse Apoe with human Apoe*2. *J Clin Invest* **102**, 130-135 (1998).
89. J. Kim, J. M. Basak, D. M. Holtzman, The role of apolipoprotein E in Alzheimer's disease. *Neuron* **63**, 287-303 (2009).
90. R. Jolivet, P. J. Magistretti, B. Weber, Deciphering neuron-glia compartmentalization in cortical energy metabolism. *Front Neuroenergetics* **1**, 4-4 (2009).
91. J. Fan *et al.*, Hormonal modulators of glial ABCA1 and apoE levels. *J Lipid Res* **54**, 3139-3150 (2013).
92. J. Zhao *et al.*, Retinoic acid isomers facilitate apolipoprotein E production and lipidation in astrocytes through the retinoid X receptor/retinoic acid receptor pathway. *The Journal of biological chemistry* **289**, 11282-11292 (2014).
93. Q. Liu *et al.*, Neuronal LRP1 knockout in adult mice leads to impaired brain lipid metabolism and progressive, age-dependent synapse loss and neurodegeneration. *The Journal of neuroscience : the official journal of the Society for Neuroscience* **30**, 17068-17078 (2010).
94. G. W. Reed, J. O. Hill, Measuring the thermic effect of food. *Am J Clin Nutr* **63**, 164-169 (1996).
95. W. T. Donahoo, J. A. Levine, E. L. Melanson, Variability in energy expenditure and its components. *Curr Opin Clin Nutr Metab Care* **7**, 599-605 (2004).
96. M. Bélanger, I. Allaman, Pierre J. Magistretti, Brain Energy Metabolism: Focus on Astrocyte-Neuron Metabolic Cooperation. *Cell metabolism* **14**, 724-738.
97. M. Morikawa *et al.*, Production and characterization of astrocyte-derived human apolipoprotein E isoforms from immortalized astrocytes and their interactions with amyloid-beta. *Neurobiol Dis* **19**, 66-76 (2005).
98. G. A. Brooks, The Science and Translation of Lactate Shuttle Theory. *Cell metabolism* **27**, 757-785 (2018).
99. R. A. Sperling *et al.*, Toward defining the preclinical stages of Alzheimer's disease: recommendations from the National Institute on Aging-Alzheimer's Association

workgroups on diagnostic guidelines for Alzheimer's disease. *Alzheimer's & dementia : the journal of the Alzheimer's Association* **7**, 280-292 (2011).
100. J. C. Polanco *et al.*, Amyloid-beta and tau complexity - towards improved biomarkers and targeted therapies. *Nat Rev Neurol* **14**, 22-39 (2018).
101. T. E. Golde, S. T. DeKosky, D. Galasko, Alzheimer's disease: The right drug, the right time. *Science (New York, N.Y.)* **362**, 1250 (2018).
102. A. Altmann *et al.*, Regional brain hypometabolism is unrelated to regional amyloid plaque burden. *Brain* **138**, 3734-3746 (2015).
103. E. M. Reiman *et al.*, Preclinical evidence of Alzheimer's disease in persons homozygous for the epsilon 4 allele for apolipoprotein E. *N Engl J Med* **334**, 752-758 (1996).
104. E. M. Reiman *et al.*, Declining brain activity in cognitively normal apolipoprotein E epsilon 4 heterozygotes: A foundation for using positron emission tomography to efficiently test treatments to prevent Alzheimer's disease. *Proc Natl Acad Sci U S A* **98**, 3334-3339 (2001).
105. L. Mosconi, S. De Santi, H. Rusinek, A. Convit, M. J. de Leon, Magnetic resonance and PET studies in the early diagnosis of Alzheimer's disease. *Expert Rev Neurother* **4**, 831-849 (2004).
106. K. N. Frayn, Calculation of substrate oxidation rates in vivo from gaseous exchange. *J Appl Physiol Respir Environ Exerc Physiol* **55**, 628-634 (1983).
107. S. A. McClave *et al.*, Clinical use of the respiratory quotient obtained from indirect calorimetry. *JPEN J Parenter Enteral Nutr* **27**, 21-26 (2003).
108. N. Troubat, M.-A. Fargeas-Gluck, M. Tulppo, B. Dugué, The stress of chess players as a model to study the effects of psychological stimuli on physiological responses: an example of substrate oxidation and heart rate variability in man. *European Journal of Applied Physiology* **105**, 343-349 (2009).
109. S. F. Al-Naher A, Barber TM, Modulation of Metabolic Rate in Response to a Simple Cognitive Task. *Arch Med* **8**, (2016).
110. M. E. Raichle, D. A. Gusnard, Appraising the brain's energy budget. *Proceedings of the National Academy of Sciences of the United States of America* **99**, 10237-10239 (2002).
111. J. M. Arbones-Mainar *et al.*, Metabolic shifts toward fatty-acid usage and increased thermogenesis are associated with impaired adipogenesis in mice expressing human APOE4. *International Journal Of Obesity* **40**, 1574 (2016).
112. R. Brookmeyer, S. Gray, C. Kawas, Projections of Alzheimer's disease in the United States and the public health impact of delaying disease onset. *American journal of public health* **88**, 1337-1342 (1998).
113. E. H. Corder *et al.*, The biphasic relationship between regional brain senile plaque and neurofibrillary tangle distributions: modification by age, sex, and APOE polymorphism. *Ann N Y Acad Sci* **1019**, 24-28 (2004).
114. J. S. Damoiseaux *et al.*, Gender modulates the APOE epsilon4 effect in healthy older adults: convergent evidence from functional brain connectivity and spinal fluid tau levels. *The Journal of neuroscience : the official journal of the Society for Neuroscience* **32**, 8254-8262 (2012).
115. M. S. Goyal *et al.*, Loss of Brain Aerobic Glycolysis in Normal Human Aging. *Cell metabolism* **26**, 353-360.e353 (2017).

116. P. J. Magistretti, Imaging brain aerobic glycolysis as a marker of synaptic plasticity. *Proceedings of the National Academy of Sciences of the United States of America* **113**, 7015-7016 (2016).
117. A. G. Vlassenko *et al.*, Spatial correlation between brain aerobic glycolysis and amyloid-β (Aβ) deposition. *Proceedings of the National Academy of Sciences* **107**, 17763 (2010).
118. E. C. B. Johnson *et al.*, Large-scale proteomic analysis of Alzheimer's disease brain and cerebrospinal fluid reveals early changes in energy metabolism associated with microglia and astrocyte activation. *Nature medicine*, (2020).
119. A. G. Vlassenko *et al.*, Aerobic glycolysis and tau deposition in preclinical Alzheimer's disease. *Neurobiology of aging* **67**, 95-98 (2018).
120. H. C. Williams *et al.*, APOE alters glucose flux through central carbon pathways in astrocytes. *Neurobiology of Disease* **136**, 104742 (2020).
121. A. L. Orr *et al.*, Neuronal Apolipoprotein E4 Expression Results in Proteome-Wide Alterations and Compromises Bioenergetic Capacity by Disrupting Mitochondrial Function. *J Alzheimers Dis* **68**, 991-1011 (2019).
122. K. C. Sonntag *et al.*, Late-onset Alzheimer's disease is associated with inherent changes in bioenergetics profiles. *Sci Rep* **7**, 14038 (2017).
123. X. Zhu, G. Perry, M. A. Smith, X. Wang, Abnormal mitochondrial dynamics in the pathogenesis of Alzheimer's disease. *Journal of Alzheimer's disease : JAD* **33 Suppl 1**, S253-S262 (2013).
124. T. Nakamura, A. Watanabe, T. Fujino, T. Hosono, M. Michikawa, Apolipoprotein E4 (1-272) fragment is associated with mitochondrial proteins and affects mitochondrial function in neuronal cells. *Molecular neurodegeneration* **4**, 35-35 (2009).
125. M. D. Tambini *et al.*, ApoE4 upregulates the activity of mitochondria-associated ER membranes. *EMBO reports* **17**, 27-36 (2016).
126. B. C. Farmer, J. Kluemper, L. A. Johnson, Apolipoprotein E4 Alters Astrocyte Fatty Acid Metabolism and Lipid Droplet Formation. *Cells* **8**, (2019).
127. J. TCW *et al.*, Cholesterol and matrisome pathways dysregulated in human APOE ε4 glia. *bioRxiv*, 713362 (2019).
128. L. Liu, K. R. MacKenzie, N. Putluri, M. Maletic-Savatic, H. J. Bellen, The Glia-Neuron Lactate Shuttle and Elevated ROS Promote Lipid Synthesis in Neurons and Lipid Droplet Accumulation in Glia via APOE/D. *Cell metabolism* **26**, 719-737.e716 (2017).
129. J. T. Newington, R. A. Harris, R. C. Cumming, Reevaluating Metabolism in Alzheimer's Disease from the Perspective of the Astrocyte-Neuron Lactate Shuttle Model. *Journal of neurodegenerative diseases* **2013**, 234572 (2013).
130. A. Tabernero, C. Vicario, J. M. Medina, Lactate spares glucose as a metabolic fuel in neurons and astrocytes from primary culture. *Neuroscience Research* **26**, 369-376 (1996).
131. P. Rasmussen, M. T. Wyss, C. Lundby, Cerebral glucose and lactate consumption during cerebral activation by physical activity in humans. *Faseb j* **25**, 2865-2873 (2011).

132. A. K. Bouzier-Sore *et al.*, Competition between glucose and lactate as oxidative energy substrates in both neurons and astrocytes: a comparative NMR study. *The European journal of neuroscience* **24**, 1687-1694 (2006).
133. D. Smith *et al.*, Lactate: a preferred fuel for human brain metabolism in vivo. *Journal of cerebral blood flow and metabolism : official journal of the International Society of Cerebral Blood Flow and Metabolism* **23**, 658-664 (2003).
134. L. F. Barros *et al.*, Aerobic Glycolysis in the Brain: Warburg and Crabtree Contra Pasteur. *Neurochem Res*, (2020).
135. R. L. Smith, M. R. Soeters, R. C. I. Wust, R. H. Houtkooper, Metabolic Flexibility as an Adaptation to Energy Resources and Requirements in Health and Disease. *Endocr Rev* **39**, 489-517 (2018).
136. S. L. Jackson *et al.*, Glucose challenge test screening for prediabetes and early diabetes. *Diabet Med* **34**, 716-724 (2017).
137. M. A. Welte, Expanding roles for lipid droplets. *Curr Biol* **25**, R470-R481 (2015).
138. S. Cohen, Lipid Droplets as Organelles. *Int Rev Cell Mol Biol* **337**, 83-110 (2018).
139. T. C. Walther, R. V. Farese, Jr., Lipid droplets and cellular lipid metabolism. *Annual review of biochemistry* **81**, 687-714 (2012).
140. S. Missaglia, R. A. Coleman, A. Mordente, D. Tavian, Neutral Lipid Storage Diseases as Cellular Model to Study Lipid Droplet Function. *Cells* **8**, 187 (2019).
141. A. Dichlberger, S. Schlager, P. T. Kovanen, W. J. Schneider, Lipid droplets in activated mast cells - a significant source of triglyceride-derived arachidonic acid for eicosanoid production. *Eur J Pharmacol* **785**, 59-69 (2016).
142. H. A. Saka, R. Valdivia, Emerging roles for lipid droplets in immunity and host-pathogen interactions. *Annual review of cell and developmental biology* **28**, 411-437 (2012).
143. P. T. Bozza, J. P. Viola, Lipid droplets in inflammation and cancer. *Prostaglandins, leukotrienes, and essential fatty acids* **82**, 243-250 (2010).
144. P. T. Bozza, I. Bakker-Abreu, R. A. Navarro-Xavier, C. Bandeira-Melo, Lipid body function in eicosanoid synthesis: An update. *Prostaglandins, Leukotrienes and Essential Fatty Acids* **85**, 205-213 (2011).
145. V. Puri *et al.*, Fat-specific protein 27, a novel lipid droplet protein that enhances triglyceride storage. *The Journal of biological chemistry* **282**, 34213-34218 (2007).
146. A. Gemmink, B. H. Goodpaster, P. Schrauwen, M. K. C. Hesselink, Intramyocellular lipid droplets and insulin sensitivity, the human perspective. *Biochimica et biophysica acta. Molecular and cell biology of lipids* **1862**, 1242-1249 (2017).
147. V. Puri *et al.*, Cidea is associated with lipid droplets and insulin sensitivity in humans. *Proc Natl Acad Sci U S A* **105**, 7833-7838 (2008).
148. J. A. Hamilton, C. J. Hillard, A. A. Spector, P. A. Watkins, Brain uptake and utilization of fatty acids, lipids and lipoproteins: application to neurological disorders. *Journal of molecular neuroscience : MN* **33**, 2-11 (2007).
149. J. Zhang, Q. Liu, Cholesterol metabolism and homeostasis in the brain. *Protein Cell* **6**, 254-264 (2015).
150. D. Puchkov, V. Haucke, Greasing the synaptic vesicle cycle by membrane lipids. *Trends Cell Biol* **23**, 493-503 (2013).

151. K. D. Bruce, A. Zsombok, R. H. Eckel, Lipid Processing in the Brain: A Key Regulator of Systemic Metabolism. *Frontiers in Endocrinology* **8**, (2017).
152. A. Meyers *et al.*, The protein and neutral lipid composition of lipid droplets isolated from the fission yeast, Schizosaccharomyces pombe. *Journal of Microbiology* **55**, 112-122 (2017).
153. C. Sztalryd, D. L. Brasaemle, The perilipin family of lipid droplet proteins: Gatekeepers of intracellular lipolysis. *Biochimica et biophysica acta. Molecular and cell biology of lipids* **1862**, 1221-1232 (2017).
154. T. C. Walther, J. Chung, R. V. Farese, Jr., Lipid Droplet Biogenesis. *Annual review of cell and developmental biology* **33**, 491-510 (2017).
155. C. A. Harris *et al.*, DGAT enzymes are required for triacylglycerol synthesis and lipid droplets in adipocytes. *J Lipid Res* **52**, 657-667 (2011).
156. Y. Zhu *et al.*, In vitro exploration of ACAT contributions to lipid droplet formation during adipogenesis. *J Lipid Res* **59**, 820-829 (2018).
157. G. Gao *et al.*, Control of lipid droplet fusion and growth by CIDE family proteins. *Biochimica et biophysica acta. Molecular and cell biology of lipids* **1862**, 1197-1204 (2017).
158. F. Wilfling *et al.*, Triacylglycerol synthesis enzymes mediate lipid droplet growth by relocalizing from the ER to lipid droplets. *Developmental cell* **24**, 384-399 (2013).
159. T. B. Nguyen *et al.*, DGAT1-Dependent Lipid Droplet Biogenesis Protects Mitochondrial Function during Starvation-Induced Autophagy. *Developmental cell* **42**, 9-21.e25 (2017).
160. A. S. Rambold, S. Cohen, J. Lippincott-Schwartz, Fatty acid trafficking in starved cells: regulation by lipid droplet lipolysis, autophagy, and mitochondrial fusion dynamics. *Developmental cell* **32**, 678-692 (2015).
161. A. Lass *et al.*, Adipose triglyceride lipase-mediated lipolysis of cellular fat stores is activated by CGI-58 and defective in Chanarin-Dorfman Syndrome. *Cell metabolism* **3**, 309-319 (2006).
162. H. Wang *et al.*, Unique regulation of adipose triglyceride lipase (ATGL) by perilipin 5, a lipid droplet-associated protein. *The Journal of biological chemistry* **286**, 15707-15715 (2011).
163. J. Montesinos, C. Guardia-Laguarta, E. Area-Gomez, The fat brain. *Current opinion in clinical nutrition and metabolic care* **23**, 68-75 (2020).
164. J. A. Olzmann, P. Carvalho, Dynamics and functions of lipid droplets. *Nature Reviews Molecular Cell Biology* **20**, 137-155 (2019).
165. K. Etschmaier *et al.*, Adipose triglyceride lipase affects triacylglycerol metabolism at brain barriers. *J Neurochem* **119**, 1016-1028 (2011).
166. F. Cingolani, M. J. Czaja, Regulation and Functions of Autophagic Lipolysis. *Trends in endocrinology and metabolism: TEM* **27**, 696-705 (2016).
167. R. Zechner *et al.*, FAT SIGNALS--lipases and lipolysis in lipid metabolism and signaling. *Cell metabolism* **15**, 279-291 (2012).
168. A. G. Cabodevilla *et al.*, Cell survival during complete nutrient deprivation depends on lipid droplet-fueled beta-oxidation of fatty acids. *The Journal of biological chemistry* **288**, 27777-27788 (2013).

169. E. L. Arrese, F. Z. Saudale, J. L. Soulages, Lipid Droplets as Signaling Platforms Linking Metabolic and Cellular Functions. *Lipid Insights* **7**, 7-16 (2014).
170. J. K. Zehmer *et al.*, A role for lipid droplets in inter-membrane lipid traffic. *Proteomics* **9**, 914-921 (2009).
171. J. Marschallinger *et al.*, Lipid-droplet-accumulating microglia represent a dysfunctional and proinflammatory state in the aging brain. *Nat Neurosci*, (2020).
172. L. K. Hamilton, K. J. L. Fernandes, Neural stem cells and adult brain fatty acid metabolism: Lessons from the 3xTg model of Alzheimer's disease. *Biology of the Cell* **110**, 6-25 (2018).
173. M. S. Ioannou *et al.*, Neuron-Astrocyte Metabolic Coupling Protects against Activity-Induced Fatty Acid Toxicity. *Cell* **177**, 1522-1535 e1514 (2019).
174. S. C. Lee, G. R. Moore, G. Golenwsky, C. S. Raine, Multiple sclerosis: a role for astroglia in active demyelination suggested by class II MHC expression and ultrastructural study. *Journal of neuropathology and experimental neurology* **49**, 122-136 (1990).
175. M. K. Shimabukuro *et al.*, Lipid-laden cells differentially distributed in the aging brain are functionally active and correspond to distinct phenotypes. *Scientific Reports* **6**, 23795 (2016).
176. F. Doetsch, J. M. Garcia-Verdugo, A. Alvarez-Buylla, Regeneration of a germinal layer in the adult mammalian brain. *Proc Natl Acad Sci U S A* **96**, 11619-11624 (1999).
177. E. A. Stoll *et al.*, Neural Stem Cells in the Adult Subventricular Zone Oxidize Fatty Acids to Produce Energy and Support Neurogenic Activity. *Stem cells (Dayton, Ohio)* **33**, 2306-2319 (2015).
178. F. Doetsch, J. M. Garcia-Verdugo, A. Alvarez-Buylla, Cellular composition and three-dimensional organization of the subventricular germinal zone in the adult mammalian brain. *The Journal of neuroscience : the official journal of the Society for Neuroscience* **17**, 5046-5061 (1997).
179. S. Lucken-Ardjomande Hasler, Y. Vallis, H. E. Jolin, A. N. McKenzie, H. T. McMahon, GRAF1a is a brain-specific protein that promotes lipid droplet clustering and growth, and is enriched at lipid droplet junctions. *J Cell Sci* **127**, 4602-4619 (2014).
180. M. Bouab, G. N. Paliouras, A. Aumont, K. Forest-Berard, K. J. Fernandes, Aging of the subventricular zone neural stem cell niche: evidence for quiescence-associated changes between early and mid-adulthood. *Neuroscience* **173**, 135-149 (2011).
181. L. K. Hamilton *et al.*, Aberrant Lipid Metabolism in the Forebrain Niche Suppresses Adult Neural Stem Cell Proliferation in an Animal Model of Alzheimer's Disease. *Cell stem cell* **17**, 397-411 (2015).
182. C. Yin *et al.*, ApoE attenuates unresolvable inflammation by complex formation with activated C1q. *Nature medicine* **25**, 496-506 (2019).
183. S. Kaushik *et al.*, Autophagy in hypothalamic AgRP neurons regulates food intake and energy balance. *Cell metabolism* **14**, 173-183 (2011).
184. L. C. Ceafalan *et al.*, Age-related ultrastructural changes of the basement membrane in the mouse blood-brain barrier. *Journal of cellular and molecular medicine* **23**, 819-827 (2019).

185. A. Khatchadourian, S. D. Bourque, V. R. Richard, V. I. Titorenko, D. Maysinger, Dynamics and regulation of lipid droplet formation in lipopolysaccharide (LPS)-stimulated microglia. *Biochimica et biophysica acta* **1821**, 607-617 (2012).
186. L. L. Lee *et al.*, Triglyceride-rich lipoprotein lipolysis products increase blood-brain barrier transfer coefficient and induce astrocyte lipid droplets and cell stress. *Am J Physiol Cell Physiol* **312**, C500-C516 (2017).
187. Y. H. Kwon *et al.*, Hypothalamic lipid-laden astrocytes induce microglia migration and activation. *FEBS Lett* **591**, 1742-1751 (2017).
188. S.-J. Lee, J. Zhang, A. M. K. Choi, H. P. Kim, Mitochondrial Dysfunction Induces Formation of Lipid Droplets as a Generalized Response to Stress. *Oxidative Medicine and Cellular Longevity* **2013**, 327167 (2013).
189. J. Lee, T. Homma, T. Kurahashi, E. S. Kang, J. Fujii, Oxidative stress triggers lipid droplet accumulation in primary cultured hepatocytes by activating fatty acid synthesis. *Biochemical and Biophysical Research Communications* **464**, 229-235 (2015).
190. Y. Jin, Y. Tan, L. Chen, Y. Liu, Z. Ren, Reactive Oxygen Species Induces Lipid Droplet Accumulation in HepG2 Cells by Increasing Perilipin 2 Expression. *Int J Mol Sci* **19**, (2018).
191. A. Islam *et al.*, FABP7 Protects Astrocytes Against ROS Toxicity via Lipid Droplet Formation. *Mol Neurobiol* **56**, 5763-5779 (2019).
192. L. Liu *et al.*, Glial lipid droplets and ROS induced by mitochondrial defects promote neurodegeneration. *Cell* **160**, 177-190 (2015).
193. A. P. Bailey *et al.*, Antioxidant Role for Lipid Droplets in a Stem Cell Niche of Drosophila. *Cell* **163**, 340-353 (2015).
194. E. Tiryaki, H. A. Horak, ALS and other motor neuron diseases. *Continuum (Minneapolis, Minn.)* **20**, 1185-1207 (2014).
195. T. Vandoorne, K. De Bock, L. Van Den Bosch, Energy metabolism in ALS: an underappreciated opportunity? *Acta Neuropathol* **135**, 489-509 (2018).
196. G. Pennetta, M. A. Welte, Emerging Links between Lipid Droplets and Motor Neuron Diseases. *Developmental cell* **45**, 427-432 (2018).
197. M. Sanhueza *et al.*, Network analyses reveal novel aspects of ALS pathogenesis. *PLoS genetics* **11**, e1005107 (2015).
198. A. Kassan *et al.*, Acyl-CoA synthetase 3 promotes lipid droplet biogenesis in ER microdomains. *Journal of Cell Biology* **203**, 985-1001 (2013).
199. T. Yagi, D. Ito, Y. Nihei, T. Ishihara, N. Suzuki, N88S seipin mutant transgenic mice develop features of seipinopathy/BSCL2-related motor neuron disease via endoplasmic reticulum stress. *Human molecular genetics* **20**, 3831-3840 (2011).
200. J. Branchu *et al.*, Loss of spatacsin function alters lysosomal lipid clearance leading to upper and lower motor neuron degeneration. *Neurobiol Dis* **102**, 21-37 (2017).
201. Y. Liu *et al.*, A C9orf72-CARM1 axis regulates lipid metabolism under glucose starvation-induced nutrient stress. *Genes & development* **32**, 1380-1397 (2018).
202. E. P. Simpson, Y. K. Henry, J. S. Henkel, R. G. Smith, S. H. Appel, Increased lipid peroxidation in sera of ALS patients: a potential biomarker of disease burden. *Neurology* **62**, 1758-1765 (2004).
203. P. McColgan, S. J. Tabrizi, Huntington's disease: a clinical review. *European journal of neurology* **25**, 24-34 (2018).

204. K. R. Croce, A. Yamamoto, A role for autophagy in Huntington's disease. *Neurobiol Dis* **122**, 16-22 (2019).
205. M. Martinez-Vicente *et al.*, Cargo recognition failure is responsible for inefficient autophagy in Huntington's disease. *Nature neuroscience* **13**, 567-576 (2010).
206. K. Aditi, M. N. Shakarad, N. Agrawal, Altered lipid metabolism in Drosophila model of Huntington's disease. *Sci Rep* **6**, 31411 (2016).
207. L. V. Kalia, A. E. Lang, Parkinson's disease. *Lancet* **386**, 896-912 (2015).
208. N. B. Cole *et al.*, Lipid droplet binding and oligomerization properties of the Parkinson's disease protein alpha-synuclein. *The Journal of biological chemistry* **277**, 6344-6352 (2002).
209. T. F. Outeiro, S. Lindquist, Yeast cells provide insight into alpha-synuclein biology and pathobiology. *Science (New York, N.Y.)* **302**, 1772-1775 (2003).
210. C. Klemann *et al.*, Integrated molecular landscape of Parkinson's disease. *NPJ Parkinson's disease* **3**, 14 (2017).
211. C. R. Scherzer, M. B. Feany, Yeast genetics targets lipids in Parkinson's disease. *Trends in genetics : TIG* **20**, 273-277 (2004).
212. C. R. Scherzer, R. V. Jensen, S. R. Gullans, M. B. Feany, Gene expression changes presage neurodegeneration in a Drosophila model of Parkinson's disease. *Human molecular genetics* **12**, 2457-2466 (2003).
213. S. Fanning *et al.*, Lipidomic Analysis of alpha-Synuclein Neurotoxicity Identifies Stearoyl CoA Desaturase as a Target for Parkinson Treatment. *Molecular cell* **73**, 1001-1014.e1008 (2019).
214. A. L. Marcos *et al.*, The Parkinson-associated human P5B-ATPase ATP13A2 modifies lipid homeostasis. *Biochimica et biophysica acta. Biomembranes* **1861**, 182993 (2019).
215. S. Fanning, D. Selkoe, U. Dettmer, Parkinson's disease: proteinopathy or lipidopathy? *NPJ Parkinson's disease* **6**, 3 (2020).
216. S. Karantzoulis, J. E. Galvin, Distinguishing Alzheimer's disease from other major forms of dementia. *Expert Rev Neurother* **11**, 1579-1591 (2011).
217. A. Alzheimer, Uber eine eigenartige Erkrankung der Hirnrinde. *Zentralbl. Nervenh. Psych.* **18**, 177-179 (1907).
218. A. Alzheimer, R. A. Stelzmann, H. N. Schnitzlein, F. R. Murtagh, An English translation of Alzheimer's 1907 paper, "Uber eine eigenartige Erkankung der Hirnrinde". *Clinical anatomy (New York, N.Y.)* **8**, 429-431 (1995).
219. J. Derk *et al.*, Diaphanous 1 (DIAPH1) is Highly Expressed in the Aged Human Medial Temporal Cortex and Upregulated in Myeloid Cells During Alzheimer's Disease. *J Alzheimers Dis* **64**, 995-1007 (2018).
220. R. van der Kant *et al.*, Cholesterol Metabolism Is a Druggable Axis that Independently Regulates Tau and Amyloid-beta in iPSC-Derived Alzheimer's Disease Neurons. *Cell stem cell* **24**, 363-375.e369 (2019).
221. Y.-T. Lin *et al.*, APOE4 Causes Widespread Molecular and Cellular Alterations Associated with Alzheimer's Disease Phenotypes in Human iPSC-Derived Brain Cell Types. *Neuron* **98**, 1141-1154.e1147 (2018).
222. T. Lo Giudice, F. Lombardi, F. M. Santorelli, T. Kawarai, A. Orlacchio, Hereditary spastic paraplegia: clinical-genetic characteristics and evolving molecular mechanisms. *Exp Neurol* **261**, 518-539 (2014).

223. P. V. S. de Souza, W. B. V. de Rezende Pinto, G. N. de Rezende Batistella, T. Bortholin, A. S. B. Oliveira, Hereditary Spastic Paraplegia: Clinical and Genetic Hallmarks. *Cerebellum (London, England)* **16**, 525-551 (2017).
224. J. M. Inloes *et al.*, Functional Contribution of the Spastic Paraplegia-Related Triglyceride Hydrolase DDHD2 to the Formation and Content of Lipid Droplets. *Biochemistry* **57**, 827-838 (2018).
225. C. Papadopoulos *et al.*, Spastin binds to lipid droplets and affects lipid metabolism. *PLoS genetics* **11**, e1005149 (2015).
226. Y. Arribat *et al.*, Spastin mutations impair coordination between lipid droplet dispersion and reticulum. *PLoS genetics* **16**, e1008665 (2020).
227. C. Hooper, S. S. Puttamadappa, Z. Loring, A. Shekhtman, J. C. Bakowska, Spartin activates atrophin-1-interacting protein 4 (AIP4) E3 ubiquitin ligase and promotes ubiquitination of adipophilin on lipid droplets. *BMC biology* **8**, 72 (2010).
228. T. L. Edwards *et al.*, Endogenous spartin (SPG20) is recruited to endosomes and lipid droplets and interacts with the ubiquitin E3 ligases AIP4 and AIP5. *The Biochemical journal* **423**, 31-39 (2009).
229. B. Renvoisé, J. Stadler, R. Singh, J. C. Bakowska, C. Blackstone, Spg20-/- mice reveal multimodal functions for Troyer syndrome protein spartin in lipid droplet maintenance, cytokinesis and BMP signaling. *Human molecular genetics* **21**, 3604-3618 (2012).
230. A. Urbanczyk, R. Enz, Spartin recruits PKC-ζ via the PKC-ζ-interacting proteins ZIP1 and ZIP3 to lipid droplets. *J Neurochem* **118**, 737-748 (2011).
231. B. J. Andreone *et al.*, Blood-Brain Barrier Permeability Is Regulated by Lipid Transport-Dependent Suppression of Caveolae-Mediated Transcytosis. *Neuron* **94**, 581-594.e585 (2017).
232. L. Du *et al.*, Starving neurons show sex difference in autophagy. *The Journal of biological chemistry* **284**, 2383-2396 (2009).
233. D. S. Cornett, M. L. Reyzer, P. Chaurand, R. M. Caprioli, MALDI imaging mass spectrometry: molecular snapshots of biochemical systems. *Nature methods* **4**, 828-833 (2007).
234. B. Fuchs, R. Süss, J. Schiller, An update of MALDI-TOF mass spectrometry in lipid research. *Progress in lipid research* **49**, 450-475 (2010).
235. R. C. Murphy, J. A. Hankin, R. M. Barkley, Imaging of lipid species by MALDI mass spectrometry. *Journal of Lipid Research* **50**, S317-S322 (2009).
236. M. M. Paula-Barbosa, R. M. Cardoso, M. L. Guimaraes, C. Cruz, Dendritic degeneration and regrowth in the cerebral cortex of patients with Alzheimer's disease. *J Neurol Sci* **45**, 129-134 (1980).
237. K. Miyazu *et al.*, Membranous lipodystrophy (Nasu-Hakola disease) with thalamic degeneration: report of an autopsied case. *Acta Neuropathol* **82**, 414-419 (1991).
238. L. Eriksson, P. Westermark, Age-related accumulation of amyloid inclusions in adrenal cortical cells. *Am J Pathol* **136**, 461-466 (1990).
239. C. M. Hulette, N. L. Earl, D. C. Anthony, B. J. Crain, Adult onset Niemann-Pick disease type C presenting with dementia and absent organomegaly. *Clin Neuropathol* **11**, 293-297 (1992).

240. A. Ozsvar *et al.*, Quantitative analysis of lipid debris accumulation caused by cuprizone induced myelin degradation in different CNS areas. *Brain Res Bull* **137**, 277-284 (2018).
241. M. Smialek, B. Gajkowska, R. P. Ostrowski, P. Piotrowski, Experimental squalene encephaloneuropathy in the rat. *Folia Neuropathol* **35**, 262-264 (1997).
242. M. Ahdab-Barmada, J. Moossy, E. M. Nemoto, M. R. Lin, Hyperoxia produces neuronal necrosis in the rat. *Journal of neuropathology and experimental neurology* **45**, 233-246 (1986).
243. J. R. Brawer, R. J. Walsh, Response of tanycytes to aging in the median eminence of the rat. *Am J Anat* **163**, 247-256 (1982).
244. R. F. de Estable-Puig, J. F. Estable-Puig, Intraneuronal lipid droplets in irradiated nervous tissue. *Virchows Arch B Cell Pathol* **14**, 117-125 (1973).
245. T. J. Benstead, P. J. Dyck, V. Sangalang, Inner perineurial cell vulnerability in ischemia. *Brain Res* **489**, 177-181 (1989).
246. J. C. Stokreef, C. W. Reifel, S. H. Shin, A possible phagocytic role for folliculo-stellate cells of anterior pituitary following estrogen withdrawal from primed male rats. *Cell Tissue Res* **243**, 255-261 (1986).
247. B. Gajkowska, A. Zareba-Kowalska, [Effect of ischemia on the ultrastructure of the hypothalamo-hypophyseal system in rats]. *Neuropatol Pol* **27**, 367-381 (1989).
248. S. M. Marasigan, M. Sato, K. Miyoshi, Experimental striatal degeneration induced by kainic acid administration: relevance to morphological changes in Huntington's disease. *Jpn J Psychiatry Neurol* **40**, 113-121 (1986).
249. H. Kamada *et al.*, Changes of free cholesterol and neutral lipids after transient focal brain ischemia in rats. *Acta Neurochir Suppl* **86**, 177-180 (2003).
250. H. Kamada *et al.*, Spatiotemporal changes of free cholesterol and neutral lipids after transient middle cerebral artery occlusion in rats. *Ann N Y Acad Sci* **977**, 115-122 (2002).
251. M. Ueno *et al.*, Ultrastructural and permeability features of microvessels in the hippocampus, cerebellum and pons of senescence-accelerated mice (SAM). *Neurobiol Aging* **22**, 469-478 (2001).
252. R. R. Sturrock, A light microscopic and scanning electron microscopic study of intraventricular macrophages in the brains of aged mice. *J Anat* **136**, 761-771 (1983).
253. R. R. Sturrock, An ultrastructural study of intraventricular macrophages in the brains of aged mice. *Anat Anz* **165**, 283-290 (1988).
254. S. Nakajima, M. Gotoh, K. Fukasawa, K. Murakami-Murofushi, H. Kunugi, Oleic acid is a potent inducer for lipid droplet accumulation through its esterification to glycerol by diacylglycerol acyltransferase in primary cortical astrocytes. *Brain Res* **1725**, 146484 (2019).
255. D. S. Yang *et al.*, Defective macroautophagic turnover of brain lipids in the TgCRND8 Alzheimer mouse model: prevention by correcting lysosomal proteolytic deficits. *Brain* **137**, 3300-3318 (2014).
256. F. Chali *et al.*, Lipid markers and related transcripts during excitotoxic neurodegeneration in kainate-treated mice. *Eur J Neurosci* **50**, 1759-1778 (2019).
257. E. Rawish *et al.*, Telmisartan prevents development of obesity and normalizes hypothalamic lipid droplets. *J Endocrinol* **244**, 95-110 (2020).

258. S. Kim *et al.*, Tanycytic TSPO inhibition induces lipophagy to regulate lipid metabolism and improve energy balance. *Autophagy*, 1-21 (2019).
259. X. Han *et al.*, Plin4-Dependent Lipid Droplets Hamper Neuronal Mitophagy in the MPTP/p-Induced Mouse Model of Parkinson's Disease. *Front Neurosci* **12**, 397 (2018).
260. R. R. Sturrock, A comparative quantitative and morphological study of ageing in the mouse neostriatum, indusium griseum and anterior commissure. *Neuropathol Appl Neurobiol* **6**, 51-68 (1980).
261. D. Crespo, R. Verduga, C. Fernandez-Viadero, M. Megias, Structural changes induced by cytidine-5'-diphosphate choline (CDP-choline) chronic treatment in neurosecretory neurons of the supraoptic nucleus of aged CFW-mice. *Mech Ageing Dev* **84**, 183-193 (1995).
262. P. P. Liberski, R. Yanagihara, C. J. Gibbs, Jr., D. C. Gajdusek, White matter ultrastructural pathology of experimental Creutzfeldt-Jakob disease in mice. *Acta Neuropathol* **79**, 1-9 (1989).
263. M. Ogrodnik *et al.*, Obesity-Induced Cellular Senescence Drives Anxiety and Impairs Neurogenesis. *Cell metabolism* **29**, 1061-1077 e1068 (2019).
264. L. K. Hamilton *et al.*, Widespread deficits in adult neurogenesis precede plaque and tangle formation in the 3xTg mouse model of Alzheimer's disease. *Eur J Neurosci* **32**, 905-920 (2010).
265. M. J. Cabirol-Pol, B. Khalil, T. Rival, C. Faivre-Sarrailh, M. T. Besson, Glial lipid droplets and neurodegeneration in a Drosophila model of complex I deficiency. *Glia* **66**, 874-888 (2018).
266. V. Kis, B. Barti, M. Lippai, M. Sass, Specialized Cortex Glial Cells Accumulate Lipid Droplets in Drosophila melanogaster. *PLoS One* **10**, e0131250 (2015).
267. A. P. Bailey *et al.*, Antioxidant Role for Lipid Droplets in a Stem Cell Niche of Drosophila. *Cell* **163**, 340-353 (2015).
268. Y. Nakai, S. Shioda, N. Tashiro, Y. Honma, Fine structures of the cerebrospinal fluid-contacting neurons in the hypothalamus of the lamprey, Lampetra japonica. *Arch Histol Jpn* **42**, 337-353 (1979).
269. L. Calderon-Garciduenas *et al.*, Air pollution and brain damage. *Toxicol Pathol* **30**, 373-389 (2002).
270. A. E. Libby *et al.*, Lipoprotein lipase is an important modulator of lipid uptake and storage in hypothalamic neurons. *Biochem Biophys Res Commun* **465**, 287-292 (2015).
271. R. E. Gregg *et al.*, Abnormal in vivo metabolism of apolipoprotein E4 in humans. *The Journal of Clinical Investigation* **78**, 815-821 (1986).
272. R. W. Mahley, K. H. Weisgraber, Y. Huang, Apolipoprotein E4: a causative factor and therapeutic target in neuropathology, including Alzheimer's disease. *Proc Natl Acad Sci U S A* **103**, 5644-5651 (2006).
273. A. B. Wolf, R. J. Caselli, E. M. Reiman, J. Valla, APOE and neuroenergetics: an emerging paradigm in Alzheimer's disease. *Neurobiol Aging* **34**, 1007-1017 (2013).
274. N. A. Elshourbagy, W. S. Liao, R. W. Mahley, J. M. Taylor, Apolipoprotein E mRNA is abundant in the brain and adrenals, as well as in the liver, and is present in other peripheral tissues of rats and marmosets. *Proceedings of the National Academy of Sciences of the United States of America* **82**, 203-207 (1985).

275. R. E. Pitas, J. K. Boyles, S. H. Lee, D. Foss, R. W. Mahley, Astrocytes synthesize apolipoprotein E and metabolize apolipoprotein E-containing lipoproteins. *Biochimica et biophysica acta* **917**, 148-161 (1987).
276. D. M. Holtzman, J. Herz, G. Bu, Apolipoprotein E and Apolipoprotein E Receptors: Normal Biology and Roles in Alzheimer Disease. *Cold Spring Harbor Perspectives in Medicine* **2**, a006312 (2012).
277. V. Hirsch-Reinshagen *et al.*, Deficiency of ABCA1 impairs apolipoprotein E metabolism in brain. *The Journal of biological chemistry* **279**, 41197-41207 (2004).
278. H. N. Yassine *et al.*, ABCA1-Mediated Cholesterol Efflux Capacity to Cerebrospinal Fluid Is Reduced in Patients With Mild Cognitive Impairment and Alzheimer's Disease. *Journal of the American Heart Association* **5**, (2016).
279. J. Edmond, R. A. Robbins, J. D. Bergstrom, R. A. Cole, J. de Vellis, Capacity for substrate utilization in oxidative metabolism by neurons, astrocytes, and oligodendrocytes from developing brain in primary culture. *Journal of Neuroscience Research* **18**, 551-561 (1987).
280. D. Ebert, R. G. Haller, M. E. Walton, Energy contribution of octanoate to intact rat brain metabolism measured by 13C nuclear magnetic resonance spectroscopy. *J Neurosci* **23**, 5928-5935 (2003).
281. D. Lovatt *et al.*, The Transcriptome and Metabolic Gene Signature of Protoplasmic Astrocytes in the Adult Murine Cortex. *The Journal of Neuroscience* **27**, 12255 (2007).
282. J. N. Jernberg, C. E. Bowman, M. J. Wolfgang, S. Scafidi, Developmental regulation and localization of carnitine palmitoyltransferases (CPTs) in rat brain. *J Neurochem* **142**, 407-419 (2017).
283. A. Panov, Z. Orynbayeva, V. Vavilin, V. Lyakhovich, Fatty acids in energy metabolism of the central nervous system. *Biomed Res Int* **2014**, 472459 (2014).
284. M. A. Welte, A. P. Gould, Lipid droplet functions beyond energy storage. *Biochimica et Biophysica Acta (BBA) - Molecular and Cell Biology of Lipids* **1862**, 1260-1272 (2017).
285. N. Krahmer, R. V. Farese, T. C. Walther, Balancing the fat: lipid droplets and human disease. *EMBO Molecular Medicine* **5**, 905-915 (2013).
286. S. Xu, X. Zhang, P. Liu, Lipid droplet proteins and metabolic diseases. *Biochimica et biophysica acta. Molecular basis of disease* **1864**, 1968-1983 (2018).
287. M. D. Tambini *et al.*, ApoE4 upregulates the activity of mitochondria-associated ER membranes. *EMBO Reports* **17**, 27-36 (2016).
288. S. Lucken-Ardjomande Häsler, Y. Vallis, H. E. Jolin, A. N. McKenzie, H. T. McMahon, GRAF1a is a brain-specific protein that promotes lipid droplet clustering and growth, and is enriched at lipid droplet junctions. *Journal of Cell Science* **127**, 4602-4619 (2014).
289. A. J. Wensaas *et al.*, Cell-based multiwell assays for the detection of substrate accumulation and oxidation. *J Lipid Res* **48**, 961-967 (2007).
290. F. K. Huynh, M. F. Green, T. R. Koves, M. D. Hirschey, Measurement of fatty acid oxidation rates in animal tissues and cell lines. *Methods Enzymol* **542**, 391-405 (2014).

291. B.-C. Cohen, A. Shamay, N. Argov-Argaman, Regulation of Lipid Droplet Size in Mammary Epithelial Cells by Remodeling of Membrane Lipid Composition—A Potential Mechanism. *PLOS ONE* **10**, e0121645 (2015).
292. N. M. Heinsinger, M. A. Gachechiladze, G. W. Rebeck, Apolipoprotein E Genotype Affects Size of ApoE Complexes in Cerebrospinal Fluid. *Journal of Neuropathology & Experimental Neurology* **75**, 918-924 (2016).
293. D. R. Riddell *et al.*, Impact of apolipoprotein E (ApoE) polymorphism on brain ApoE levels. *The Journal of neuroscience : the official journal of the Society for Neuroscience* **28**, 11445-11453 (2008).
294. Y. Z. Feng *et al.*, Loss of perilipin 2 in cultured myotubes enhances lipolysis and redirects the metabolic energy balance from glucose oxidation towards fatty acid oxidation. *J Lipid Res* **58**, 2147-2161 (2017).
295. S. Senthivinayagam, A. L. McIntosh, K. C. Moon, B. P. Atshaves, Plin2 inhibits cellular glucose uptake through interactions with SNAP23, a SNARE complex protein. *PLoS One* **8**, e73696 (2013).
296. M. Ueno *et al.*, Cardiac overexpression of perilipin 2 induces dynamic steatosis: prevention by hormone-sensitive lipase. *American journal of physiology. Endocrinology and metabolism* **313**, E699-e709 (2017).
297. H. B. Shi *et al.*, Adipocyte differentiation-related protein promotes lipid accumulation in goat mammary epithelial cells. *Journal of dairy science* **98**, 6954-6964 (2015).
298. M. Miyata, J. D. Smith, Apolipoprotein E allele-specific antioxidant activity and effects on cytotoxicity by oxidative insults and beta-amyloid peptides. *Nature genetics* **14**, 55-61 (1996).
299. X. Shen, H. Liu, Z. Hu, H. Hu, P. Shi, The relationship between cerebral glucose metabolism and age: report of a large brain PET data set. *PloS one* **7**, e51517-e51517 (2012).
300. B. Horwitz, C. L. Grady, N. L. Schlageter, R. Duara, S. I. Rapoport, Intercorrelations of regional cerebral glucose metabolic rates in Alzheimer's disease. *Brain Res* **407**, 294-306 (1987).
301. N. Zhong, K. H. Weisgraber, Understanding the Association of Apolipoprotein E4 with Alzheimer Disease: Clues from Its Structure. *The Journal of biological chemistry* **284**, 6027-6031 (2009).
302. R. Chouinard-Watkins, M. Plourde, Fatty Acid Metabolism in Carriers of Apolipoprotein E Epsilon 4 Allele: Is It Contributing to Higher Risk of Cognitive Decline and Coronary Heart Disease? *Nutrients* **6**, 4452-4471 (2014).
303. R. P. Patrick, Role of phosphatidylcholine-DHA in preventing APOE4-associated Alzheimer's disease. *Faseb j* **33**, 1554-1564 (2019).
304. H. N. Yassine *et al.*, DHA brain uptake and APOE4 status: a PET study with [1-(11)C]-DHA. *Alzheimer's Research & Therapy* **9**, 23 (2017).
305. T. Nuriel *et al.*, Neuronal hyperactivity due to loss of inhibitory tone in APOE4 mice lacking Alzheimer's disease-like pathology. *Nature communications* **8**, 1464 (2017).
306. R. W. Mahley, S. C. Rall, Jr., Apolipoprotein E: far more than a lipid transport protein. *Annu Rev Genomics Hum Genet* **1**, 507-537 (2000).

307. R. W. Mahley, Apolipoprotein E: from cardiovascular disease to neurodegenerative disorders. *J Mol Med (Berl)* **94**, 739-746 (2016).
308. E. M. Reiman *et al.*, Exceptionally low likelihood of Alzheimer's dementia in APOE2 homozygotes from a 5,000-person neuropathological study. *Nature communications* **11**, 667 (2020).
309. R. Fallaize *et al.*, APOE genotype influences insulin resistance, apolipoprotein CII and CIII according to plasma fatty acid profile in the Metabolic Syndrome. *Scientific Reports* **7**, 6274 (2017).
310. J. M. Aburto, F. Villavicencio, U. Basellini, S. Kjærgaard, J. W. Vaupel, Dynamics of life expectancy and life span equality. *Proceedings of the National Academy of Sciences* **117**, 5250 (2020).
311. E. R. Tuminello, S. D. Han, The apolipoprotein e antagonistic pleiotropy hypothesis: review and recommendations. *International journal of Alzheimer's disease* **2011**, 726197 (2011).
312. C. R. Mondadori *et al.*, Better memory and neural efficiency in young apolipoprotein E epsilon4 carriers. *Cerebral cortex (New York, N.Y. : 1991)* **17**, 1934-1947 (2007).
313. P. J. Babin *et al.*, Both apolipoprotein E and A-I genes are present in a nonmammalian vertebrate and are highly expressed during embryonic development. *Proc Natl Acad Sci U S A* **94**, 8622-8627 (1997).
314. B. Maloney, Y. W. Ge, G. M. Alley, D. K. Lahiri, Important differences between human and mouse APOE gene promoters: limitation of mouse APOE model in studying Alzheimer's disease. *J Neurochem* **103**, 1237-1257 (2007).
315. J. E. Hixson, L. A. Cox, S. Borenstein, The baboon apolipoprotein E gene: structure, expression, and linkage with the gene for apolipoprotein C-1. *Genomics* **2**, 315-323 (1988).
316. P. Huebbe, G. Rimbach, Evolution of human apolipoprotein E (APOE) isoforms: Gene structure, protein function and interaction with dietary factors. *Ageing research reviews* **37**, 146-161 (2017).
317. R. M. Corbo, R. Scacchi, Apolipoprotein E (APOE) allele distribution in the world. Is APOE*4 a 'thrifty' allele? *Annals of human genetics* **63**, 301-310 (1999).
318. A. M. McIntosh *et al.*, The apolipoprotein E (APOE) gene appears functionally monomorphic in chimpanzees (Pan troglodytes). *PLoS One* **7**, e47760 (2012).
319. S. C. Anton, W. R. Leonard, M. L. Robertson, An ecomorphological model of the initial hominid dispersal from Africa. *J Hum Evol* **43**, 773-785 (2002).
320. D. M. Bramble, D. E. Lieberman, Endurance running and the evolution of Homo. *Nature* **432**, 345-352 (2004).
321. S. Craft, The role of metabolic disorders in Alzheimer disease and vascular dementia: two roads converged. *Arch Neurol* **66**, 300-305 (2009).
322. J. M. Walker, F. E. Harrison, Shared Neuropathological Characteristics of Obesity, Type 2 Diabetes and Alzheimer's Disease: Impacts on Cognitive Decline. *Nutrients* **7**, 7332-7357 (2015).
323. K. M. Narayan, J. P. Boyle, L. S. Geiss, J. B. Saaddine, T. J. Thompson, Impact of recent increase in incidence on future diabetes burden: U.S., 2005-2050. *Diabetes Care* **29**, 2114-2116 (2006).

324. R. E. González-Reyes, M. O. Nava-Mesa, K. Vargas-Sánchez, D. Ariza-Salamanca, L. Mora-Muñoz, Involvement of Astrocytes in Alzheimer's Disease from a Neuroinflammatory and Oxidative Stress Perspective. *Frontiers in molecular neuroscience* **10**, 427 (2017).
325. N. Auestad, R. A. Korsak, J. W. Morrow, J. Edmond, Fatty acid oxidation and ketogenesis by astrocytes in primary culture. *J Neurochem* **56**, 1376-1386 (1991).
326. J. Edmond, R. A. Robbins, J. D. Bergstrom, R. A. Cole, J. de Vellis, Capacity for substrate utilization in oxidative metabolism by neurons, astrocytes, and oligodendrocytes from developing brain in primary culture. *J Neurosci Res* **18**, 551-561 (1987).
327. D. M. Muoio, Metabolic inflexibility: when mitochondrial indecision leads to metabolic gridlock. *Cell* **159**, 1253-1262 (2014).
328. L. Mosconi, A. Pupi, M. J. De Leon, Brain glucose hypometabolism and oxidative stress in preclinical Alzheimer's disease. *Ann N Y Acad Sci* **1147**, 180-195 (2008).
329. S. Stoykovich, K. Gibas, APOE ε4, the door to insulin-resistant dyslipidemia and brain fog? A case study. *Alzheimers Dement (Amst)* **11**, 264-269 (2019).
330. K. Morgen, L. Frolich, The metabolism hypothesis of Alzheimer's disease: from the concept of central insulin resistance and associated consequences to insulin therapy. *J Neural Transm (Vienna)* **122**, 499-504 (2015).
331. K.-C. Sonntag *et al.*, Late-onset Alzheimer's disease is associated with inherent changes in bioenergetics profiles. *Scientific Reports* **7**, (2017).
332. N. R. Sims, J. M. Finegan, J. P. Blass, Altered metabolic properties of cultured skin fibroblasts in Alzheimer's disease. *Annals of Neurology* **21**, 451-457 (1987).
333. W. S. Liang *et al.*, Alzheimer's disease is associated with reduced expression of energy metabolism genes in posterior cingulate neurons. *Proc Natl Acad Sci U S A* **105**, 4441-4446 (2008).
334. T. Terada *et al.*, In vivo mitochondrial and glycolytic impairments in patients with Alzheimer disease. *Neurology* **94**, e1592 (2020).
335. M. J. de Leon *et al.*, Prediction of cognitive decline in normal elderly subjects with 2-[(18)F]fluoro-2-deoxy-D-glucose/poitron-emission tomography (FDG/PET). *Proc Natl Acad Sci U S A* **98**, 10966-10971 (2001).
336. R. Laforce, Jr., G. D. Rabinovici, Amyloid imaging in the differential diagnosis of dementia: review and potential clinical applications. *Alzheimer's research & therapy* **3**, 31 (2011).
337. J. P. Blass, Alzheimer's disease and Alzheimer's dementia: distinct but overlapping entities. *Neurobiol Aging* **23**, 1077-1084 (2002).
338. J. V. Haxby *et al.*, Longitudinal study of cerebral metabolic asymmetries and associated neuropsychological patterns in early dementia of the Alzheimer type. *Arch Neurol* **47**, 753-760 (1990).
339. C. L. Grady, J. V. Haxby, N. L. Schlageter, G. Berg, S. I. Rapoport, Stability of metabolic and neuropsychological asymmetries in dementia of the Alzheimer type. *Neurology* **36**, 1390-1392 (1986).
340. R. Mullins, D. Reiter, D. Kapogiannis, Magnetic resonance spectroscopy reveals abnormalities of glucose metabolism in the Alzheimer's brain. *Annals of Clinical and Translational Neurology* **5**, 262-272 (2018).

341. K. E. Weaver *et al.*, Posterior Cingulate Lactate as a Metabolic Biomarker in Amnestic Mild Cognitive Impairment. *Biomed Res Int* **2015**, 610605 (2015).
342. E. T. Poehlman, R. V. Dvorak, Energy expenditure in Alzheimer's disease. *The journal of nutrition, health & aging* **2**, 115-118 (1998).
343. D. A. Andres *et al.*, Improved workflow for mass spectrometry-based metabolomics analysis of the heart. *J Biol Chem*, (2020).
344. J. Xia, D. S. Wishart, Using MetaboAnalyst 3.0 for Comprehensive Metabolomics Data Analysis. *Curr Protoc Bioinformatics* **55**, 14.10.11-14.10.91 (2016).
345. R. Wei *et al.*, Missing Value Imputation Approach for Mass Spectrometry-based Metabolomics Data. *Scientific Reports* **8**, 663 (2018).
346. L. A. Johnson *et al.*, Apolipoprotein E4 exaggerates diabetic dyslipidemia and atherosclerosis in mice lacking the LDL receptor. *Diabetes* **60**, 2285-2294 (2011).

VITA

Brandon C. Farmer

EDUCATION

University of Kentucky College of Medicine

(2015-present)

MD/PhD Candidate

Western Kentucky University - B.S. Biology, Chemistry, Spanish
(2010-2015)

Summa Cum Laude

Carol Martin Gatton Academy of Mathematics and Science in Kentucky

(2010-2012)

Graduated with Honors

Bourbon County High School
(2008-2012)

Valedictorian

FUNDING

2019-2022 ***NRSA Research Fellowship Award*** **(1F30AG063422-01A1),** National Institutes of Health / National Institute on Aging

2018-2019 ***Predoctoral Fellowship*** **(19PRE34380094) ,** American Heart Association

2018 ***Fellowship for Excellence in Graduate Research,*** College of Medicine Office of Biomedical Education, University of Kentucky

2016-2017 ***Professional Student Mentored Research Fellowship***, Center for Clinical and Translational Science, University of Kentucky

AWARDS

Saha Cardiovascular Center MD/PhD Student Award, Saha Cardiovascular Research Center

Travel Award, 2019 American Neurological Association Annual Meeting

Travel Award, 2018 Southeastern Regional Lipid Conference

60-second Blitz Awardee, 2018 UK Dept of Physiology Research Retreat

Best Graduate Student Poster, 6th Annual Meeting of the Kentucky Chapter of the American Physiological Society

MD/PhD Student Scholarship, University of Kentucky MD PhD Program

Thomas Batterton Fund Trust for Health Care Students, Kentucky Bank

L.Y. Lancaster Award for Excellence in Pre-Medical Studies, Western Kentucky University

Tier 1 Gatton Academy Scholarship Recipient, Western Kentucky University

WKU Faculty Undergraduate Student Engagement (FUSE) Grant, Western Kentucky University

William Ralph Walls Jr. International Travel Award, WKU Modern Languages Department

RESEARCH EXPERIENCE

MD/PhD Lab

(Nov 6, 2017 – May 15th, 2020)

University of Kentucky College of Medicine

Department of Physiology

Mentor: Lance Johnson, PhD

Apolipoprotein E4 Contributes to Neurodegeneration via Cerebral Metabolic Derangements

MD/PhD Program Rotation

(July 3, 2017 – Nov 3, 2017)

University of Kentucky College of Medicine

Mentor: Brad Taylor, PhD

Sphingosine-1-Phosphate Signaling Mediates Descending Nociception in the Central Amygdala

MD/PhD Program Rotation – CCTS/PSMRF Project

(June 13, 2016 - Nov 30, 2016)

University of Kentucky College of Medicine

Mentor: Romulo Albuquerque, MD, PhD

Gender Specific Responses to Alu-RNA in the Corneal-Trigeminal Axis

MD/PhD Program Rotation

(June 25, 2015 - July 24, 2015)

University of Kentucky College of Medicine

Mentor: Paul M. Murphy, PhD

APP/PS1 Model for Determining the Role of Amyloid-β Peptide in Inclusion Body Myositis

Undergraduate Clinical Research Internship Program

(June 1, 2014 - July 30, 2014)

Vanderbilt University School of Medicine

Mentor: Agnes Fogo, MD

Fibroblast-Specific Knockdown of PAI-1 Attenuates Kidney Interstitial Fibrosis

2014 Partners in Caring: Medicine in Kenya Program

(December 28, 2013 - January 13, 2013)

Western Kentucky University

Mentor: Nancy Rice, PhD

A Pilot Study of the Occurrence of Trachoma in Kasigau, Kenya

WKU Honors College Thesis Project

(August 28, 2011 - May 15, 2015)

Western Kentucky University Honors College

Mentor: Kenneth Crawford, PhD

Endothelin-1 Promotes Bovine Corneal Endothelial Cell Proliferation via a MAPK Pathway: Implications for Keratopathy and Deturgescence

Kentucky Biomedical Research Infrastructure Network Undergraduate Internship

(May 4, 2011 - August 10, 2011)

University of Louisville Division of Nephrology

Mentor: Eleanor Lederer, MD

Cardioglycoside stimulated association b/w Na-K-ATPase & NHE-1: A TIRF & FRET Analysis

NSF Research Experience for Undergraduates: The Mammoth Cave/ Upper Green River Watershed

(May 31, 2011 - August 5, 2011)

Western Kentucky University

Mentor: Matthew Nee, PhD

Synthesis of Porous Nanomeric Non-Polar Beads for Solid Phase Micro Extraction

WKU Biology Department Research Field Study

(January 4, 2011 - January 19, 2011)

Cloudbridge Nature Preserve, Costa Rica

Mentor - Keith Philips, PhD

Elevational Disparity in Mammal Presence in Cloudbridge Nature Preserve

PEER REVIEWED PUBLICATIONS

Williams HC, **Farmer BC**, Piron MA, Walsh AE, Bruntz RC, Gentry MS, Sun RC, Johnson LA. APOE alters glucose flux through central carbon pathways in astrocytes. *Neurobiology of Disease*. 2020 Jan. PMID: 31931141

Yao L, Wright MF, **Farmer BC**, Peterson LS, Khan AM, Zhong J, Gewin L, Hao CM, Yang HC, Fogo AB. Fibroblast Specific plasminogen activator inhibitor-1 depletion ameliorates renal interstitial fibrosis after unilateral ureteral obstruction. *Nephrology Dialysis Transplantation*. 2019 Dec. PMID: 3107122

Farmer BC, Kluemper JC, Johnson LA. Apolipoprotein E4 Alters Astrocyte Fatty Acid Metabolism and Lipid Droplet Formation. *Cells*. 2019 Feb. PMID: 30791549

Farmer BC, Johnson LA, Hanson AJ. Effects of apolipoprotein E on nutritional metabolism in dementia. *Current Opinion in Lipidology*. 2019 Feb. PMID: 30550413

Brandon JA, **Farmer BC**, Williams HC, Johnson L. APOE and Alzheimer's Disease: Neuroimaging of metabolic and cerebrovascular dysfunction. *Frontiers in Aging Neuroscience*. 2018 March 28: PMID: 379433

Syed J Khundmiri, Ph.D.; Sarah A Salyer, MS; **Brandon Farmer**; Natia Qipshidze, Ph.D; Rebecca D Murray, BS; Barbara J Clark, Ph.D.; Zijian Xie, Ph.D; Thomas A Pressley, Ph.D; Eleanor D Lederer, MD. Structural determinants for the ouabain-stimulated increase in Na-K ATPase activity. *Biochim Biophys Acta*. Volume 1843. June 2014. Pages 1089–1102. PMID: 24566089

Farmer B, McKinley M, Nee M. Concave porosity non-polar beads by a modified microbubble fabrication. *Materials Letters*, Volume 98, 17 Feb 2013, Pages 105–107.

RESEARCH PRESENTATIONS

Farmer BC, Golden L, Kluemper N, Johnson LA. Apolipoprotein E4 is Associated with Increased Lipid Droplet Formation in Glia. 9th Annual Markesbery Symposium on Aging and Dementia. Lexington, KY. 11/6/19

***Farmer BC**, Nation G, Williams HC, Carter DJ, Khanal RB, Wilwerding A, Brandon JA, Gentry M, Sun R, Johnson LA. Indirect Calorimetry as a Novel Method to Study APOE's Role in Cerebral Metabolism and Alzheimer's Disease Risk. 144th Annual American Neurological Association Meeting. Annals of Neurology. Volume 86, Suppl 24. St Louis, MO. 10/14/19

***travel awardee**

Farmer BC, Kluemper JC, Johnson LA. Apolipoprotein E4 Alters Astrocyte Fatty Acid Metabolism and Lipid Droplet Formation. Kern Lipid Conference. Vail, CO. 8/14/19

Khanal R, Nation GK, **Farmer BC**, Carter DJ, Johnson LA. Early-Life Changes in Peripheral Metabolism: A Study of *APOE* Genotype Effects Using Indirect Calorimetry. Alzheimer's Association International Conference. Los Angeles, CA. 7/16/19

Farmer BC, Kluemper JC, Johnson LA. Apolipoprotein E4 Promotes Lipid Droplet Accumulation in Astrocytes. Alzheimer's Association International Conference. Los Angeles, CA. 7/14/19

***Farmer BC**, Nation GK, Khanal R, William H, Carter DJ, Brandon JA, Johnson LA. APOE's Cognitive and Metabolic Effects Revealed through Indirect Calorimetry. UK 2019 MD/PhD Program Retreat. 6/6/2019

***invited speaker**

Farmer BC, Nation GK, Khanal R, William H, Carter DJ, Brandon JA, Johnson LA. APOE's Cognitive and Metabolic Effects Revealed through Indirect Calorimetry. UK College of Medicine 2019 Physiology Research and Education Day. 5/22/2019

***Farmer BC**, Johnson LA. APOE's Cognitive and Metabolic Effects Revealed through Indirect Calorimetry. UK College of Medicine 2019 Physiology Research and Education Day 90-Second Blitz Competition. 5/22/2019

***Blitz award winner**

Kluemper, J., **Farmer, B. C**., Johnson, L.A. The effects of oxidative stress on lipid droplet formation in APOE expressing astrocytes. UK College of Medicine 2019 Physiology Research and Education Day. 5/22/2019

Khanal R, Nation GK, **Farmer BC**, Williams HC, Carter DJ, Brandon JA and Johnson LA. Using Plasma and Breath Measures to Detect APOE-dependent Changes in Metabolism. Undergraduate Research Showcase. Lexington, KY. 4/24/19

Khanal R, Nation GK, **Farmer BC**, Williams HC, Carter DJ, Brandon JA and Johnson LA. Using Plasma and Breath Measures to Detect APOE-dependent Changes in Metabolism. UK Center for Clinical and Translational Science Conference. Lexington, KY, 4/15/19.

Kluemper J, **Farmer BC**, Johnson LA. The effects of oxidative stress on lipid droplet formation in APOE expressing astrocytes. UK Center for Clinical and Translational Science Conference. Lexington, KY, 4/15/2019

***Farmer BC**. Apolipoprotein E4 Alters Astrocyte Fatty Acid Metabolism and Lipid Droplet Formation. University of Kenutcky CCTS 2019 Annual Conference. Lexington, KY 4/15/19

***selected for oral presentation**

Farmer BC. Apolipoprotein E4 Increases Lipid Droplet Formation in Astrocytes. UK Department of Physiology Seminar. Lexington, KY, 3/27/19

***Farmer BC**. Disovering APOE's Metabolic Role in Humans, Mice, and Astrocytes. WKU Department of Biology Seminar. Bowling Green, KY 2/15/19

***invited speaker**

***Farmer BC,** Kluemper JC, Johnson LA. Apolipoprotein E Isoforms Modulate Astrocytic Lipid Metabolism. Southeastern Regional Lipid Conference. Cashiers, NC, 11/8/18

***selected for oral presentation**

***selected for travel award**

***Farmer BC,** Carter DJ, Nation GK, Khanal R, Johnson LA. APOE Genotype Effect on Respiratory Quotient – A Potential Biomarker for Alzheimer's Disease Risk. 2018 Neuroscience Clinical-Translational Research Symposium, Kentucky Neuroscience Institute, 10/5/18

***selected for oral presentation**

Khanal R, **Farmer BC**, Brandon JA, Carter DJ, Kluemper J, Johnson LA. APOE and Fatty Acid Metabolism: E4 Increases Astrocyte Lipid Droplet Formation. Cardiovascular Research Day, University of Kentucky, 9/21/18

*Brandon JA, **Farmer BC**, Carter DJ, Williams HC, Khanal R, Kluemper J, Johnson LA. APOE and Energy Substrate Balance: E2 Promotes Glucose Uptake and Utilization in Astrocytes. Neurobiology of Brain Disorders, Gordon Research Conference, Barcelona, Spain, 8/6/18

*** selected for oral presentation**

***Farmer BC.** "60-second Blitz". Apolipoprotein E ε4 Promotes Lipid Droplet Formation in Astrocytes. UK Dept of Physiology Research Retreat. Lexington, KY. May 16, 2018.

***competition awardee**

Farmer BC, Kluemper J, Williams HC, Fields L, Carter DJ, Brandon JA, Johnson L. Apolipoprotein E ε4 Promotes Lipid Droplet Formation in Astrocytes. UK Dept of Physiology Research Retreat. Lexington, KY. May 16, 2018.

Carter DJ, **Farmer BC**, Brandon JA, Johnson LA. APOE Metabolism and Cognitive Function: An Assessment via Indirect Calorimetry. American Physician Scientists Association, Chicago, IL, 4/21/18

Farmer BC. APOE Metabolism and Cognitive Function: An Assessment via Indirect Calorimetry. "60-Second Pitch", UK 13th Annual CCTS Spring Conference, Lexington, KY, 4/13/18

Carter DJ, **Farmer BC**, Brandon JA, Johnson LA. APOE Metabolism and Cognitive Function: An Assessment via Indirect Calorimetry. UK 13th Annual CCTS Spring Conference, Lexington, KY, 4/13/18

*** Farmer BC**, Kluemper J, Williams HC, Fields LW, Carter DJ, Brandon JA, Johnson LA. Apolipoprotein E ε4 Promotes Lipid Droplet Formation in Astrocytes. Kentucky Chapter of the American Physiological Society, Annual Conference, University of Louisville, 2018 Apr 7

**** won Best Poster Award***

Williams HC, **Farmer BC**, Carter DJ, Brandon JA, Johnson LA. Apolipoprotein E4 Decreases Glycolysis and Reduces Glucose Uptake and Lactate Secretion in Astrocytes.

Kentucky Chapter of the American Physiological Society, Annual Conference, University of Louisville, 2018 Apr 7

Farmer B, Cho J, Albuquerque R. Gender Specific Inflammasome Activation in the Trigeminal Ganglion. *2017 Annual CCTS Spring Conference*. 2017 Mar 30; Lexington, KY

Farmer, B, Beckett T, Murphy P. APP/PS1 Model for Determining the Role of Amyloid-Beta Peptide in Inclusion Body Myositis. *2016 AOA Groves Memorial and MD/PhD Program Student Research Symposium*. 2016 Feb 4; Lexington, KY

Farmer, Brandon C., "Endothelin-1 Promotes Bovine Corneal Endothelial Cell Proliferation via a MAPK Pathway: Implications for Keratopathy and Deturgescence" (2015). College Capstone Experience/Thesis Projects. 557.

Brandon Farmer, Haichun Yang, MD/PhD, Agnes Fogo, MD.; Fibroblast-Specific Knockdown of PAI-1 Attenuates Kidney Interstitial Fibrosis. *2014 Southeastern Medical Scientist Symposium*; 2014 Aug 23-24; Atlanta, GA

Brandon Farmer, Leah Frazier, BS, Akhila Bethi, MS.; Ken Crawford, Ph. D.; Endothelin-1 induces phosphorylation of ERK 1/2 in bovine corneal endothelial cells. *2014 Annual Meeting of the Association for Research in Vision and Ophthalmology*; 2014 May 4-8; Orlando, Fl.

Farmer B, Bethi A. Endothelin-1 Induces Phosphorylation of ERK 1/2 in Bovine Corneal Endothelial Cells. *99th Annual Kentucky Academy of Sciences Conference.* Murray, KY,9 Nov 2013.

Farmer B, Bethi A. Endothelin-1 Induces Phosphorylation of ERK 1/2 in Bovine Corneal Endothelial Cells. *WKU Student Research Conference*. Undergraduate Paper Session 6: Natural Sciences.

Farmer B, Murray R, Khundmiri S. Cardioglycoside stimulated association between Na-K-ATPase and NHE-1 : A TIRF and FRET Analysis. *KAS 2012 Annual Meeting*. Undergraduate Poster Session. 20 Oct 2012.